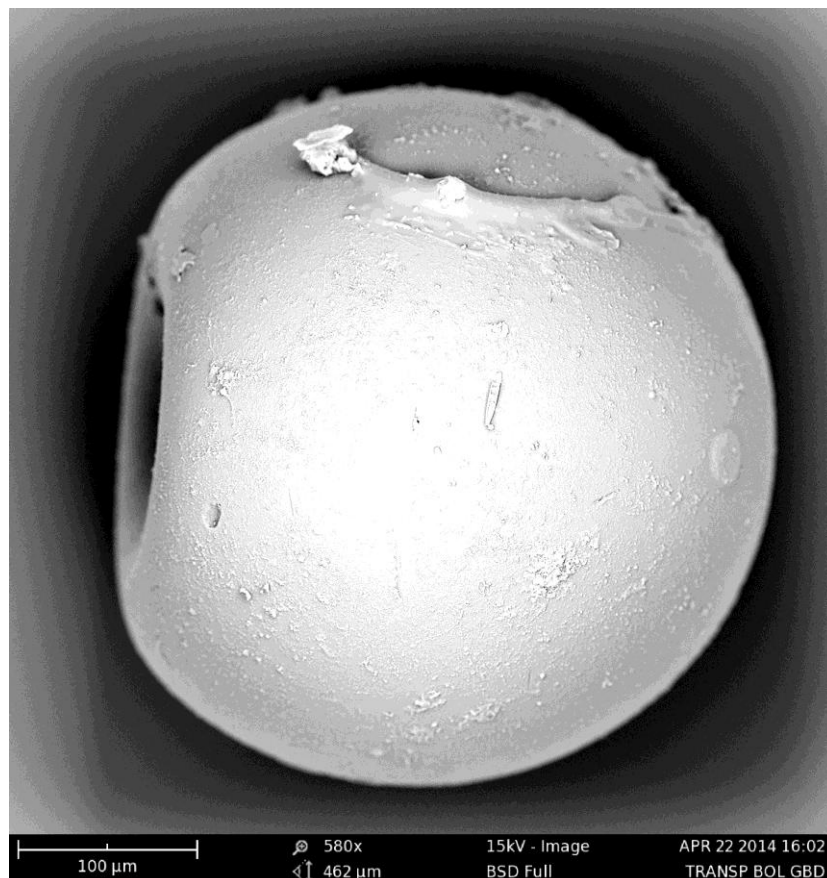**Open Universiteit**
www.ou.nl

Master's thesis for
Master of Science Environmental Sciences

Department of Science, Faculty of Management, Science &
Technology, Open University of the Netherlands, Heerlen.

Microplastics in the rivers Meuse and Rhine

Developing guidance for a possible
future monitoring program.

Wilco Urgert
October 16th, 2015

"Environmental Science is about analyzing, preventing and solving societal problems. For that, you need different disciplines. Which disciplines you will need, depends on the specific problems at hand. Integration of knowledge from different disciplines is a key characteristic of the Environmental Scientist."

Quoted from prof. dr. A.M.J. (Ad) Ragas, professor at the Department of Science, Faculty of Management, Science & Technology, Open University of the Netherlands, Heerlen.

In this study, to a greater or lesser extent, I tried to integrate insights from Biology, Hydrology, Analytical chemistry, Organic chemistry, Physics and Mathematics into one coherent whole.

The graduation committee consists of the following members:

First OU supervisor:	dr. A.J. (Ansje) Löhr, assistant professor at the Department of Science, Faculty of Management, Science & Technology, Open University of the Netherlands, Heerlen.
Second OU supervisor:	dr. F.G.A.J. (Frank) van Belleghem, assistant professor at the Department of Science, Faculty of Management, Science & Technology, Open University of the Netherlands, Heerlen.
External supervisor:	dr. G. (Gerard) Stroomberg, program manager operational water quality monitoring at Rijkswaterstaat, Lelystad. From October 1st 2014: director at RIWA-Rijn, Nieuwegein.
External supervisor:	prof. dr. N.M. (Nico) van Straalen, professor at the Department of Ecological Science, Faculty of Earth And Life Sciences, VU University, Amsterdam.
External supervisor:	dr. ir. C.A.M. (Kees) van Gestel, associate professor at the Department of Ecological Science, Faculty of Earth And Life Sciences, VU University, Amsterdam.
Coordinator/secretary:	drs. P. (Pieter) Geluk, study coordinator at the Department of Science, Faculty of Management, Science & Technology, Open University of the Netherlands, Heerlen.

The image on the front cover represents a transparent spherule collected from the Rhine river. The image was created by a Phenom Scanning Electron Microscope (model 800 07334/PW-100-017) on April 24th, 2014. For optimal image resolution the spherule was first covered with a thin layer of gold.

Acknowledgements

Abstract

Microplastics, plastics fragments smaller than 5 mm, are found in aquatic ecosystems all over the world. Marine life may be harmed when they ingest microplastics, as they can form blockades in the gastro-intestinal tract or carry adhered pollutants. To assess the scale and the urgency of this environmental threat, scientists stress the need build up accurate and comparable datasets on the abundance and composition of microplastics in aquatic systems, among which rivers. Research in rivers, however, is still in its infancy. In this master thesis, an in-depth study on the abundance and composition of microplastics in the Dutch parts of the European rivers Meuse and Rhine was carried out. This study is one of the first, if not the first, that includes an extending series of synchronized samples, collected at exactly the same locations and using the same method, in two running European rivers.

From January 10th 2014 up to June 23rd 2014, 17 weekly samples were taken by leading river water through a cascade of soil sieves for 72 hours. Two size fraction are acknowledged: 0.125-0.250 mm and 0.250-5 mm. The samples were cleared from organic debris, inorganic particulate matter and occasionally coal. Hereto a method is developed comprising successively the following steps: digestion with hydrogen peroxide, an interim filtration step using a mini-sieve, sample splitting, density separation with sodium chloride and sonication. Microplastics were visually indentified, counted, and sorted out into four groups: films, white spherules, transparent spherules and miscellaneous microplastics. Occasionally scrubs were sorted out form the latter group as well. Fibres were not taken into account. For each sample, the individual groups were weighed separately.

Raman and Fourier Transform spectroscopy were used in combination with Principal Component Analysis (PCA) to indentify the composition of the handpicked particles. Differences between both rivers were observed as in the Meuse no spherules were found. In both rivers films, scrubs and the majority of the miscellaneous microplastics were identified as polyethylene. The white spherules in the Rhine were verified as polystyrene, just as the transparent spherules up to 0.250 mm. For the larger transparent spherules, temporal variations in composition were observed comprising polyethylene, polypropylene and polystyrene. Also a yet unidentifiable polymer was observed.

For the size range of 0.125-5 mm, average concentrations of 0.14 mg or 9.7 microplastics per m^3 were calculated for the Meuse, and 0.56 mg or 56 microplastics per m^3 for the Rhine. These figures form an under limit, as particles can become lost and unevenly distributed during the laboratory processing and demonstrated is that even with secure visual selection, microplastics can become overlooked. Indications were found that the sampled water is not representative for the water column and river width. PCA showed to be a useful tool for studying large numbers of spectral recordings simultaneously.

Proper clearing of the microplastics samples improves the distinctiveness and certainty of determination but also increases the processing time. Some of tested clearing methods, among which sonication, is likely to affect microplastics with weak molecular bonds. Spectral quality improvements will increase the certainty of determination and decrease the processing time. Temporal abundance and composition variations could not be related to varying river discharges or turbidity levels. More research is needed on the upstream emission sources, the associated emission intensities and the behaviour of microplastics in relation to the complex river dynamics.

Samenvatting

Microplastics, kunststof fragmenten kleiner dan 5 mm, worden wereldwijd gevonden in zeeën en zoete wateren. Onderzoek heeft uitgewezen dat microplastics potentiële risico's kunnen vormen voor de dieren die in die wateren leven. Om de risico's in kaart te kunnen brengen is er behoefte aan een eenduidige en integrale registratie van de soorten microplastics die wereldwijd worden gevonden. Het meeste onderzoek is tot op heden uitgevoerd in de zeeën, terwijl rivieren juist gezien worden als belangrijke aanvoerroutes van microplastics naar die zeeën toe. In deze studie is het rivierwater van de Maas en Rijn, ter hoogte van de landsgrenzen, onderzocht op de hoeveelheid en samenstelling van microplastics.

Op drie locaties waar Rijkswaterstaat onderzoek doet naar de chemische rivierwaterkwaliteit, te weten Eijsden (Maas), Lobith (Rijn) en Bimmen (Rijn), zijn tussen 10 januari 2014 en 23 juni 2014 wekelijks monsters genomen. Daarbij is gedurende 72 uur een bekende hoeveelheid rivierwater over een stapel bodemzeven geleid, waardoor twee groottefracties ontstonden: 0.125-0.250 mm and 0.250-5 mm. De monsters zijn geschoond van organisch en anorganisch materiaal en in sommige gevallen van steenkool. De microplastics zijn gedetermineerd onder een stereomicroscoop, geteld en op basis van uiterlijke kenmerken gerangschikt naar vier groepen: folies, witte bollen, transparante bollen en overige microplastics. Vanuit de laatstgenoemde groep zijn in sommige gevallen ook scrubs als aparte groep onderscheiden. Vezels zijn buiten beschouwing gelaten. Groepsgewijs is per monster het gewicht vastgesteld.

De groepen microplastics zijn met Raman en Fourier Transform spectroscopie bestudeerd. Grootschalige vergelijking van de spectrale data vond plaats door middel van Principale Componenten Analyse. Tussen de beide rivieren zijn verschillen gevonden in hoeveelheid en soorten microplastics. In de Maas en Rijn zijn films, scrubs en overige (ongeclassificeerde) deeltjes gevonden, waarvan spectroscopie heeft uitgewezen dat dit voornamelijk polyethyleen betreft. Bollen zijn alleen gevonden in de Rijn, waarvan de witte bollen en de transparante bollen tot 0.250 mm zijn geïdentificeerd als polystyreen. Voor de grotere transparante bollen zijn tussen verschillende samples ook verschillen in samenstelling vastgesteld: polyethyleen, polystyreen en polypropyleen, alsook een polymeer waarvoor geen match kon worden gevonden. Een omvangrijkere dataset en verbeteringen in de spectroscopische methode opzet zullen leiden tot betere determinatie binnen minder tijd.

Gegeven de bestudeerde groottefractie van 0.125-5 mm zijn gemiddelde concentraties berekend van 0.14 mg of 9.7 microplastics per m^3 voor de Maas, en 0.56 mg of 56 microplastics per m^3 voor de Rijn. Deze getallen gelden als onderste waarden, omdat testen hebben uitgewezen dat tijdens de verwerking van de samples microplastics verloren kunnen gaan, dat splitsing kan leiden tot ongelijke verdeling en dat zelfs bij zorgvuldige handmatige selectie, microplastics over het hoofd kunnen worden gezien. Het zorgvuldig schonen van zoetwater monsters leidt tot een betere herkenning van microplastics, maar maakt het een tijdsintensief proces.

Daarbij zijn ook inzichten naar voren gekomen over het mogelijke verlies van microplastics tijdens het laboratoriumwerk. Sommige beproefde methodes, zoals ultrasoon behandeling, zijn verdacht van het beschadigen van sommige microplastics. Verbeteringen op het vlak van spectroscopie zullen bijdragen aan het nauwkeuriger identificeren van microplastics in kortere tijd. Daarbij zijn er aanwijzingen dat het ingenomen water niet representatief was ten opzichte van de hele waterkolom en ten opzichte van de breedte van de rivier. De gevonden concentraties konden niet worden gerelateerd aan rivierafvoeren of de hoeveelheid zwevend stof. Het transport van zwevend stof in het algemeen, en dat van microplastics in het bijzonder, is thans nog onbekend terrein.

Index

1. Introduction

1.1 The demand for global and European plastics

Plastics, synthetic polymers such as polyethylene (PE), polypropylene (PP), polystyrene (PS), polyethylene terephthalate (PET) and polyvinyl chloride (PVC) have become an inseparable part of our daily lives. Societal beneficial applications are numerous: examples of light weight packaging, building & construction, household goods, automotive, aviation and safety control are within easy reach.

In 2012, 288 million tons of plastics were produced worldwide, of which 57 million tons in the European Union (Plastics Europe, 2013). Markets in Europe that lead to plastic demand are packaging (39.4%), building & construction (20.3%), automotive (8.2%), electrical and electronic applications (5.5%) and agricultural applications (4.2%). Other sectors like appliances, household and consumer products, furniture, sport health and safety comprise a total of 22.4% of the European plastics demand (Plastics Europe, 2013). The global and European plastics demand in 2012 were geographically distributed as presented in table 1. Obviously, 25% of the total European demand is induced by Germany. Italy is good for 15% and France for 10%. Most of the EU members' individual share remain below 5%.

Table 1 Global and European plastics demand in 2012 (Plastics Europe, 2013). Included in these number are the polymer groups polyethylene, polypropylene, polystyrene, polyethylene terephthalate and polyvinyl chloride. Excluded are elastomers (rubbers) and thermosetting polymers such as Teflon®, Bakelite, acrylonitrile butadienestyrene (ABS) and polyurethane (PUR).

Geographical unit	Mtons	Share
China	58	23.9%
Europe	49	20.4%
NAFTA (North American Free Trade Agreement, i.e. U.S.A., Canada and Mexico)	48	19.9%
Asia without China, CIS and Japan	38	15.8%
Middle east and Africa	17	7.2%
Japan	12	4.9%
Latin America	12	4.9%
CIS (Common wealth of Independent States (i.e. 11 former Soviet republics including Russia)	7	3.0%
Total	**241**	**100%**

EU member	Share
Germany	~25%
Italy	~15%
France	~10%
Spain	~ 8%
United Kingdom	~ 8%
Poland	~ 6%
Others combined, including the Netherlands	~28%

1.1 Plastics in the natural environment

Plastics become accidentally lost, emitted or disposed in the natural environment and have become one of the most common and persistent pollutants in ocean waters and beaches worldwide (Andrady, 2011; Moore, 2008). Due to its buoyancy, plastic debris is widely dispersed in oceans and accumulation takes place in gyres (Law et al., 2010; Pichel et al., 2007). An European coastal submarine study by Pham et al. (2014) showed that plastics – even buoyant polymers – are also accumulating on the sea floor, especially in submarine canyons.

The first encounters between animals and marine debris were reported in the 1960's and since then have been increasingly reported. The number of animals affected has also been increasingly reported. (Gall & Thompson, 2015). Ingestion of plastics, entanglement in plastics and the presence of adhered pollutants can cause physical harm to marine wildlife, at every level of the food web (Derraik, 2002; Moore, 2008; Wright, Thompson & Galloway, 2013).

In previous decades, most research on synthetic polymers focused on large (visible) fragments like fishing nets, household materials, packages and industrial pellets due to the observable physical effects (Wright et al., 2013). However, smaller (microscopic) particles are of growing interest and concern due to their uptake by smaller marine life, their possible transfer into the human food chain and possible additional negative physical-chemical effects (Rocha-Santos & Duarte, 2015; Setala, Fleming-Lehtinen & Lehtiniemi, 2014). These smaller microscopic polymers are referred to as microplastics. Their characterization is explained in the following subsection.

1.2 **The distinction of the size, shape and origin of microplastics**

Plastics entering the marine environment are - based on their size - divided into three groups (Arthur, Baker & Bamford, 2009; Leslie, Van der Meulen, Kleissen & Vethaak, 2011).

1) Macroplastics   : polymer products and parts of this, larger than 5 mm.
2) Microplastics   : polymer particles between 100 μm and 5 mm.
3) Nanoplastics   : polymer particles beneath 100 μm.

In literature the boundaries of microplastics (MPs) are not uniformly set. Some authors divide them into just macro size and micro sizes. Practical factors such as mesh sizes used for probing may also lead to different boundaries. Due to the sampling method in this study, whenever MPs are addressed in this report, they range from 125 μm up to 5 mm. Furthermore, in addition to their size distinction, MPs are based on their origin arranged in two groups: primary MPs and secondary MPs (Arthur et al., 2009; Cole, Lindeque, Halsband & Galloway, 2011):

Primary MPs are intentionally produced either for direct use or as precursors to other products . Examples include pre-production plastic pellets, industrial abrasives and exfoliants (i.e. skin scrubbers).

Secondary MPs are formed from the breakdown of originally larger plastic materials. Often, polymer degradation is a combination of abiotic and biotic mechanisms (Beyler & Hirschler, 2001; Eubeler, Bernhard & Knepper, 2010; Lucas et al., 2008) such as:

a) Light degradation by UV-radiation.
   The energy carried by photons can cause instability in the polymer chemical bonds and hence damage the original macromolecular structure.

b) Chemical degradation.
   Atmospheric pollutants and agrochemicals may interact with polymers changing its polymer properties. Free radicals originating from atmospheric oxygen (O_2, O_3) are known to attack covalent bonds and cause cross linking reactions and/or polymer chain scissions. Hydrolysis can occur on covalent bonds between the polymer backbone and functional groups such as ester, ether, anhydride, and ester amide (urethane). Hydrolysis depends on various factors such as the type of chemical bond, pH, temperature, salinity, pressure and water uptake.

c) Mechanical degradation.
   Compression, tension and/or sheer forces may lead to embrittlement, cracking or breaking. Examples are numerous, like car crashes, fibre loss during washing of clothes, abrasion against rough surfaces, waste shredding, wind force, snow force, and coastal ground swell.

d) Thermal degradation
   The loss of physical, mechanical or electrical properties under influence of heat is called thermal degradation . For synthetic polymers, the associated temperatures are not easily achieved under environmental conditions. However, thermal degradation may have occurred prior to emission to the environment.

e) Biotic degradation.
   Specific (groups of) bacteria and fungi are - often as a successive step after one or more of the above processes - able to break down the macromolecular structure of the polymer with enzymes or secreted products. Oligomers and monomers can enter the cell cytoplasm in which mineralization leads to further breakdown for use as sources of energy, electrons and cell structure elements (i.e. carbon, nitrogen, oxygen, phosphorus, sulphur). Biotic degradation processes are mainly studied under laboratory conditions in dry form, or mixed with soil. The great number of possible natural parameters in aqueous media cannot be entirely reproduced and controlled. Biotic degradation in aqueous media, especially in salty surroundings, occurs most likely at a slower rate.

MPs come in numerous forms of shapes. Due to this, for their clarification, different nomenclatures are used, such as: cylindrical, flat, ovoid, spheruloid, rounded, subrounded, subangular, angular, irregular, elongated, degraded, rough, broken edges, fibre (Hidalgo-Ruz, Gutow, Thompson & Thiel, 2012).

1.3 The uptake, transfer and effects of microplastics

In 2014, Ivar do Sul and Costa (2014) reviewed 37 studies on the uptake of MPs, of which 26 by vertebrates and 11 by invertebrates. The number of reports however is still growing. The reviewed studies include species from the whole sea water column and comprise both small and large species. Examples of benthic and demersal species demonstrating to ingest MPs are: marine algae (*Scenedesmus*), marine ciliates (*Strombidium sulcatum),* scleractinian corals (*Dipsastrea pallida),* lugworms (*Arenicola marina),* sea cucumbers (*Holothuria floridana),* lobsters (*Nephrops norvegicus*), blue mussels (*Mytilus edulis*), red gurnard (*Aspitrigla cuculus),* dragonet (*Callionymus lyra*), redband fish (*Cepola macrophthalma),* solenette (*Buglossisium luteum)* and thickback sole (*Microchirus variegates*).

Examples of pelagic fish species demonstrated to ingest MPs are whiting (*Merlangius erlangus),* blue whiting (*Micromesistius poutassou,) A*tlantic horse mackerel (*Trachurus trachurus),* poor cod (*Trisopterus minutes)* and John Dory (*Zeus faber).* Drifting Meso zooplankton demonstrated to ingest MPs are *Echinoderm* larvae, *calanoid copepods and chaetognaths.* (Lusher, McHugh & Thompson, 2013; Wright et al., 2013)

Natural uptake of MPs by marine life
The natural uptake of MPs is demonstrated by studying field collected samples, such as: 1) Common periwinkles (*Littorina littorea*), 2) Amphipods (*Gammarus sp.*), 3) Pacific oysters (*Crassostrea gigas) and 4)* Blue mussels (*Mytilus edulis*) (Leslie, Van Velzen & Vethaak, 2013). In the latter, no particles were found in field collected crabs (*Carcinus maenas)*.

The transfer of MPs within food webs
The natural transfer of MPs through the food web has not been demonstrated yet. Laboratory experiments by Farrell and Nelson (2013) showed the trophic transfer of 0.5 µm PE particles from mussels *Mytilus edilus* to crabs *(Carcinus maenas)* and Setala et al. (2014) demonstrated the transfer of ingested MPs from meso zooplankton to macro zooplankton (i.e. the mysid shrimp *Neomysis integer*). The presence of microplastics in myctophid fish guts on one hand and Hooker's sea lion and fur seal scats on the other, suggest the microplastic transfer through this pelagic food chain: zooplankton -> myctophid fish -> Hooker's sea lions/fur seals (Wright et al., 2013).

The transfer of MPs within the human food chain
The transfer of MPs to humans has also not been proven yet, but the transfer may be likely as marine biota like mussels, oysters and common periwinkles can be part of human diet. In medical science, small polymeric particles are widely studied as drug delivery carriers for at least two decades (Andrianov & Payne, 1998). In a laboratory setting, Wick et al. (2010) demonstrated that PE spheres with diameters of 50, 80 and 240 µm are capable of transplacental transfer in humans. PE microspheres were found capable of entering the gastro-intestinal tract of humans, after which they can spread via the lymphatic and cardiovascular systems (Hussain, Jaitley & Florence, 2001).

The effects of microplastics on marine wildlife
A rapidly growing number of experiments show that MPs can induce negative effects on smaller marine life after ingestion or uptake. Also here, these studies are in situ based and the concentrations used exceed those (yet) reported in the environment. Non-exhaustively, examples of negative effects found in the literature are:

- Reduced photosynthesis, oxidative stress and growth limitation to the green algae *Scenedesmus* (Besseling, Wang, Lurling & Koelmans, 2014; Bhattacharya, Lin, Turner & Ke, 2010).
- Tissue inflammation in the mussel *Mytilus edulis L.* (Von Moos, Burkhardt-Holm & Kohler, 2012).
- Influences on growth, mortality and neonate production of *Daphnia magna* and malformations to its neonates (Besseling et al., 2014).

Not all experiments show negative effects. Kaposi, Mos, Kelaher and Dworjanyn (2014) fed PE microspheres to larvae of the sea urchin (*Tripneustes gratilla*) and found a small nondose (i.e. not proportional to the amount of particles fed) effect on growth, and no significant effect on survival. The highest environmental concentration found up to date, 0.1 MP particle per liter (Noren & Naustvoll, 2010), appeared to have no effect at all.

Microplastics as pollution carriers
Apart from physical harm, additional toxicological risks may arise from pollutants that are present in, or at, MPs. As polymers are hydrophobic, in aqueous surroundings hydrophobic pollutants prefer to adhere to polymer particles present, rather than to dissolve in water. Field collected PE and PE samples in the North Pacific Gyre (Rios, Moore & Jones, 2007) and field collected PE samples at the San Diego, California beach (Van et al., 2012), showed increased concentrations of polycyclic aromatic hydrocarbons (PAH), polychlorinated biphenyls (PCB), dichlorodiphenyl-trichloroethane (DDT) and aliphatic hydrocarbons.

1.4 **The presence of microplastics in rivers**
Rivers are increasingly being seen as carriage systems for land-based originated MPs to the seas (Hidalgo-Ruz et al., 2012; Wagner et al., 2014). Several emission routes leading to the presence of MPs in freshwater ecosystems are acknowledged (Habib, Locke & Cannone, 1998; Verschoor, De Poorter, Roex & Bellert, 2014):

Examples of land based emissions of MPs into fresh water systems:
- Industrial and domestic sewage overflows discharge unfiltered or partly filtered sewage water.
- Remote households not being connected to collective sewage treatment plants (STP)
- The running-off of MPs from STP sediments, that in the past were used as soil fertilizer.
- MPs being blown away from land to surface water during transport, from adjacent construction sites or from polymer factory facilities.
- The shattering of agriculture plastics or disposed packages during road side or agriculture mowing.

The number of studies on plastic litter and MPs in rivers is gradually growing. European studies comprise amongst other the Thames (Morritt, Stefanoudis, Pearce, Crimmen & Clark, 2014), the Danube (Lechner et al., 2014) and the Meuse (Kroes, Tweehuysen & Löhr, 2014; Van Paassen, 2010). Regarding the Rhine, the abundance of microplastics were studied in the Rhine-Mainz area (Klein, Worch & Knepper, 2015) and the Dutch Rhine estuary (Leslie, Van Velzen & Vethaak, 2013).

Policy makers are called upon to classify plastic waste as hazardous (Rochman et al., 2013) and are also called to focus more on finding preventive measures than to search for more evidence on the factual fates and effects of plastics in the environment. Assuming that rivers are contributing to MP pollution of the seas, monitoring programs would help to understand and regulate the processes that lead to the marine pollution with MPs. However, to date nor for fresh, nor for saline water systems legal obligations are determined for water quality representatives to monitor MPs. This could change, as policy developments lie ahead.

1.5 **European legislation on microplastic monitoring**
The EU Marine Strategy Framework Directive (MSFD 2008/56/EC) has established a framework within each EU Member stating that they must act to achieve or maintain a good environmental status of their marine waters by 2020. Marine litter, including MPs, is specifically addressed.
The MSFD brings with it the incentive for water quality representatives to work towards a monitoring of MPs in their surveillance zones and to commit efforts to mitigate emissions. A Technical Subgroup on Marine Litter (TSG ML) provides support by means of technical recommendations for the implementation of the MSFD requirements for marine litter. One of their scopes includes the specification of monitoring methods for (all) litter in the different marine compartments (Galgani, Hanke, Werner & De Vrees, 2013)

Another European Directive, the European Water Framework Directive (EWFD 2000/60/EC) commits European Union members to achieve good qualitative and quantitative statuses of all water bodies, including the fresh surface waters. For rivers, the so-called river basin district plans were introduced. In these plans the communal objectives can be set, including the required time limits to meet these objectives. In the prevailing plans ranging from 2009-2015, MPs are not addressed (LNV, V&W, VROM en LNV, 2009; 2009a) .

Successive river basin district plans ranging from 2016-2021 for the rivers Meuse and Rhine are expected to be established at the end of 2015. A published draft version learns that MPs are just briefly addressed. In European policies however, plastic litter including MPs is pointed out as undesirable and its presence should be decreased. In spite of this, monitoring obligations nor concentrations levels have been determined so far (personal communication drs. B. Bellert, Rijkswaterstaat).

1.6 The monitoring of microplastics in the rivers Meuse and Rhine

Rijkswaterstaat is the executive branch of the Dutch Ministry of Infrastructure and Environment and has been given the task to monitor and report on the ecological and chemical status of the main Dutch water bodies. To fulfill this task, Rijkswaterstaat operates several monitoring stations along and in their fresh water bodies. With regard to the Meuse and Rhine, monitoring stations are located along the Dutch borders: at Eijsden (Meuse) and at Lobith and Bimmen (Rhine). Their geographical locations are visually presented in appendix 1. For these stations, chemical monitoring parameter targets are concentrations of heavy metals, volatile solvents, polar compounds, fluorine and ammonium. Physical parameter targets are radio-activity, conductivity, acidity, salinity and turbidity. MPs are no target parameter yet.

The physical parameter turbidity is often positively related to the abundance of chemical compounds (personal communication dr. G. Stroomberg, Rijkswaterstaat). Turbidity stands for the amount of suspended matter in the river stream that comprise a mix of organic and inorganic material in different sizes, shapes and specific gravity. A deeper clarification of turbidity is included as appendix 2. The positive relation is caused by hydrophobic and metallic pollutants that become adsorbed to the suspended matter. As turbidity rises, chemical concentrations can rise along.

According to Asselman (1999) and Doomen, Wijma, Zwolsman and Middelkoop (2008), turbidity is often positively related to the discharge rates of the Meuse and Rhine. As a river discharges more water, the energy to carry suspended matter increases. Varying discharge levels can cause sediment to be deposited and re-suspended in time intervals. MPs in the water column can be regarded as suspended matter as well. It is unknown whether a positive relation between MP particle concentrations and turbidy levels exists.

1.7 Main objective and research questions

With regard to the rivers Meuse and Rhine, the presence of MPs was already demonstrated. However, their abundance, their nature and temporal variations are still largely unknown. With possible monitoring obligations in sight, Rijkswaterstaat would like to investigate the possibilities and the obstacles that can be encountered with sampling MPs in current rivers. The main aim of this MSc project to study whether the stationary monitoring stations at Eijsden, Bimmen and Lobith can facilitate a future monitoring program for MPs in the rivers Meuse and Rhine.

Main objective
This research aims at developing guidance for a monitoring program in the rivers Meuse and Rhine to determine abundance, composition and behavior of microplastics. Five research questions were formulated to help support the main objective.

Research question 1.
Is it possible to quantitatively determine microplastic concentrations in rivers? Which factors are involved?

Research question 2.
Are the present monitoring locations at Lobith, Bimmen and Eijsden suitable when it comes to quantitatively and qualitatively measuring microplastics? Under what conditions can they be included in a future monitoring program?

Research question 3.
Do the rivers Meuse and Rhine differ with regard to the abundance and composition of microplastics?
Is it possible to point out sources?

Research question 4.
What is the temporal variation in abundance and composition of microplastics in river water?

Research question 5.
Is there a relationship between the abundance and composition of microplastics on one hand, and discharge and turbidity of the river water on the other?

1.8 **Structure of this report**

To help answering the research questions, the methods for sampling, laboratory processing, quantitative analysis and qualitative analysis were written out beforehand. However, as developing guidance was the main objective of this study, during the project new approaches were tested and the methods were altered at some occasions. For this reason the Method section is split into four successive chapters:

- Chapter 2: Methods for sampling and the collection of samples (page 7).
- Chapter 3: Methods for laboratory processing (page 12).
- Chapter 4: Methods for quantitative analysis: microscopy and sampling targets (page 18).
- Chapter 5: Methods for qualitative analysis (page 21).

The used methods and the method improvements are discussed in the associated chapters. Aspects that are directly related to the research questions, are being discussed in the final discussion chapter (chapter 9, page 70) and conclusion chapter (chapter 10, page 75) .

With regard to the results, the qualitative aspects, which include MP characteristics such as shapes and compositions, are discussed first in chapter 6 (page 25). After this the quantitative results, which adress the abundance and their associated weights, are discussed in chapter 7 (page 52).

2. Methods for sampling and the collection of samples

2.1 Building up a method strategy: several pilot runs

In extensive reviews by Hidalgo-Ruz et al. (2012), Rocha-Santos and Duarte (2015) and Eerkes-Medrano, Thompson and Aldridge (2015) can be read that with regard to MP sampling, up to date basically two methods are being used:

- Neuston/zooplankton nets that are being towed by a boat or fixed to a stationary object.
- Sediment collection from beaches or estuarine shores.

Due to the fact that the monitoring stations have a permanent water inlet, and that several options to tap river water are present, a soil sieve method was proposed. In the literature, however, sampling MPs with soil sieves was not reported before. Also, at the monitoring stations themselves, no practical insights on the proposed method were available. For this reason, before the actual start of this research, in the second half of 2013 several pilots were run at each of the monitoring stations. The pilot details are presented in appendix 3. The insights obtained in these pilots were used for the development of the sampling method that is written out in this chapter.

2.2 Sampling locations: monitoring stations

In relation to the rivers Meuse and Rhine, one pontoon is berthed in the river Meuse at the east river bank at Eijsden, which is closely to the Dutch-Belgium border. In the Rhine, at the Dutch-German border, a pontoon is berthed at the north river bank at Lobith. At Bimmen, which is at short distance to Lobith but situated on the opposite river bank, an onshore laboratory is present. This onshore laboratory is a cooperation between Rijkswaterstaat and the Landesamt für Natur, Umwelt und Verbraucherschutz Nordrhein-Westfalen, Germany (LANUV). A fourth shore-based monitoring station situated on the right bank of the river Rhine at Bad Honnef, which is located in Germany 240 km upstream to Lobith, is briefly addressed in this study. The characteristics of the Meuse and Rhine are described in chapter 8.1. River contour maps near to Lobith/Bimmen (Rhine) and Eijsden (Meuse) are presented in appendices 7 and 8.

Lobith and Eijsden

The monitoring stations Eijsden and Lobith are two similar pontoons (figure 1). The pontoons are stabilized in a sense that they can move vertically along two bollards to follow changing water levels, but they are fixed horizontally. Water was taken in permanently at a depth of -0.80 meters under water surface. An electric centrifugal pump in the underwater part of the pontoon draws water in at a rate of 30 m^3 per hour. Unused water is released at the other end. In between the inlet and the outlet, several output taps along the pipe provide river water for measuring and research purposes.

Figure 1. Monitoring station at Lobith (Rhine). The station at Eijsden is similar. Water is taken in permanently by the yellow crane jib and released at the other front. Several taps are available for analytical purposes, of which one was reserved for this study on microplastics.

Bimmen and Bad Honnef

The monitoring stations at Bimmen and Bad Honnef are shore based laboratories to monitor Rhine river water. Bad Honnef lies 240 Rhine kilometer upstream of Bimmen and approximately 20 kilometers upstream the city of Bonn (Germany). Consequently Bad Honnef also lies upstream of the large industrial Ruhr region. At both Bimmen and Bad Honnef river water was taken in by an eccentric screw pump and transported via a pipe system to the labs. At Bimmen the pump rate and the transport distance between inlet and onshore laboratory are 28 m^3/h and 200 meters. For Bad Honnef these figures read 25 m^3/h and 100 meters.

The inlet of Bimmen is (similar to Lobith and Eijsden) fixed at -0.80 m under the surface. At Bad Honnef however, the inlet is fixed at the river bottom (plus 1.20 meter). For the latter, the inlet depth depends on the river discharge. The actual depth during sampling is not exactly known; the personnel at the laboratory estimated it at 3 to 4 meters below the surface. The details of the monitoring stations used in this study are presented in table 2.

Table 2. Summary of monitoring stations where MPs were collected, including their position and inlet characteristics. Except for Bad Honnef, the stations are situated along the Dutch border. Except for Bad Honnef, a weekly sampling series was exerted. River km express the distance along the river stream.

River	Station	Kind of station	River km	River bank	GPS-coordinates	Inlet depth (under surface)	Pump type C/E	Intake rate (m³/h)	MPs sampling frequency
Meuse	Eijsden (NL)	Pontoon	Meuse km 2.5	Right	N 50.779377° E 5.699805°	-0.80	C	30	Weekly
Rhine	Lobith (NL)	Pontoon	Rhine km 861	Right	N 51.851230° E 6.098189°	-0.80	C	30	Weekly
Rhine	Bimmen (GE)	Onshore lab	Rhine km 864	Right	N 51.859921° E 6.067801°	-0.80	E	28	Weekly
Rhine	Bad Honnef (GE)	Onshore lab	Rhine km 640	Left	N 50.630452° E: 7.214981°	-3.00 (estimated)	E	25	Single sample

C: centrifugal pump
E: eccentric screw pump

2.3 Sampling materials

Taps from the water intake systems were made available for the present research. A ball valve on each tap offers the possibility to adjust the flow rates to the desired level. Three Ø20 cm, ISO 3310-1 standardized metal cloth soil sieves, flange height 5 cm each, were placed under the tap. Sieved water could pass through a hole in the tableau. The mesh sizes were arranged from top to down: 1 mm, 0.25 mm and 0.125 mm. Wooden spacers were placed between the 0.125 mm and 0.250 mm sieve, so that if the smallest sieve got clogged, water could run out freely without influencing the upper two sieves. The sieve set up is displayed in figure 2.

Figure 2 Three stacked sieves with descending mesh sizes were used to filter microplastics out of plain river water.

2.3.1 Sampling series

From January 10th 2014, up to May 26th 2014, a series of 17 weekly samples were taken at each of these monitoring locations: Eijsden (E), Lobith (L) and Bimmen (B). For the sampling a measuring protocol was provided to the laboratory staff. Additionally, at May 20th one sample was taken at Bad Honnef (BH).

Each sample is seen as unique. Each monitoring station has its own abbreviation (E, L, B, BH) and successive sample series were numbered upwards. Sampling was planned for 72 hours, starting on Friday morning and completing on Monday morning, under comparable conditions regarding tap flow rate, and duration. In some cases sampling could not be continued as no sieves were available or due to pump system maintenance. For samples E1, E2, B1, B2, L1, L2 (further E1 to L2), between January 10th up to February 6th, only 1 stack of sieves was available. Measurements starting with series 3 (further E3 to B17) were synchronized.

In table 3, the sampling details are shown. For the overview yellow lines indicate Eijsden, blue ones indicate Lobith and green ones indicate Bimmen. The single sample at Bad Honnef is purple.

Table 3 Overview of microplastics sampling details at Eijsden (E), Lobith (L), Bimmen (B) and Bad Honnef (BH). The sample duration was recorded at the sampling location. The sieved volume was calculated by multiplying the average tap flow (not shown) with the duration of the sampling. The river discharge and turbidity were recorded during sampling, here the average values over the sampling period are shown.

Location	Nr	Start Date	End Date	Duration (hours)	Sieved volume (m³)	Upper sieve 1.0 mm	Middle sieve 250 µm	Bottom sieve 125 µm	Average discharge (m³/s) during sampling	Average turbidity during sampling
Eijsden	E1	10/01	13/01	68.0		Flushed	Clogged	Clogged	517	25
Lobith	L1	13/01	16/01	70.5	49.4	Whole	Whole	Whole	2512	25
Bimmen	B1	20/01	22/01	44.0	43.4			Clogged	2224	11
Eijsden	E2	29/01	31/01	48.5	46.9			Clogged	505	23
Lobith	L2	24/01	27/01	69.0	55.1	Whole	Whole	Whole	2109	11
Bimmen	B2	3/02	6/02	69.0	60.5	Lost	Lost	Lost	2102	15
Eijsden	E3	14/02	15/02	21.0		Flushed	Clogged	Clogged	630	27
Lobith	L3	14/02	17/02	72.5	55.5				2631	22
Bimmen	B3	14/02	17/02	71.0	61.0			Clogged	2677	24
Eijsden	E4	21/02	24/02	72.0	45.8				463	20
Lobith	L4	21/02	24/02	72.0	56.3				2721	38
Bimmen	B4	21/02	24/02	72.0	62.5				2695	36
Eijsden	E5	No sample	No sample	No sample	No sample	No sample	No sample	No sample	No sample	No sample
Lobith	L5	28/02	3/03	71.5	53.7	N.p.	N.p.	N.p.	2082	13
Bimmen	B5	28/02	3/03	72.0	54.7			Lost	2083	13
Eijsden	E6	7/03	10/03	73.0	46.8				263	8
Lobith	L6	6/03	9/03	72.0	56.4				1923	8
Bimmen	B6	6/03	9/03	72.0	58.2				1918	8
Eijsden	E7	14/03	17/03	73.5	46.3				187	4
Lobith	L7	14/03	17/03	72.0	56.3				1561	7
Bimmen	B7	No sample	No sample	No sample	No sample	No sample	No sample	No sample	No sample	No sample
Eijsden	E8	21/03	24/03	72.0	46.7				167	3
Lobith	L8	21/03	24/03	72.0	58.9				1401	9
Bimmen	B8	21/03	24/03	70.5	58.4				1400	9
Eijsden	E9	No sample	No sample	No sample	No sample	No sample	No sample	No sample	No sample	No sample
Lobith	L9	28/03	31/03	72.0	54.0			Lost	1539	8
Bimmen	B9	28/03	31/03	72.3	55.5			Clogged	1538	7
Eijsden	E10	4/04	7/04	72.0	44.8				113	3
Lobith	L10	4/04	7/04	71.5	53.6				1318	11
Bimmen	B10	4/04	7/04	72.0	63.3			Clogged	1317	11
Eijsden	E11	11/04	14/04	72.0	44.6				101	3
Lobith	L11	11/04	14/04	72.0	58.9				1257	15
Bimmen	B11	11/04	14/04	72.0	64.8			Clogged	1259	14
Eijsden	E12	18/04	21/04	72.0	46.2				85	3
Lobith	L12	18/04	21/04	71.0	53.3				1202	15
Bimmen	B12	18/04	21/04	69.0	59.1				1200	15
Eijsden	E13	25/04	28/04	72.8	46.7	N.p	N.p	N.p.	88	3
Lobith	L13	25/04	28/04	71.8	50.7	N.p.	N.p.	N.p.	1179	19
Bimmen	B13	25/04	28/04	72.3	53.1	N.p.	N.p.	N.p.	1179	19
Eijsden	E14	2/05	5/05	72.0	46.3				78	2
Lobith	L14	3/05	6/05	73.0	59.7				1656	15
Bimmen	B14	3/05	6/05	70.0	51.5				1666	15
Eijsden	E15	9/05	12/05	72.0	46.6				151	3
Lobith	L15	9/05	12/05	72.0	63.3				1872	13
Bimmen	B15	9/05	12/05	72.0	51.4				1874	13
Eijsden	E16	16/05	19/05	72.0	45.2	N.p.	N.p.	N.p.	97	1
Lobith	L16	16/05	19/05	72.0	51.8	N.p.	N.p.	N.p.	1829	12
Bimmen	B16	16/05	19/05	72.0	66.6	N.p.	N.p.	N.p.	1833	12
Eijsden	E17	23/05	26/05	72.0	46.0			Lost	82	2
Lobith	L17	23/05	26/05	72.0	58.9				1568	23
Bimmen	B17	23/05	26/05	72.0	51.8				1565	22
Bad Honnef	BH	20/05	21/05	13.0	10.4				n.d.	n.d.

Clogged	: water could not pass through the metal cloth bed, resulting in overflow.
Whole	: the sample was not split into small size and the large size fractions.
Flushed	: the middle sieve clogged, leading the upper sieve to overflow.
No sample	: no sieves were available or no set up was possible due to maintenance of the pump system.
Lost	: sample was lost during laboratory processing
N.p.	: not processed; sample is stored
N.d.	: not determined

Determination of the volume sieved
Just prior to and directly after sampling the tap flow rate was determined by measuring the time needed to fill a standard volume. At Eijsden, Lobith and Bad Honnef a 5 liter measuring cup was used, for Bimmen a 10 liter bucket with ticks. The flow rate at the start and at the end were averaged and used to estimate (calculate) the amount of river water that was sieved.

A data registration form was used to accompany the sieve sets during transport and to submit the following sample characteristics:
- Dates and times of start and finish.
- Tap flow rates at both start and finish.
- Discrepancies pertaining to the sample protocol (like deviations in sampling time, a maintenance stop or clogging sieves).

Desired tap flow rate
At the start of the project, the tap flow rate was set to approximately 800 liters per hour. Due to consecutive clogging problems at Eijsden with sampling series E1, E2 and E3, the tap flow rate at Eijsden was reduced to approximately 600 liters per hour. For Lobith and Bimmen the flow rate remained unchanged.

Blank control
The aim of this study is to filter exclusively MPs from river water. To see whether MPs could have landed on the sieves by another route, one set of sieves was set up at Bimmen, next to the tap, for a period of 24 hours.

2.4 Sample transport and collection of samples from the sieves
The phrase sample collection is used to describe the method by which the samples were taken from the sieves. Sampling was carried out at the monitoring stations, but sample processing took place in a laboratory. For this, the samples were transported from the monitoring stations to the laboratory facilities. For better understanding of this subsection it is important to know that the samples E1 up to B2, and all the other succeeded samples (i.e. E3 up to B17 and the Bad Honnef sample), were collected by two different procedures. The contents on the three sieves of E1 up to B2 were combined. As it was noticed that possibly detailed qualitative information might become lost by following this method, were the contents of the other samples split into two size fractions, as is described below.

Samples E1 up to B2
Samples E1 up to B2 were collected at the monitoring stations. Here, with a gentle stream of purified water from a tap with flexible hose, the contents of the upper two sieves were washed onto the bottom sieve (0.125 mm). The combined contents were washed with pure analytical grade water (milliQ) from wash bottles above a glass funnel that was placed in an empty and clean 250 ml PE bottle. This resulted in one combined sample and are marked as 'whole' (see table 3). As these contents were still wet during collection; scraping the contents was not necessary. Before removing the funnel, the inside and the outside of the funnel tube were rinsed inside the bottle. To avoid cross contamination, the funnel and scoop were cleaned under the tap before using it again. Samples E1 up to B2 were transported under environmental conditions, and stored under refrigerated conditions (4ºC), before processing.

Samples E3 up to B17 and the Bad Honnef sample
All other samples, which are E3 up to B17 and the Bad Honnef sample, were collected at the central laboratory of Rijkswaterstaat at Lelystad. Directly after sampling, the sieve sets were covered by a receiver below and a cover lid on top and placed in sample transport containers. Pre-mounted rubber rings provided seals in between the receiver, cover lid and the sieves which avoided contamination or sample loss during transport. Samples E3 up to B17 and the Bad Honnef sample were stored and transported under refrigerated conditions (4ºC), before processing.

At the laboratories, a gentle stream of purified water was obtained from a tap with a flexible hose. First, the material on the sieve bed was soaked to loosen any dried material from the metal wire cloth. A metal spatula was used to help directing the contents towards the sieve edges. Then the hose was used to gently rinse the contents of the upper sieve on top of the middle sieve. A glass funnel was placed in an empty and clean 250 ml PE bottle on which the majority of the material was transferred with a metal scoop into the funnel. The metal cloth was rinsed twice again by using wash bottles, while directing the remaining contents to the sieve edges and gently rinsing them above the

funnel. The scoop and the funnel were rinsed inside the bottle. To avoid cross contamination, all materials were cleaned before using it for the other fraction or another sample.

The contents of the bottom sieve were washed into a separate 250 ml PE bottle, following the same procedure as described above. As a result of this, two size fractions were obtained:
    1) 0.250 mm – 5 mm   (also: the large size fraction)
    2) 0.125 mm- 0.250 mm   (also: the small size fraction)

All bottles were marked with the associated unique sample numbers and size fractions.

2.5 Discussion on the method of sampling

This study demonstrated that at the considered monitoring stations, with little effort and simple materials, MPs could be sampled from the rivers Meuse and Rhine. It also brought forth some additional insights that deserve to be discussed.

For sampling, metal wire cloth sieves were used. A detailed view under the stereomicroscope learned that the meshes have a square shape, which means that the space is not congruent in all directions. Regarding the 250 micron sieve, measurements range from 238 µm (horizontally) via 263 µm (vertically) up to 345 µm (diagonally). The 125 µm sieve ranges accordingly from 114 µm, 131 µm and 161 µm. Depending on the individual shapes, this could result in the risk of target MPs escaping through the mesh without being noticed, especially fibres, with their strong length-width ratio. On the other hand, deposited organic or inorganic material could form a blockade to MPs yet smaller than the target size. It is supposed that neuston nets encounter similar disadvantages and it is thereto concluded that precise under or upper size limits for MPs sampling are difficult to achieve.

The sample set up was not tested on the possible loss of MPs during sampling. Possibly the descending tap water can cause sample material to splatter over the top sieve edge. For further sampling it is suggested to put an additional sieve on top, for example 8 mm square, which additional flange height declines the risk of material being splattered over the sieve edge.

In this study, the tap flow rate and the sampling duration were set random arbitrarily. A weekly 72 hour sampling series covers 40% of the time and was chosen to level temporal variations in MP abundance in the rivers. At several occasion this method yielded more particles can could be processed within one week. It is suggested to study the temporal variation on a shorter interval basis, using a new series of measurements at the monitoring stations, to study the temporal variation between these shorter intervals.

3. Methods for laboratory processing

Samples E1 to B4 were processed and studied at the Department of Ecological Science, Faculty of Earth And Life Sciences, VU University, Amsterdam. Samples E5 to B17 and the Bad Honnef sample were processed and studied at the central laboratory of Rijkswaterstaat located at Lelystad. The method of laboratory processing is described in the successive subsections.

Unless pointed out otherwise in this chapter, milliQ is obtained from unique wash bottles that were newly purchased and only used for this study. All laboratory processing is carried out under a fume hood and for heating up of samples a Schott electrical heating plate was used.

3.1 Hot digestion with hydrogen peroxide

In the laboratories, the PE 250 ml bottles containing the MP samples were shaken and the contents were decanted into 250 ml glass, Teflon (PTFE) or Perfluoroalkoxy alkane (PFA) beakers. The PE bottles and the caps were washed above the beakers three times with milliQ. This resulted in an aqueous solution. Samples that visibly contained organic material were subject to digestion. Samples that showed a clear solution were not digested but directly subjected to density separation (as described in 3.2.2).

The beakers were marked with the sample characteristics read on the bottles and placed on a heating plate under a fume hood. The contents were heated up to 85-95°C (exact temperature could not be determined) to concentrate the sample. When almost all the water had evaporated, the sample was digested with hydrogen peroxide (H_2O_2, 35%), still remaining on the heating plate at 85-95°C. Aliquots of 10 ml H_2O_2 were flushed along the beaker wall with a 10 ml pipette without actually touching the wall. An aliquot of H_2O_2 was added as soon as the reaction responses in the beaker faded out. The number of aliquots of H_2O_2 were not recorded as digestion depended heavily on the amount of organic material in the sample. Indicatively, in between one and 15 aliquots were used per sample, with an estimated average of 10.

3.2 Successive cold and hot digestion

All samples up to E13 were heated up on heating plates till approximately 80-95 °C (exact temperature could not be determined). This was for two reasons:
- To evaporate water, as higher H_2O_2 concentrations increases the oxidation reactions.
- Adding heat (i.e. energy) increases oxidation reactions.

Warming up however, showed some disadvantages as well: First, warming up can increase oxidation reaction. As a result bubbles can rise up, overflow the beaker and cause a loss of particles.
Second, warming up increases the risk of samples drying up inside the beaker. As soon as all liquid is evaporated, the buffering effect of the liquid is gone and contents may be warmed up to temperatures that can induce thermal degradation.

In an experiment the heat supply step was omitted. The PTFE beakers were placed under a fume hood and just exposed to room temperature conditions (further: cold digestion). Aliquots of 10 ml H_2O_2 were added three times a day, for a period of 8 working days. After this, the sample was processed as usual, as described in the succeeding subsections.
Microscopic analysis pointed out that with just cold digestion, considerable amounts of organic residue were still present in the sample

Directly after this observations, the beaker was placed on an electrical heating plate again and the contents were heated up to approximately 60-80 °C (exact temperature could not be determined) for four hours, adding aliquots of 7 ml H_2O_2 every hour. Oxidation reaction, i.e. the generation of gas bubbles, was observed. Microscopic study showed significantly less organic remnants.

> Conclusions:
> - Heat supply can cause a risk of losing particles due to instantaneous reactions of H_2O_2.
> - Cold digestion with H_2O_2 may lead to less distinctiveness during microscopic study as not all organic material gets digested.
> - Successive cold and warm H_2O_2 digestion tends to offer a fair compromise between sample weight loss risk and distinctiveness during microscopic study.

For samples B14, and all successive samples that visibly contained organic matter, the following procedure is followed. The sample material from the PE 250 ml beakers was washed into the beakers as described in subsection 3.1. After this, the beakers were not placed on an electrical heating plate but on the working floor of the fume hood. During a period of 10 working days, aliquots of 7 ml H_2O_2 were added three times a day. After this, the beaker was placed on a heating plate, 25 ml H_2O_2 was added and the contents were heated up to approximately 60-70ºC (the exact temperature could not be determined). Aliquots of 7 ml were added once an hour, to a maximum of four times. This time path is rather arbitrarily chosen: when directly starting in the morning, the afternoon could be used for microscopic study.

3.3 Digestion with Nitric acid
After the H_2O_2 digestion step, samples E1 up to L3 were successively digested with Nitric acid (HNO_3, 65%) to remove possible inorganic remnants. As soon as H_2O_2 did not cause any visible reaction anymore, one aliquot of 7 ml HNO_3 was added. The sample was left on the heating plate for one hour at approx 85-95°C (the exact temperature could not be determined).

Starting with series E4, the acidification step was omitted because of a probable damaging effect to MPs. This is demonstrated by an acid destruction test described in appendix 4. However the procedure in the acid destruction test is not similar to the procedure described above, it cannot be excluded that acids are affecting any present MPs.

3.4 Density separation in a saline solution
The MPs samples that were collected from the sieve mostly contained sand particles. Density separation in saline water (NaCl saturated: density 1.2 g/cm^3) is commonly used to separate most MPs from sediment particles (Hidalgo-Ruz et al., 2012). It is known that some polymer types are denser than NaCl saturated water, such as PVC (up to 1.58 g/cm^3) and PET (up to 1.45 g/cm^3). For this reason, both the floated and the settled part were studied under the microscope (section 4).

Directly after the digestion step, samples were decanted above a 200 ml glass PTFE or PFA graduated cylinder. Then the beaker was washed three times above the cylinder with saline water and the graduated cylinder was filled with saline water till 1 cm under the top. The mixture was left to equilibrate for at least one hour, allowing sediment to settle, and lighter material to float.

3.5 Filtration over a micro pore filter
Density separation resulted in a floating layer and a settled layer which were both filtered separately one after the other. First the floating and possibly suspended particles were retrieved by decanting the graduated cylinder above a ø47 mm glass fibre or cellulose micro pore filter on a vacuum pump. The cylinder wall was carefully rinsed with milliQ, without disturbing the settled layer. The pump beaker was duly rinsed with milliQ to loosen material adsorbed to the pump beaker wall and to wash residues of acid and/or salt. After this, the graduated cylinder was decanted and rinsed with MilliQ above a second micro pore filter to filtrate the settled layer and remove residues of acid and/or salt.

At start, Whatman ø47 mm 0.7µm glass fibre filters were used for filtration on the vacuum pump. Starting with sample E4, they were replaced by ø47 mm cellulose micro pore filter as the latter offered advantages for microscopic analysis:
- Cellulose filters have a flatter surface, which makes picking up of particles with tweezers easier.
- Cellulose membrane filter can be brushed better, which increases distinctiveness (section 4.2.1).
- Contrary to glass fibre filters, cellulose membrane filter do not release small fibres that can influence sample weight determination.

3.6 Interim filtration step
The digestion of organic debris with H_2O_2 brought forth a brownish suspension (figure 3a) that after filtration over a micro pore filter, became a nuisance for subsequent microscopic study for several reasons:
- It covered target MPs resulting in overlooking them.
- It disguised target MPs with similar colour characteristics, resulting in overlooking them.
- It adhered to particles, disturbing secure weight measurements.

As the reaction products of H_2O_2 and organic hydrocarbons are gaseous CO_2 and H_2O, it is suggested that the brownish suspension comprise a mix of non-carbon compounds such as mineral elements and partly digested organic debris.

Experiment including a mini-sieve to investigate whether the brownish suspension could be removed without jeopardizing the present MPs in the samples.
In an experiment, during the processing of sample L5, an interim filtration step was fitted in using a Ø 0.125 mm mini-sieve, with a nylon net mesh at one side and a collector tube at the other side (figure 3b). Such a mini-sieve is commonly used to catch small marine life with a plankton net.

After the digestion step, the contents were rinsed with milliQ into a clean and empty 150 ml PFA beaker (figure 3a). Then the contents were decanted and rinsed in the collector tube of the sieve (figure 3c), allowing the brownish suspension to pass through the mesh. After this, the mini-sieve was turned upside down above another empty and clean PFA 150 ml beaker. The contents were rinsed from the sieve bed with milliQ (not shown in figure 3). The collector tube of the mini-sieve was rinsed above the PFA beaker twice to make sure that adhesive particles were rinsed as well. After this, the sample is decanted above a Ø 47 mm cellulose micro pore filter on a vacuum pump (figure 3d). Under the stereomicroscope it was observed that the brownish suspension was completely gone. Some organic remnants were present, which could be easily identified by its cellulose structures, and formed no further hindrance for identification of the MPs.
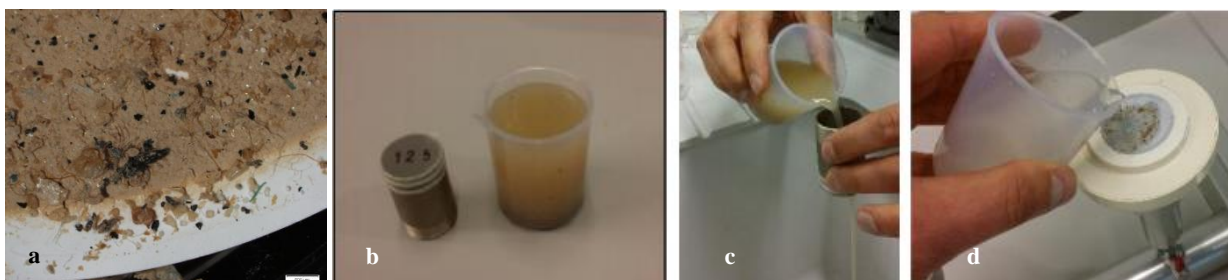

Figure 3. Illustration of the interim filtration step to remove digestion remnants from the MPs samples. The aim is to improve distinctiveness during the microscopic work. (a) An example of a clogged micro pore filter caused by the brownish suspension that remains after the H_2O_2 digestion of organic debris in the microplastic samples. Scale bar = 0.5 mm. (b) The 125 μm mini-sieve and the brownish suspension that remained after H_2O_2 digestion. (c) The suspension being led through the mini-sieve. Target MPs remained in the collector tube while fine organic debris passed through into the sink. (d) Decanting the cleared suspension over a Ø 47 mm cellulose micro pore filter.

Analysis of the mini-sieve filtrate to determine the possible loss of MPs
The general aim was to get rid of suspended matter of non polymeric origin without jeopardizing the MPs appearance. A test was performed on the filtrate of the small size fraction of sample E7. Its filtrate was not discharged into the sink (as shown in figure 3c), but the mini-sieve was placed on top of a ø 47mm cellulose micro pore filter on a vacuum pump. The filtrate that normally was discarded was now filtered over the micro pore filter and studied under the stereomicroscope. Based on visual judgement, no particles suspected to be of polymer nature were identified.

Conclusions:
- Interim filtration decreases the amount of disturbing material on the micro pore filter, among which the brownish layer that remains after organic digestion, and hence increases distinctiveness with microscopic study.
- An interim step, however, may increase the risk of losing particles. Whenever there is no organic material in the sample, an interim step is not needed.
- When applying the interim step, the mesh size of the mini sieves must correspond to the target fraction (i.e. 0.125 mm or 0.250 mm) to avoid the risk of target plastics becoming lost in the sink.

Starting with series E7, an interim filtration step with mini-sieves was included to remove the occurring brownish suspension. For each size fraction, separate mini-sieves were used (0.125 or 0.250 mm). The interim step was only attended as organic material was present in the sample and was fitted in between the digestion step and the density separation step.

Previous (earlier) processed samples were studied afterwards by washing the contents of the micro pore filters into a clean and empty 250 ml beaker and leaving it for at least one day while stirring the suspension a few times. This suspension was further processed according to the description of the interim filtration step.

3.7 Sonication to remove coal fragments

Some Meuse and Rhine samples contained black flat opaque fragments that were resistant to both H_2O_2 and HNO_3 digestion. However, during microscopic study they did not seem to resist gentle pressure between tweezers points. These black fragments are likely to be coal. A Scanning Electron Microscopic (SEM) image is included as figure 4.

Generally, if present, their appearance was a nuisance to microscopic work as they diminish distinctiveness, due to the fact that:
- Coal fragments covered target MPs.
- Coal fragments tended to stick to the tweezers.
- Coal fragments easily outnumbered target MPs, resulting in MPs being overlooked.

Figure 4. Scanning Electron Microscopic image of the surface (above) and fracture (front) of a coal sheet-like shaped fragment. Scale bar = 20 μm

An experiment to see whether sonication can be used to remove coal fragments

Microscopic study of the smaller size fraction of sample L17 revealed the presence of relatively large amounts of coal particles.
In an experiment, the contents on the filter were washed with milliQ into a 150 ml beaker and filled up to 100 ml. Then the beaker was placed in a Branson 5510 ultrasonic cleaner and sonicated for 30 minutes at full power (20 khz) without pulsation. After this, the suspension was led through a 0.125 mm mini-sieve and filtered over a cellulose micro pore filter. It could be observed that the filtrate through the mini-sieve was blackish, what was not observed earlier. Visual interpretation under the microscope demonstrated that considerably less black particles were present after sonication.

The possible deteriorating effects of sonication tot microplastics was briefly studied. This is reported in section 6.15.

> Conclusions:
> - Sonication demonstrated the ability to fracture present coal fragments to a size beneath the under limit of this study (0.125 mm). Interim filtration can be used to separate target MPs from the fractured coal.

Determining whether samples contained coal

After the digestion step, the presence of coal could be observed with the bare eye. If coal was observed, samples were filtered according to the interim filtration step (3.6), then sonicated, and after sonication, filtered according the interim filtration step again. Sonication was carried out as follows:

The contents which were caught on the mini-sieve during the interim filtration step were washed with miliQ in a 150 ml PFA beaker and filled up to 100 ml. Then the beaker was placed under the sonicator for 30 minutes at full power (20 khz) without pulsation. Then again the interim filtration step was performed. The coal fragments which were now reduced in size were able to pass through the mini sieve, resulting in considerably less coal fragments on the micro pore filter and hence increased microscopic distinction.
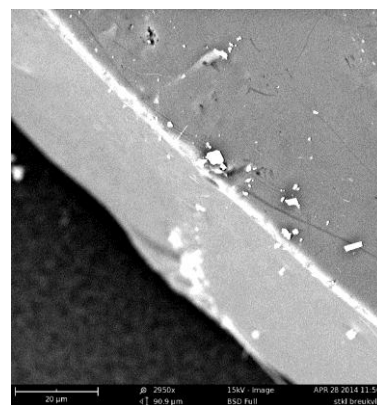
3.8 **Splitting samples**

The time needed to go through samples under the stereomicroscope differed widely. Components like sediment, organic remnants, coal fragments and the number of MPs were of great influence on the total time needed to finish samples. Therefore, starting with series L5 and based on visual inspection, samples were split in 4, 5, 6 or 8 parts. Exceptional clean samples were processed without splitting them.

Sample splitting was carried out as follows: A magnetic stirring bar was placed in an empty and clean PFA 250 ml beaker on a balance (Type: Sartorius L420S). The balance was then set to zero. The sample was added to the beaker and filled up with milliQ to a total weight of 120 grams. Then the beaker was placed on a magnetic stirring device (IKA Big Squid). Stirring started and rotation was increased until a vortex appeared (figure 5c).

Another empty and clean PFA 150 ml beaker was placed on the balance and set to zero. In steps of 7 ml, aliquots were pipetted and brought in the PFA 150 ml beaker, until the desired weight part was reached. The pipette was manually adjusted in the last step to obtain the required part.

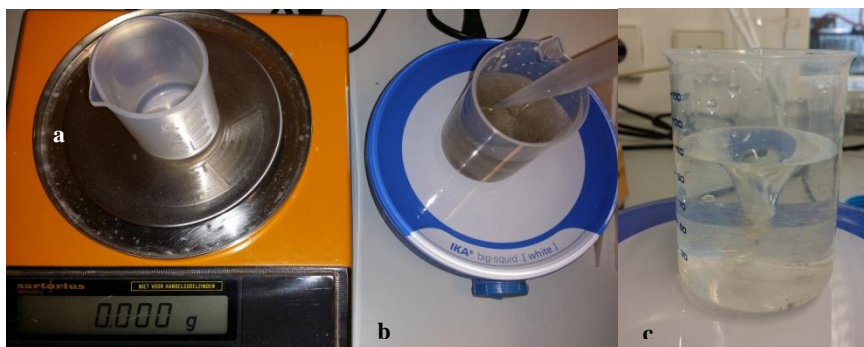The possible uncertainties that arise with sample separation on a weight basis is discussed in section 7.1.

Figure 5. Illustration of the method used to split samples into parts. (a) An empty and clean 150 ml beaker was placed on a balance which after this was set to zero. (b) The MPs sample on a magnetic stirring device to obtain a suspension. (c) A suspension obtained with a magnetic stirring bar.

3.9 **Discussion on the method of laboratory processing**

Methods to separate plastics from other material are generally based on salt water samples and sediment samples. A standardized method is not known, but repeatedly mentioned separation techniques that were also included in this study are density separation, filtration, sieving and visual sorting (Eerkes-Medrano et al., 2015; Hidalgo-Ruz et al., 2012). Processing samples from the Meuse and Rhine brought forth additional challenges, by means of the varying abundance and composition of the suspended matter that ended up at the sieve beds. Organic matter is almost any time observed and can comprise a major part of the mix. Mostly sand was noticed, regularly observed were fly ash particles and incidentally coal. Improved laboratory processing led to clearer MP samples which benefits the successive microscopic work. There are however some issues to be discussed.

In this study, most MP river samples could be processed with relative simple means: a handful of laboratory glasswork, wash bottles, a pipette, a heating plate, a magnetic stirrer, H_2O_2, MilliQ, NaCl and a small sieve. Besides glass, also Teflon and PFA laboratory were tested. Due to this, trial-and-error learned that PFA had advantages to the other two. Contrary to glass and Teflon, no sediment layer was formed at the walls, that could hold larger particles, including MPs. Also, decantation was easiest carried out with PFA, as no drops of water adhered to its wall. A disadvantage of PFA is that it is much more expensive than glass.

Heating of the samples is required to clear the MP samples from organic debris. Heating up brings with it some additional risks. It was noted that heating can bring oxidation bubbles to rise above the beaker and to overflow MPs. In addition to this, heating might also physically affect the present MPs, especially when the samples are cooked dry. For PE, degradation under atmospheric conditions is detectable above 150ºC, for PP above 227ºC and for PS above 300ºC. A polymer like PTFE, of which beakers were partly used for H_2O_2 digestion, is reported to show degradation above 477 ºC (Beyler & Hirschler, 2001). Present additives could decompose at temperatures below the polymer decomposition temperature (Lobo & Bonilla, 2003). This study has also shown that oxidizing reactions can cause sample material to become lost. Successive cold and (a shorter period of) heat digestion is suggested for future processing.

For sample clearance, an interim sieve step was tested and found useful. The used sieve was fitted with a nylon square mesh which may cause target MPs to be washed away (see also section 2.5). The presence of coal is a nuisance for microscopic work; they can easily outnumber MPs. In literature, the elimination of coal from fresh water samples was not found. Sonication is suggested, however this method may bring possible damage to MPs and jeopardize accurate measurements (see section 6.15).

4. Methods for quantitative analysis: microscopy and sampling targets

Quantitative analysis stands for the selection of MPs, based on beforehand framed selection criteria, and the recording of their numbers and associated weights. In this chapter the methods used for quantitative analysis are addressed.

Directly after filtration, the samples were studied under a stereo microscope. For series E1 to B4 a Leica M8 was used (magnification 6-50x). For the other samples an Olympus SZX12 (magnification 7-90x) and an Olympus SZH-ILLD-200 (magnification 7.5-64x) were used. All stereomicroscopes were illuminated from below, whereby additionally three adjustable cold light beams from above were used for better light conditions. All samples were only studied by the author of this thesis.

4.1 Sampling targets

During microscopic study, the recognition of MPs was actually based on visual interpretation. Criteria applied for MPs identification were:
- Insoluble in water.
- Resistant to digestion steps.
- Unnatural appearance, by means of colour or shape. In case of doubt a microbiologist specialized in fresh water biota at Rijkswaterstaat was consulted.
- Resistant to pressures between tweezer points, without crumbling and/or smearing.
- Solid but yet not able to make scratches in a plastic Petri dish or to make scratching sounds.
- Recognition of examples earlier reported in literature (spherules, scrubs, films).
- Comparison to self derived polymer examples.

Following the pilot, at the start of this study, three groups of MPs were distinguished:
1) Films   : Thin, foldable but yet hardly tearable semi-transparent sheets.
2) Spherules   : Spherical particles.
3) Miscellaneous   : Particles that appear in different characteristics like colour, shape, form.

During the study the designated groups of MPs were extended to:
1) Films   : Thin, foldable, but yet hardly tearable semi-transparent sheets.
2) White spherules   : Spherical, opaque white, cream or beige coloured particles.
3) Transparent spherules : Spherical, transparent uncoloured particles.
4) Miscellaneous   : Particles with different characteristics like colour, shape, form.

A fifth designated group is formed by scrubs.
Scrubs are described as ragged, semi-transparent, mostly uncoloured particles that are used in exfoliants and facial cleaners (Fendall & Sewell, 2009). In the first five series, they were already recognized as polymeric, but designated to the group miscellaneous. To study their particular abundance, in some occasions scrubs were distinguished as a separate group. Scrubs were isolated in both size fractions of
B6, L7, L11, B15, L15, B17, L17, E6 and E10. Scrubs were also isolated in the large size fraction of B5, L9, B9, B11, E2, E7 and E17.

Microscopic study also revealed the presence of a group of spherical particles that were not of polymeric nature, but belong to the group of aluminosilicates. This group of so called cenospheres are discussed in detail in subsection 6.8.

4.1.1 Fibres exclusion

Fibres, like nylon remnants from clothing, are generally found in MPs surveys. They were, however, excluded from this study as is explained here. Fibres are characterized by a very small diameter compared to their length. It would be likely that during sampling, the descending water would realign fibres on the filter bed repeatedly leading them to slip through the metal cloth sieve bed in its length position. Besides, in their study on North Sea fish guts, Foekema et al. (2013) concluded that in a regular (read: no ultra clean) environment, airborne fibres from the surroundings could land on samples and contaminate them. They found that the number of fibres decreased when working under special clean conditions. Is has to be noted that the soil sieve sample set up is per definition an open set up. Also laboratory analysis was carried out in a regular (no ultra clean) environment.

Because of uncertainty about the retention of fibres on the sieve bed during sampling, and uncertainty about the possible deposit of airborne fibres during sampling, fibres are excluded beforehand from this study.

4.2 Handpicking of microplastics

The samples were gravitated in saline water and filtered in two parts, so two filters for each size fraction were subject to study. The plastic particles were handpicked from the sample by precision instruments (sharp pointed tweezers) and individually transferred to a pre-weighed Eppendorf tube. During the handpicking, the isolated particles were counted and recorded. Inspection of the sample under the stereomicroscope ended when it took more than 30 seconds to find another polymer particle of any kind. After the handpicking, the Eppendorf tube was closed and its filled weight was determined on a microbalance. The remains, i.e. the micro pore filter, fibres and remnants, were stored in covered glass Petri dish for possible anew analysis.

4.2.1 Brushing particles from the micro pore filter

The used light microscopes project light from beneath the object, while observation takes place from above. As micro pore filters are white, the full background lights up white. Pale particles could be overlooked, resulting in reduced distinctiveness. Using only the additional light sources from above led to too poor light conditions. It was noticed that particles could be easier distinguished on a transparent surface.

Starting with sample E5, as soon the particles were air dried, a soft paintbrush was used to brush the contents gently from the micro pore filter onto a clean glass Petri dish. This appeared to contribute to improved distinctiveness:
- White or pale particles, such as white transparent spherules and scrubs attracted better attention against the colourless background and became less easily overlooked. Spherical, translucent particles acted as a lens as they catch light from below. The inside reflections within the sphere led to high distinctiveness. In general, the appearance changed as more or less light is projected on to them.
- The spherical particles tended to roll on the glass Petri dish surface which helped detecting them.
- Films, that were often aligned in a flattened position on the micro pore filter, were much easier distinguished.
- Organic remnants reveal cell structures when they catch in unfiltered light from below and hence became not so often mistaken for MPs.

After processing of the last sample, all previous samples were inspected again to see whether possible polymeric particles were overlooked. For these samples, all contents were gently brushed from the micro pore filter onto the glass petri dish. MPs indentified then, were additionally recorded and new Eppendorf tube weights were determined afterwards. The overall number count and final weight determination were included in the dataset (4.3).

4.3 Dataset

During this study, a dataset was built up comprising the following:

On sampling
- Duration of the sieve sampling (dates and times of start and finish).
- Tap flow rate (at start and finish).
- River discharge (in m^3). Data retrieved from river gauges from Rijkswaterstaat in time intervals of 10 minutes. For Lobith and Bimmen: river gauge at Lobith. For Eijsden: river gauge at St. Pieter (Maastricht). For Bad Honnef: estimation by monitoring station staff.
- Turbidity levels. Data retrieved from monitoring stations Lobith and Eijsden. For Bimmen, the Lobith values were used.

Quantitative data on retrieved particles (per individual sample)
- Number of particles counted per specific group, per fraction (0.125-0.250 mm and 0.250-5 mm).
- Group weight, per fraction (0.125-0.250 mm and 0.250-5 mm).

Metadata (calculated manually on collected sampling data).
- The number based concentrations of particles per sieved m^3 of river water (particles per m^3).
- The concentrations of particles per sieved m^3 of river water (mg per m^3).
- Average values of river discharge and turbidity of both rivers. Averaging data was needed to present particle numbers and/or concentration levels against either river discharge or turbidity. For this purpose, turbidity and discharge data were averaged over the sampling time. For regression analysis, daily averaged data was used).

4.4 Discussion on the microscopic analysis

Stereomicroscopic study is a well known method for the identification of MPs, but it is sensitive for false identifications (Song et al., 2015). This study demonstrated that improved laboratory processing leads to clearer samples and improved distinctiveness. However, still remnants of organic debris and inorganic light-dense particles, amongst which fly ash particles, ended up at the micro pore filter. Further improvements with the stereomicroscope were achieved with better light conditions, brushing the MPs on the transparent Petri dish and the use of the specific characteristics of the MP samples, such as internal light reflection.

In this study all MPs selected by use of a stereomicroscope and stored in the associated Eppendorf tubes for weight determination. Picking up of MPs could be directed through the binoculars, but transferring the MP to the Eppendorf tubes took place beyond binocular sight. Especially the small size fraction MPs are (barely) visible with the bare eye, it cannot be excluded that while carrying them to the Eppendorf tube, MPs became lost. MPs, coal and organic remnants can be a hindrance during microscopic work as they easily stick to the tweezers due to static electricity. An antistatic device was used to reduce static electricity on the tweezers, but its effect was partly successful. Probably due the fact that the static electricity was not on the tweezers, but yet on the particles themselves. The approach of an anti-static device on the MP led to jumping particle, which might induce MPs loss. Plastic laboratory equipment increases static electricity, as was observed with the polystyrene Petri dishes.

As will be elucidated in chapter 6, in Rhine samples specific groups of MP were observed, that were not found in Meuse samples. This observation brought along the possibility to study probable cross-contamination during laboratory processing and microscopic work. Cross contamination, by means of specific Rhine MPs to end up in Meuse samples, was not observed.

Samples appeared to contain numerous MP. Specifically for the small size fractions, precise identification could be time consuming. A single sample could take more than one working day to process.

5. Methods for qualitative analysis

The determination and isolation of MPs was based on their external characteristics. For better understanding and proper interpretation of their presence and abundance, it is important to know more about their qualitative aspects and the polymers they comprise.

For the identification of MPs, 2 types of vibrational spectroscopic techniques were used:
1) Raman scattering spectroscopy (further: Raman).
2) Fourier Transform Infra Red Spectroscopy (further: FT-IR).

FT-IR and Raman are both well established as methods of vibrational spectroscopy and both have been used for polymer analysis for decades.

The core of the techniques is based on the fact that molecules can vibrate at specific frequencies, with energies corresponding with the mid-infrared range (wavenumber 200-4000 cm^{-1}). The interaction between light and molecular vibrations results in an exchange of energy and a decrease in the photon energy, which can be recorded and visualized in a peak spectrum.

Examples of vibrations are demonstrated with a CH$_2$ group that is for example integrated in a polyethylene backbone (figure 6). Specific molecular bonds absorb energy at specific wavenumbers. Based on this characteristics, spectra of sample material – in this case MPs - can be verified with known references. Raman and FT-IR deliver spectra at the same wavenumbers, but can with the same studied polymers, show large differences in peak intensity. The two techniques are considered complementary to each other (Lobo & Bonilla, 2003).
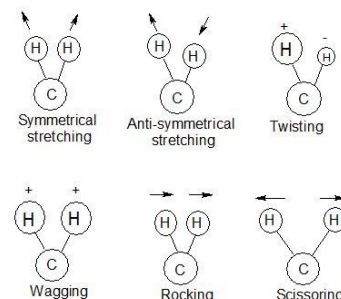

Figure 6. Examples of possible vibrations in a CH$_2$ group in a polymer backbone. Figure drawn with Chemsketch.

5.1 Raman scattering spectroscopy

Raman derives from an inelastic light scattering process. With Raman, a laser beam is aimed at the sample material. The laser is highly monochromatic, in the laser beam each emitted photon has the same energy. A laser photon is scattered and loses energy during the process due to the absorption of energy at molecule bonds, like carbon-carbon bonds in the backbone (C-C) carbon-hydrogen bonds (C-H) or bonds between the backbone and functional groups, like an aromatic ring. The amount of energy lost is seen as a change in energy (wavenumber) of the irradiating photon. This intensity loss is characteristic for a particular bond in the molecule; it depends on the atomic masses involved and the strength of the bond. A vibration is Raman active when the molecular vibration induces a net change in the bond polarizability during the vibration.

Raman spectra were recorded with a Renishaw (Wotton-under-Edge, United Kingdom) InVia Reflex Raman microscope with a 300 mW, 785-nm diode laser in combination with a spectrograph with a 1200 lines per millimeter (l/mm) grating, operating in the 1769- 672 cm^{-1} wavenumber range (polymer finger print region). Laser power is mostly set to 100%, except when particles showed physical damage, visible through the microscope's binoculars. The acquisition time is one second, repeated 0 to 20 times depending on the noise recorded without repetition.

Per group, randomly chosen particles were transferred from the Eppendorf tube by pointy tweezers onto an aluminum bar. To see whether the aluminum could disturb spectral measurements, first a blank was recorded. The microscope was focused on one randomly chosen particle. An overall area map is acquired by stitching snap shots of smaller areas, resulting in one picture presenting all particles on the computer screen. All particles were successively manually selected by mouse-clicking them, meanwhile recording the X,Y locations of the selected particles. Raman map scans were stored in .txt format.

Reference materials

For polymer recognition, Raman reference spectra were obtained from 16 regular consumer plastics, as shown in table 4. Verification of the references was done based on the resin code on the product itself, a label description or personal communication. These consumer plastics were unprocessed, i.e. not treated as the environmental MPs samples. To study the effects of colorants and possible variations within the same polymer group, for PE, PP, PS and PET, multiple references were included.

Verification of the references was done based on line plot analysis of the self derived Raman spectra. These are included in appendix 5.

Table 4. Consumer products used as reference materials for Raman spectral analysis for all groups, except for the white spherules. The abbreviations in the last column were used in the PCA plots in chapter 6.

Polymer	Source	Colour and transparency	Origin	Abbreviation used in figures
HDPE	Lid from 0,5 l water bottle	Blue, opaque	Product polymer code	HDPE blue
LDPE 1	IKEA wrapping bag	Transparent	Product polymer code	LDPE Ikea
LDPE 2	Sandwich bag	Transparent	Label description	LDWE sandw bag
PP 1	Eppendorf tube	Transparent	Label description	PP transl
PP 2	Salad cup lid	White, opaque	Product polymer code	PP white
PS 1	Plastic Petri dish	Transparent	Label description	PS Petri dish
PS 2	Coffee cup	White, opaque	Product polymer code	PS white
White Teflon	Laboratory tube lid	White, opaque	Label description	Teflon white
PET 1	Albert Heijn water bottle	Blue, transparent	Product polymer code	PET 1
PET 2	Lidl water bottle	Uncoloured, transparent	Product polymer code	PET 2
PET 3	IKEA packaging material	Uncoloured, transparent	Product polymer code	PET 3
PET 4	Shoarma sauce cup	Uncoloured, transparent	Product polymer code	PET 4
PC	Firework safety goggles	Uncoloured, transparent	Personal communication supplier	PC safety goggle
Nylon-6	White nylon bar	White, opaque	Raman	Nylon-6
Scrub	Palmolive thermal (bought in Wallonia)	Uncoloured, semi-transparent	Label description	Scrub
ABS/PC copolymer	Electricity meter device	Beige, opaque	Product polymer code	ABS/PC cop

5.2 Fourier Transform-Infrared spectroscopy

With the Raman setup, spectroscopic imaging on white spherules (both size fractions) was not successful. Spectral recording did not lead to useful spectra. For this reason, FT-IR analysis is performed on the white spherules. As the FT-IR brought with it the necessity to record individual spectra, while Raman offered the option of map scanning, all other groups were analyzed with Raman spectroscopy.

FT-IR is based on the absorption of energy when sample material is exposed to infrared radiation. The sample molecules selectively absorb radiation at specific wavenumbers corresponding with vibrational energies, but only if that vibration causes changes in dipole moment. The absorption leads to a decrease in IR intensity. In FT-IR spectra, the transmission (= I/I_0 in %) is plotted against wavenumbers, and visually presented by downward peaks. The intensity of absorption peaks is related to 1) the change of dipole moment and 2) the number of similar molecule bonds and 3) the number of exposed molecules.

White spherules are individually identified using a Shimadzu 8400S FT-IR spectrometer, type ATR, operating in the 4000–400 cm^{-1} wavenumber scanning range. A diamond compression cell (2 mm square) was used to compress the spherule onto the ATR prism. Each spectral measurement was the result of 16 repetitions.

Atmospheric compounds like water vapor (H_2O) and Carbon dioxide (CO_2) are subject to dipole changes and can therefore contribute to the IR spectrum. For this, a background measurement was first made for background correction purposes. After this, each spherule was transferred by pointy tweezers from the Eppendorf tube onto the ATR prism and subsequently tightly compressed and locked. After measurement, the sample could not be picked up again because of brittleness and was further considered as lost. Between every measurement the compressing plate and the ATR surface were cleaned with a paper tissue moistened with ethanol (70%).

All measurements are recorded by IR-solution, a software program that was provided with the Shimadzu spectrometer. Data were stored in .txt format.

Reference materials

For polymer recognition, FT-IR reference spectra were obtained from 10 regular consumer plastics, as shown in table 5. Polymer types were verified by the plastic polymer code printed on the product itself or displayed on its label. For polyethylene, polypropylene and polystyrene, multiple references were used. An organic reference was added to the reference set as it appeared also infrared active in the finger print region and the inclusion of organic material in fresh water microplastic samples cannot be excluded.The single sample of *Prunus armeniaca* seed was isolated from a consumer exfoliant (Labell Douche Gommante). All references were unprocessed, i.e. not treated such as the environmental MPs samples.

Verification of the references was done based on line plot analysis of the self derived FT-IR spectra. These are included in appendix 5.

Table 5. Consumer products used as reference materials for Fourier Transform Infrared spectral analysis on only the white spherules (both size fractions) found in this study. The abbreviations in the last column were used in the PCA plots in chapter 6.

Polymer	Source	External characteristics	Verification	Abbreviations
LDPE	IKEA transparent wrapping bag	Uncoloured, transparent	Product polymer code	LDPE
PE	Lid from juice bottle	Yellow, opaque	Product polymer code	PE
PE (scrub)	Palmolive thermal (bought at Intermarché Wallonia)	Uncoloured, transparent	Label description	Palmolive
PVC	Construction electricity pipe	Yellow, opaque	Product polymer code	PVC
PP 1	Salad cup lid	Uncoloured, transparent	Product polymer code	PP transl
PP 2	Butter cup lid	Blue, opaque	Product polymer code	PP blue
EPS	Package material	White, opaque	Product polymer code	EPS
PS	Coffee cup	White, opaque	Product polymer code	PS
Isolation foam	A fragment collected from building construction site	Dark yellow, opaque, brittle	None	Isol Foam
Prunus Armeniaca Seed	Labell Douche Gommante (bought at Intermarché Wallonia)	Brown, opaque	Label description	PR. A seed

5.3 Principal Component Analysis on spectral data

Spectral analysis is often used and recommended for polymer recognition (Hidalgo-Ruz et al., 2012; Song et al., 2015). The comparison of polymers is based on such aspects as:
- Peak positions on the x-scale (wavenumber).
- Peak number (the total number of peaks present in the spectrum).
- Mutual peak intensities (the highest peak to appear at the same wavenumber).
- Peak width.
- Other identical aspects like doublets or triplets (i.e. two or three characteristic associated peaks originating from one particular chemical bond).

In other words, two similar polymers are expected to deliver two similar spectra. In practice, however, comparison can be difficult or even uncertain as the peak positions and peak characteristics are non-identical. Examples of influences that provide variant spectra are formed by (Chen, Hay & Jenkins, 2012; Gulmine, Janissek, Heise & Akcelrud, 2002; Gulmine, Janissek, Heise & Akcelrud, 2003; Lobo & Bonilla, 2003):
- Noise recording.
- Device settings, like spectral resolution and the number of repetitions.
- Sample thickness.
- Differences in the degree of polymer christallinity.
- Differences in monomer orientation in the polymer backbone.
- The presence of non-polymeric molecules.
- The presence of additional groups like plasticizers, colourants or additional functional groups.
- (Bio)deterioration of the plastics.

For Raman, also microscopic out of focus situation and cosmic rays can influence the spectra. The Raman microscope was focused on one single particle before applying the map scan. Due to this, differently sized particles can easily be slightly out of focus, resulting in diffuse scattering and hence less sensor readings. Cosmic rays are false sensor readings caused by high energetic particles from outer space and cause a very high and sharp peak in Raman spectra. For FT-IR, the presence of infrared active atmospheric gasses such as CO_2 and H_2O can influence spectral quality.

For analytical insights, the datasets were preferably kept as raw as possible. Smoothing of data and/or cosmic ray removal were not applied. Spectral data containing failure recordings were not removed beforehand.

Principal Component Analysis
To compare the hundreds of spectra in this study, Principal Component Analysis (PCA) was carried out. With PCA it was possible to find correlations between data sets that were maybe missed with the bare eye. Besides, also with a view to a possible monitoring program, PCA could be helpful to study a large amount of retrieved data.

PCA is based on the conversion of possibly correlated variables into a set of linearly non-correlated values called principal components (PC). In more simple terms, PCA is used to find corresponding characteristics, for example the number of peaks in the spectra, their location (wavenumber) and their width. The first PC includes the maximum variance, the second PC includes the second largest variance, and so on. The PC scores were scatter plotted in a (X,Y)-diagram, in which data objects become arranged. A cluster of scatters indicate correlation. The spectral data of known polymers were included in the PCA as well, so if a cluster was formed near to a certain reference, correspondence was indicated. The references were distinguished by red dots and accompanied by its abbreviation as shown in tables 4 and 5 on pages 29 and 30.

PCA was performed with Matlab® 2014r (Student Version) statistics toolbox, on FT-IR spectral data of white spherules and on Raman spectral data of 1) transparent spherules, 2) scrubs, 3) miscellaneous MPs and 4) sample remnants of the (randomly chosen) small size fraction of sample B17. Due to poor Raman spectral data quality of films, PCA was not performed on this group. The selections of particles are included in the results chapter (chapter 6).

The .txt files were imported to Matlab® after which, the spectral data was adjusted following these successive steps:

1. Baselines correction with asymmetric least squares smoothing (Eilers & Boelens, 2005). Baseline correction is needed to correct for baseline drift (Raman) and background noise (FT-IR).

2. Scatter is caused by the reflectance of light or radiation on the surface and – when recorded – it influences the spectral data. Scatter correction was applied per Standard Normal Variate Transformation (Barnes, Dhanoa & Lister, 1989).

    The equation reads: $\frac{data-mean(data)}{standard\ deviation(data)}$.

3. Mean centering data. Centering data is needed for PCA, as PCA is based on a covariance matrix which is formed from centered data. The Matlab® PCA function does not perform this step automatically. The whole dataset, references plus studied samples together, were mean centered.

PCA was performed on the reference data. The obtained loadings, were multiplied with the mean centered data from the whole data set, resulting in scores for both references and samples. These scores were plotted in PCA plots.

To obtain maximal variance, first PC1 and PC2 were first plotted. After this, often also PC2 versus PC3, and PC3 versus PC4 were plotted for improved insights for MP identification. To study the actual similarity between a reference and studied samples, particle spectra were occasionally line plotted with reference spectra.

6. Qualitative results

6.1 Introduction to the qualitative results

In this chapter the designated groups are discussed, including their properties, their appearances in the rivers, their possible origin and the results of the spectral analysis. The latter also involves the Principal Components Analysis, which is used to simultaneously compare large numbers of spectral recordings. When applying PCA, tens to hundreds of spectra were compared with 10 (FT-IR) or 16 (Raman) references as presented in the method section. PCA arranges both the references and the MPs as scatters in a two-dimensional matrix called a PCA plot. The more a the MP spectral data approaches similarity to a certain reference, the closer it is arranged to this reference in the PCA plot. Multiple MPs of the same polymer type are expected to become arranged closely to each other, resulting in clusters of scatters. As will be noticed, not all samples were arranged near to a certain reference. Line plot comparison is applied to visually verify the spectra of individual samples with either references or other particulate specimens.

PCA has also been applied on a range of samples that during stereomicroscopic were yet not identified as polymeric. The aim for this is to see whether and to what extent MPs can be overlooked at microscopic study. Finally, a series of other qualitative aspects will pass by, among which the discovery of a spherical particle that is of abiotic nature and may be confused for microplastics: cenospheres.

6.2 Films

Films (figure 7) are classified as thin, foldable pieces of semi-transparent material. Within this study mostly uncoloured films were found and appeared in both size range. Films were found in samples derived from both the rivers Meuse and Rhine. Raman spectra were derived but their numbers were too low to perform PCA on. It appeared that specifically the group of films, even with low laser power levels (i.e. 10%), led to sensor saturation and hence to unusable spectra. Conformity to PE was tested occasionally by individual line plot comparison of Raman spectra of a handful of films from the large size fraction (not shown). A relationship to PE is considered likely, however films can be also comprise other plastics polymers, such as PP, PVC, PET, ethylene-vinyl acetate (EVA), ethylene-butyl acrylate (EBA) and linear low density polyethylene (LLDPE) (Espi, 2006; Mangaraj, Goswami & Mahajan, 2009).

Figure 7. Films found at Lobith (Rhine river), sample L16. Scale bar=500 μm

Specific applications of film fragments as they were observed under the stereomicroscope, were not found. It is suggested that these fragments originate from larger plastic fragments and thus have to be considered as secondary MPs.

6.3 White spherules

White spherules are described as spherical, opaque white, cream or beige coloured particles (figure 8). Occasionally other colours were found, like slightly pink or black, but the opaque character remains. They were commonly found moderately resistant to pinching forces by tweezers. White spherules were only found in samples collected from the river Rhine. They were observed at all times and in both size fractions, however visual interpretation suggest their top size to be limited to approximately 0.6 mm. The nature of the white spherules was tested with FT-IR spectral analysis and Principal Components analyses. These results are discussed in the following two subsections.
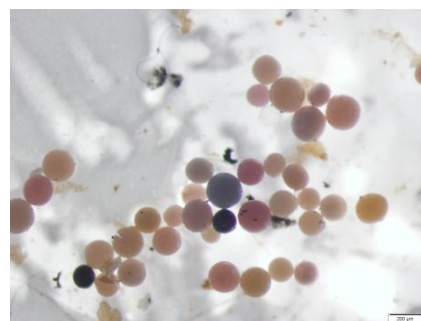

Figure 8. White spherules, size range 0.125-0.250 mm found at Lobith in sample L16. Scale bar = 200 μm

The white spherules were demonstrated to be less rigid than other derived MPs. A close up SEM image shows outside cracks (figure 40 on page 48). Household applications of white spherules were not found. It is believed that the white spherules are pre-expanded beads for the manufacturing of expanded polystyrene (EPS), that is used as packaging material and construction isolation (Raps, Hossieny, Park & Altstädt, 2015). The expansion is based on a process where hot air or steam expands pre-added pentane inside the pre-expanded spherules.

Verification of the PS references

Lobo and Bonilla (2003) point out that industrially manufactured polystyrene mainly exists as the atactic polymer in which the phenyl groups are randomly distributed over both sides of the polymer chain. The variant arrangement of functional groups (see figure 9a) lead to variant vibrations and consequently to variant peak structures in near-infrared spectra. This tactility leads in the fingerprint region to a characteristic peak in FT-IR spectra at 541 cm^{-1}. Aromatic absorptions are expected as well, such as ring vibrations at 1600 and 1500 cm^{-1} and C-H ring deformations at 757 and 699 cm^{-1}. In figure 9b the fingerprint region of the polystyrene reference is given, provided with the expected FT-IR peaks for atactic polystyrene (Lobo and Bonilla, 2003). Obviously, the polystyrene reference matches the expected characteristics. The pronounced peak at 1452 was not explained by Lobo & Bonilla (2003), but nonetheless also present in their PS example spectrum. To investigate the similarity of the two used PS references, their FT-IR spectral recordings were overlaid in figure A4 in appendix 5. Clear similarity between the EPS and the PS references is demonstrated. Pentane influences in the EPS reference spectrum were not observed.
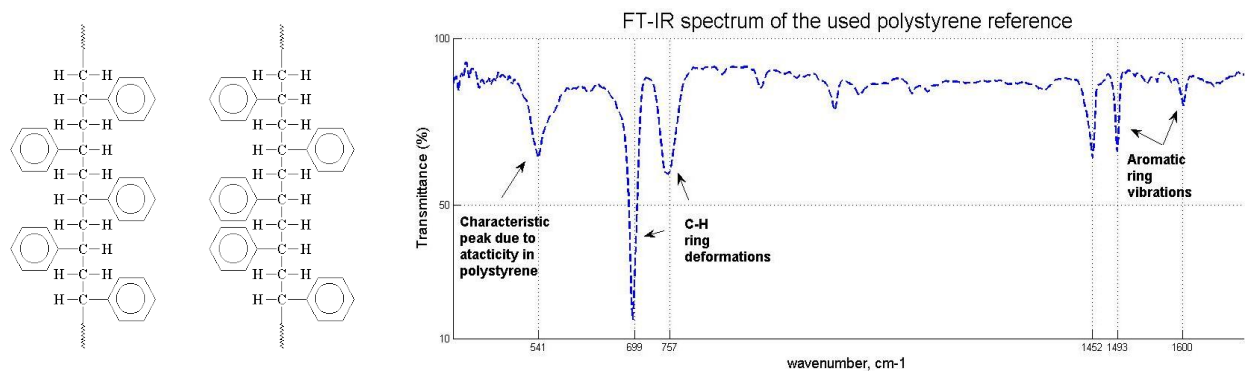

Figure 9 (a) Two manifestations of polystyrene: syndiotactic (left) and atactic (right). Isotactic PS is not shown. Source: www.plsc.ws (2015).
b) FT-IR spectum of the fingerprint region of the polystyrene reference. The expected peak characteristics for atactic polystyrene are presented (Lobo & Bonilla, 2003).

White spherules 0.125-0.250mm

Out of four MP samples, 74 white spherules in the size range 0.125-0.250 mm were selected for FT-IR spectral analysis. Three samples were obtained from Lobith and one sample from Bimmen (table 6). The sample spectral data was combined with the spectral data of the reference plastics (table 5 on page 30) and organized into one dataset for PCA. The first 10 numbers are attached to the references and the samples were numbered consecutively from here. This means that 10 references plus 74 samples lead to 84 projections in the scatter plot.

Figure 10 displays the PCA plot of PC 1 and PC 2, explaining 88% of data variance. Each Rhine MP sample has its own colour. No specific clustering around a certain reference is noticed, however PS and EPS seem more related than PVC and *Prunus Armeniaca*. The PP references and PE based references (PE, LDPE and Palmolive) are far distant as they are outlying at the other side of the PCA plot.

Table 6. White spherules in size range 0.125-0.250 mm selected for FT-IR spectral analysis and PCA.

MPs sample	Total white spherules in sample	Randomly picked for FT-IR/ PCA
L3	68	20
L8	44	10
B17	60	19
L17	82	25
Total	**254**	**74**

To investigate the relation to PS, four samples were selected for line plot analysis (figure 13). Sample 80 was chosen as it was arranged closest to PS in the PC1 and PC2 plot. The other three samples were chosen as specimens from the point cloud outer edge. Numbers 47 and 51 belong to sample L8 (blue scatters) and numbers 73 and 80 to sample L3 (magenta scatters).
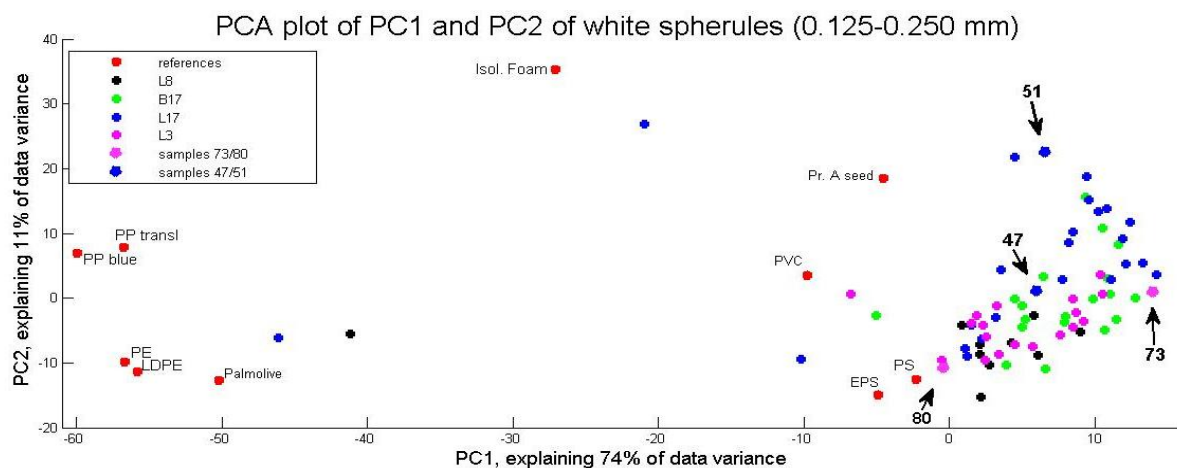
Figure 10. PCA plot of PC1 and PC2 of the FT-IR data of white spherules, size fraction 0.125-0.250 mm. The references and all four samples are distinctively printed in individual colours. Four particles at the outer edge of the scatter cloud were selected for line plot comparison (47, 51, 73, 80; figure 11).

Synthetic polymers comprise many methyl groups (CH_2) that are attached to the molecule backbone. Due to this, symmetric stretching vibrations at 2853 cm^{-1}, and asymmetric stretching vibrations at 2926 cm^{-1} are expected to appear as synthetic polymers are studied (Lobo and Bonilla (2003). These vibrations are often used for a quick view whether a sample is of synthetic nature. For the two samples in the scatter plot of PC1 and PC2 that are most distant to PS, numbers 51 and 47, pronounced stretching vibration peaks cannot be observed. This might indicate that they are not of polymeric origin. However, also the spectral quality may be debated, as sample peak intensities are low compared to the references and also noise was recorded. For all four samples, except for the one closest arranged to PS (number 80, black line), also in the fingerprint region no characteristics peaks are observed.

On their educational website, the American Chemistry Council (2015) mentions that polystyrene is a poor barrier to water vapour. In the rather open, internal structure, water originating from the sample processing may be still present, leading to the recording of noise.
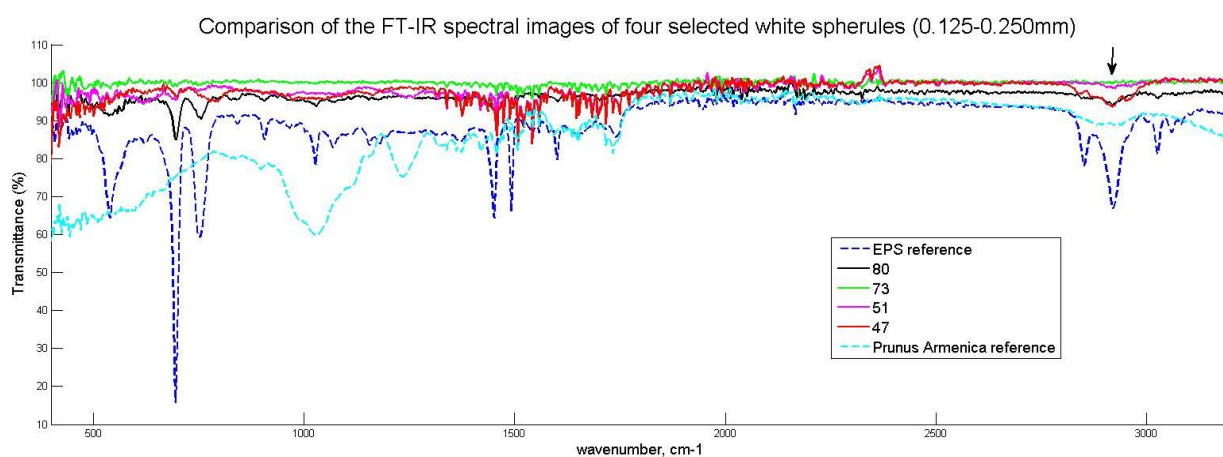

Figure 11. Line plots of the FT-IR spectra of four selected white spherules in the size range 0.125-0.250 mm (see figure 10). Also line plotted are the PS reference and the (organic) Prunus armeniaca reference (both dashed lines). The arrow indicates the lack of C-H stretch vibrations that are expected for polymeric macromolecules.

White spherules 0.250-5 mm

Out of four MP samples, 74 white spherules in the larger size range were selected for FT-IR spectral analysis. Three samples were derived from Lobith and one sample from Bimmen (table 7). In total 209 white spherules were found within these four samples and within this size range. The sample spectral data was combined with the spectral data of the reference plastics (table 5 on page 30) and organized into one dataset for PCA. The first 10 numbers were attached to the references and the samples were numbered consecutively from here. This means that 10 references plus 74 samples led to 84 projections in the scatter plot.

Table 7. White spherules in the size range 0.125-0.250 mm selected for FT-IR spectral analysis and PCA.

MP sample	Total white spherules in sample	Randomly picked for FT-IR
B3	51	15
L3	90	21
L8	38	16
L17	30	22
Total	**209**	**74**

Figure 12 displays the PCA plot of PC1 and PC2, explaining in total 88% of data variance. Red dots represent the references and the sample spectra are presented in black. Obviously, a cluster of scatters is formed near the two polystyrene references. No samples are outlying, indicating that the selected samples are mutual quite similar. All the other references than PS/EPS are more remote in the PCA plot. To verift the similarity to PS, four outer edge samples in the scatter cloud, numbers 32, 33, 51 and 69, are line plotted with the EPS reference in figure 11.
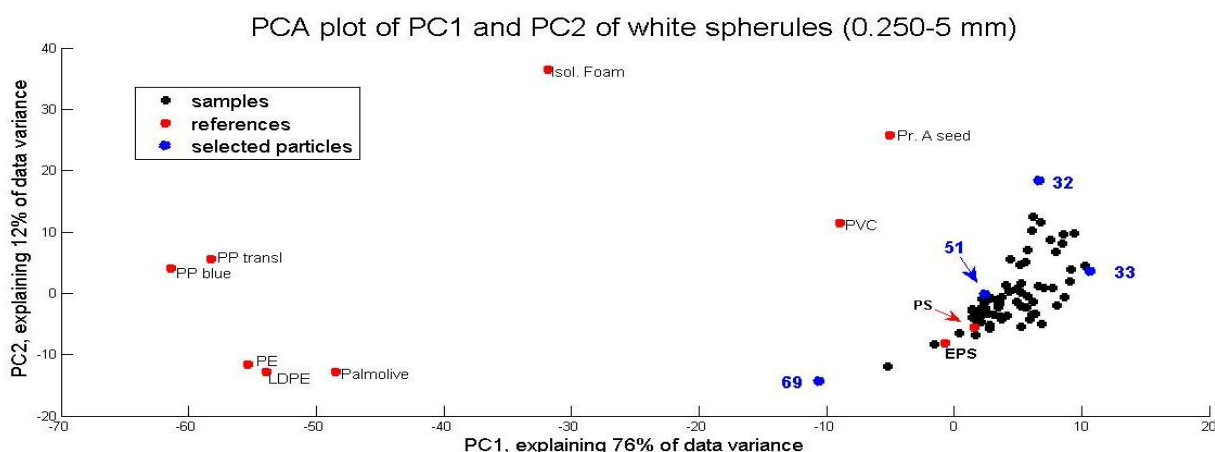

Figure 12. PCA plot of PC1 and PC2 of the FT-IR data of white spherules, size fraction 0.250-5 mm. Red dots represent references. Black dots are environmental samples. Blue dots at the outer edge of the scatter cloud indicate samples spectra that were used for line plot analysis (figure 13).

The finger print region of samples 69 and 33 (black and green lines) seem to match polystyrene. For the other two samples (51 magenta and 32 red) visual verification is difficult. Just as with the small size fraction of the white spherules, data quality is not consistent. The black arrow points at the where stretching peaks are expected, but which are not properly present. According to PCA similarity to PS is much more obvious than to the other polymer references, which is demonstrated in the following subsection.
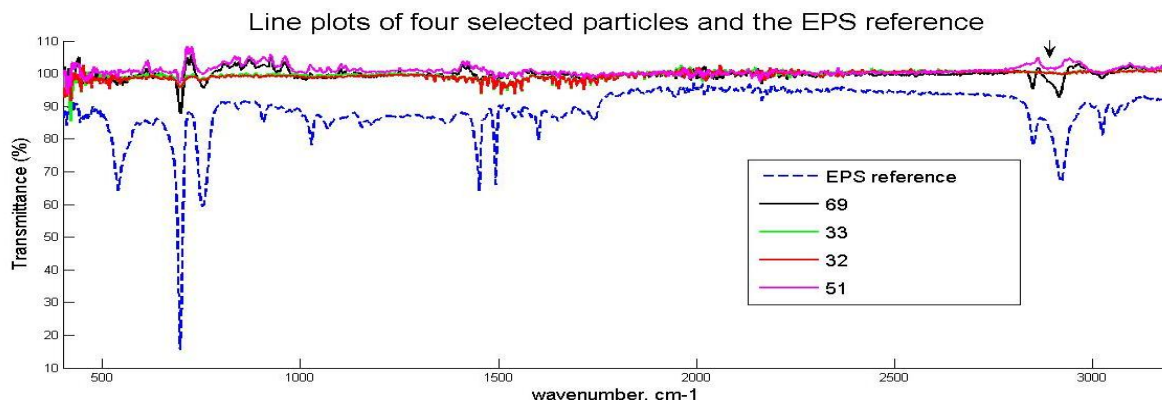

Figure 13. Line plots of the FT-IR spectra of four selected white spherules in the size range 0.250-5 mm (32, 33, 51, 69; see figure 12). Also line plotted is the EPS reference. The arrow indicates the lack of C-H stretch vibrations near 2900-3000 cm^{-1} that are expected for polymeric macromolecules.

Verification of the PCA.
In both PCA's on the white spherules was noted:
- that the references were arranged similarly in the PCA plots (figures 10 and 12),
- that in both cases, PC1 already explains more than 75% of data variance,
- that the spectral quality of the studied samples was predominantly poor, and
- that the original spectral characteristics of the references were altered due to mean centering with these studied samples.

This gave thought to the idea that possibly instead of peak positions, yet peak intensity was regarded as variance within the PCA. This could have caused a false interpretation, as the samples with low peak pronunciation in that case would have been arranged closely to the reference with the least peak pronunciation in the meancentered dataset. For this reason, also the relation between the loadings of PC1 and the meancentered data was studied. In figure A10 in appendix 5, the loadings of PC1 is line plotted with the meancentered data of 1) the PP reference, 2) the EPS reference and 3) the meancentered data of sample 80 (which is near to PS in figure 10).

The more the peaks of the PC1 loadings plot are inverse to the peaks in the line plot of the meancentered data, the less similar they are in reality. In figure A10 can be observed that PP shows pronounced inverse peaks at wavenumbers that are assigned to PS (wavenumbers 541, 699, 757). The PS reference and sample 80 do both approximately follow the line plot of PC1. Because the PS reference is less inverse to the loadings of PC1, PS was arranged near zero at the PC1 axis. PP, with was obviously inverse at several wavenumbers, is correctly arranged at a distance in the PCA plots. This comparison has also demonstrated similarity of the white spherules to PS.

Conclusions (white spherules, both size fractions):
- Household applications of white spherules were not found. It is suggested that they are the unexpanded precursors for an industrial application: the fabrication of expended polystyrene foam for packaging or construction isolation purposes. It is likely that they are emitted during production, transport and/or fabrication into end products.
- PCA on both size fractions of the white spherules resulted in high amounts of variation (over 85%) to be explained by just PC1 and PC2.
- Line plot analysis of the loadings of PC1 and the meancentered data demonstrated that peak characteristics formed the basis for PCA, and not peak intensity.
- However verification of the spectral data by the bare eye is difficult due to poor spectral quality, with PCA for the majority of white spherules similarity to polystyrene could be demonstrated.
- Improved spectral data quality can improve distinctiveness and decrease the amount of time needed for verification.

6.4 Miscellaneous microplastics

The group of miscellaneous MPs comprise MPs that do not meet the external features regarding shape and colour of the other groups, but are still thought to of polymeric origin. They were found in all samples derived from both the Meuse and Rhine and appear in all possible sizes within the full size range of this study (0.125 mm-5 mm). Obviously, the miscellaneous MPs appear in the most diverging shapes and colours (figure 14).

Examples of industrial or household applications of miscellaneous MPs were not found. It is suggested that these MPs originate from larger plastic fragments and thus have to be considered as secondary MPs (Cole et al., 2011).

Figure 14. Examples of the group of so called miscellaneous MPs, in the size range 0.250-5 mm observed in Rhine river sample L16. Scale bar = 2 mm

With Raman, only map scans were made from the larger size fraction. Out of three MP samples, 45 particles in the size range 0.250-5mm mm were selected for Raman spectral analysis and PCA (table 8). MP samples E6 and E10 are both obtained at Eijsden (the Meuse), MP sample L17 was obtained at Lobith (the Rhine). Scrubs were excluded beforehand from these three samples, so they do not contribute to the mix of particles that was studied here and hence of no influence to the PCA outcome.

The sample spectral data was combined with the spectral data of the reference plastics (table 4 on page 29) and organized into one dataset for PCA. The first 16 numbers were attached to the references and the samples were numbered consecutively from here. This means that 16 references plus 66 samples led to 82 projections in the PCA plots.

In figure 15 the PCA plot of PC1 and PC2 is shown, in total explaining 58% of data variance. Samples obtained from the Meuse (E6, E10) are represented by green dots while Rhine river specimens (L17) are indicated in blue. Alikeness to PE is suggested as the PE based references and most of the MPs are arranged into one scatter cloud.

Table 8. Miscellaneous particles in size range > 0.250 mm selected for Raman and PCA

MP sample	Total Mps found in sample	Randomly picked for Raman and PCA
E6	21	21
E10	24	24
L17	42	21
Total	**87**	**66**

PC and PET are far distant. In the PCA plot of PC3 versus PC4 (not shown), an additional 22% of data variance was explained. Here a similar distribution was found as in the first PCA plot: most samples cluster near the PE based references, two tend to PP and two to PS. About 20 samples are widely spread over the diagram, due to record failures. Regarding their distribution over the PCA plot, there is no obvious difference between the composition of the Meuse samples and the Rhine sample.
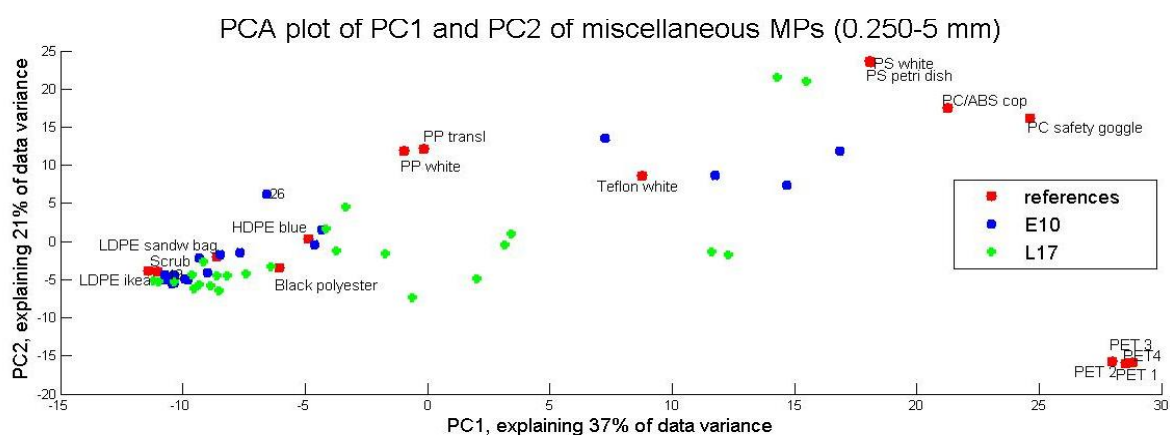

Figure 15. PCA plot PC1 and PC2 of Raman spectral data of the group of miscellaneous MPs, size range 0.250-5 mm. The Meuse sample is presented in green and Rhine in blue.

PE is the simplest polymer: it is a repeating chain of methyl groups ($-CH_2-$)$_n$. Vibrational peaks are expected by CH_2 scissors vibration at 1460 and 1440 cm^{-1}, CH_2 wagging at 1417 cm^{-1}, CH_2 twist at 1295 cm^{-1}, a backbone vibration assigned to CH_2 rocking at 1169 cm^{-1} and two C-C stretch vibrations at 1130 cm and 1061 cm^{-1}. However, crystallization, impurities and additives such as weakeners, colorants and co-monomers can lead to deviant spectral recordings as their presence would bring along molecule bond absorptions that would be expressed by additional peaks. For this reason several different PE based references were included in the PCA: translucent, flexible and coloured examples. To study their similarity, the four used PE based references are line plotted together (figure A11 in appendix 5). Obviously, the PE characteristics are met by all four and they show approximate similarity, but some spectral differences were observed. This is probably the reason that after PCA, in the PCA plots the PE-based references are mostly arranged at a slight distance to each other.

Spectral failures, such as sensor saturation and noise recording, were not removed beforehand from the dataset. Because of this, specimens with spectral failures or poor data quality become plotted somewhere in the diagram and influence the PCA outcome. Individual line plot analysis was needed to verify the similarity to the references. Considering the large number of line plots these are not all shown in this report. In figure 16 are three examples of Raman recordings that hinder verification are presented: 1) a wide peak ranging over three specific PE peaks, 2) noise recording that brings in additional variance and 3) sensor saturation resulting in an unusable spectral image. For comparison, the scrub reference is overlaid. Particle 41 displays similarity to the scrub reference, but obvious is that the noise introduces additional variance.
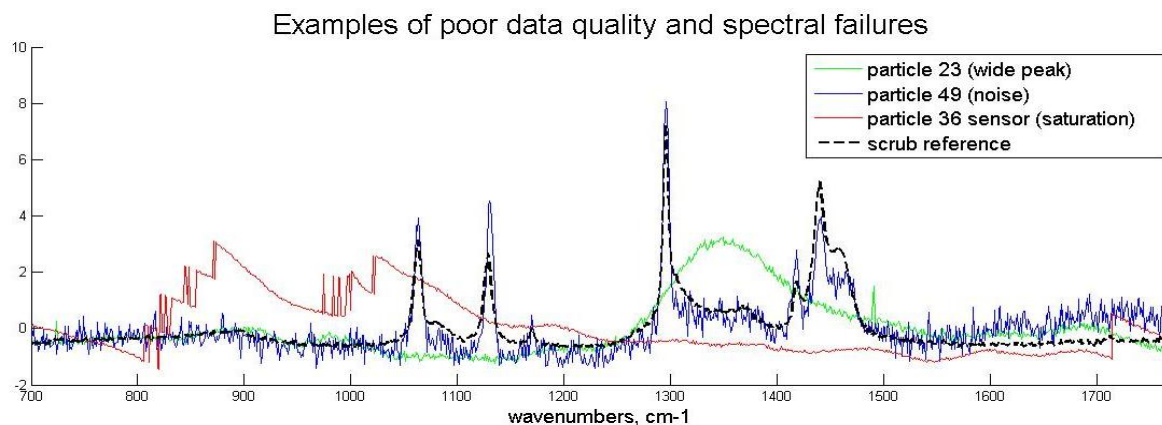

Figure 16. Three examples of Raman spectra of miscellaneous MPs (0.250-5 mm) to illustrate the effect of poor data quality to PCA. For comparison, also the scrub reference is overlaying (black dashed line). The wavenumbers are presented on the X-axis, ranging from 700 cm^{-1} to 1770 cm^{-1} (the finger print region). Before plotting, the baseline was removed, and scatter correction was applied to improve peak pronunciation. Because of this, the Y-axis is dimensionless. Laser wavelength: 785 nm.

Based on visual judgement, out of 66 studied samples, 46 correspond to PE, 2 times to PS, 2 times to PP and 4 times sensor saturation was found. For 16 samples the data was just partly matching a reference and thereto not identifiable. This might be caused by poor spectral quality as well as unknown peak characteristics, possibly induced by an unknown (co)polymer, to which a matching reference was lacking.

A closer look at the scatters in the PCA plots has learned that for four times, scatters were exactly overlying each other. This means that their characteristics are exactly the same. This occurred only with scatters with the same color, thus from the same river. It could not be determined whether these samples also had the same features. If so, it could have formed an indication that they were originated from the same origin, such as a larger plastic fragments or from the same industrial plant.

Conclusions (Miscellaneous MPs 0.250-5 mm):
- It is likely that the group of miscellaneous MPs are of secondary origin.
- Line plot analysis was still needed to verify the particle polymer types to the references. PCA showed:
    o that 46 out of 66, were related to PE,
    o that 2 MPs were identified as PP and 2 as PS,
    o that 16 out of 82 particles could not be verified. This was partly caused by poor spectral data quality and partly due to the lack of a good reference match,
    o that matches or possible relations to PET, PC and Teflon were not found.
- No obvious differences were observed in the composition of Meuse and Rhine samples.
- Comparison to the miscellaneous MPs in the smaller size fraction was not carried out as these were not studied spectroscopically.

6.5 Transparent spherules

Improvements in light microscopy, such as the interim filtration step and brushing the MPs from the white micro pore filter on the glass Petri dish, revealed the group of so-called transparent spherules (figure 17). The inside reflection within the sphere helped to distinguish them from other particles under the stereomicroscope.

Transparent spherules are described as solid, spherical, transparent, uncoloured MPs that are resistant to pinching forces by tweezers. Just like the white spherules, they were found in all samples derived from the Rhine, but were not observed at all in Meuse samples. They appeared in both sizes fractions, however the top size seemed limited to approximately 0.7 mm.

All observed transparent spherules are clear; pigmented transparent spheres, like the red spherules used for calibration measurements in section 7.1, were not once observed.

Figure 17. Examples of transparent spherules > 0.250 mm found in the Rhine river (sample L16). Scale bar = 0.5 mm

Household applications of the transparent spherules were not found. Believed is that the transparent spherules are precursors for subsequent processing into larger plastic items (Cole et al., 2011) and thus regarded as primary plastics which are emitted by industrial spillage or during transport. Spherules and pellets (which are flattened spherules) were first reported in coastal waters by Carpenter, Anderson, Harvey, Miklas and Peck (1972) and yet found worldwide (Cole et al., 2011). In Europe, their presence is demonstrated in Belgian coastal waters (Claessens, De Meester, Van Landuyt, De Clerck & Janssen, 2011) and the Danube river (Lechner et al., 2014). Their appearance, however, differs from the transparent spherules found in the Rhine. Also the reported sizes differ, as also spherules and pallets ranging above 0,7 mm were reported, which were not observed in the Rhine or Meuse in this study.

Transparent spherules 0.125-0.250mm
Out of three Rhine samples, 113 transparent spherules in the size range 0.125-0.250 mm were selected for Raman (table 9). The total number of transparent spherules found in these three samples is 177. It must be noted that the samples were split during laboratory processing.

The sample spectral data was combined with the spectral data of the reference plastics (table 4 on page 29) and organized into one dataset for PCA. The first 16 numbers were attached to the references and the samples were numbered consecutively from here. This means that 16 references plus 113 samples led to 129 projections in the PCA plots.

Table 9. Transparent spherules in the size range 0.125- 0.250 mm selected for Raman and PCA.

MP sample	Number of transparent spherules isolated from sample	Randomly picked for Raman
L3	68	24
L8	44	24
L17	65	65
Total	**177**	**113**

In figure 18 the PCA plot of PC1 and PC2 is shown, in total explaining 69% of data variance. Figure 19 displays the PCA plot of PC3 and PC4, explaining an additional 17% of data variance.
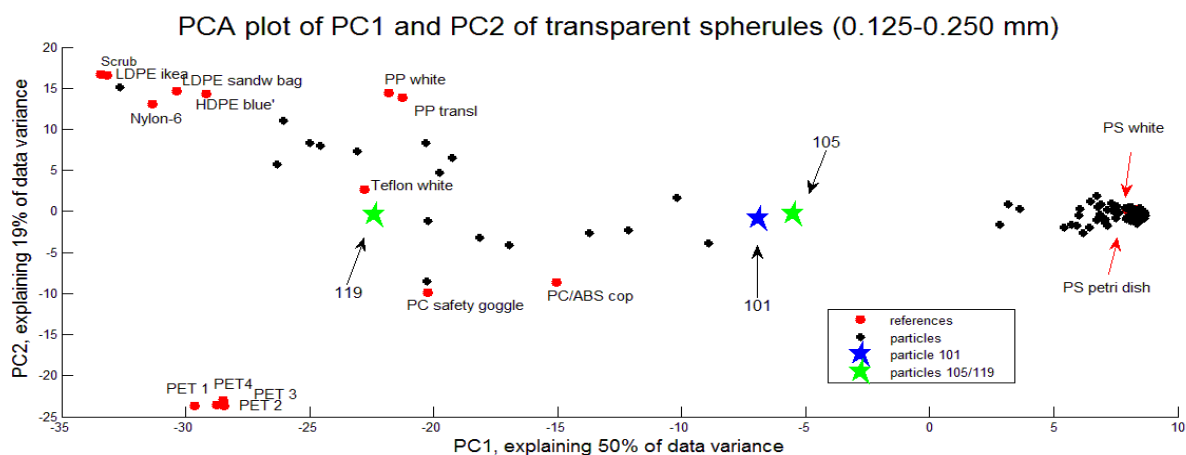

Figure 18. PCA plot of PC1 and PC2 of Raman spectral data on transparent spherules, size range 0.125-0.250 mm. In total 69% of data variance is explained. The polystyrene references are covered by the sample markers at the right. Samples 101 (blue), 105 and 119 (both green) were selected for line plot comparison (figure (20).

In both PCA plots a cluster of 92 scatters were formed around the PS references, which indicated similarity to PS. The clusters are so densely arranged, and therefore so much alike, that the PS references themselves became covered. About 20 samples are spread over the diagram.
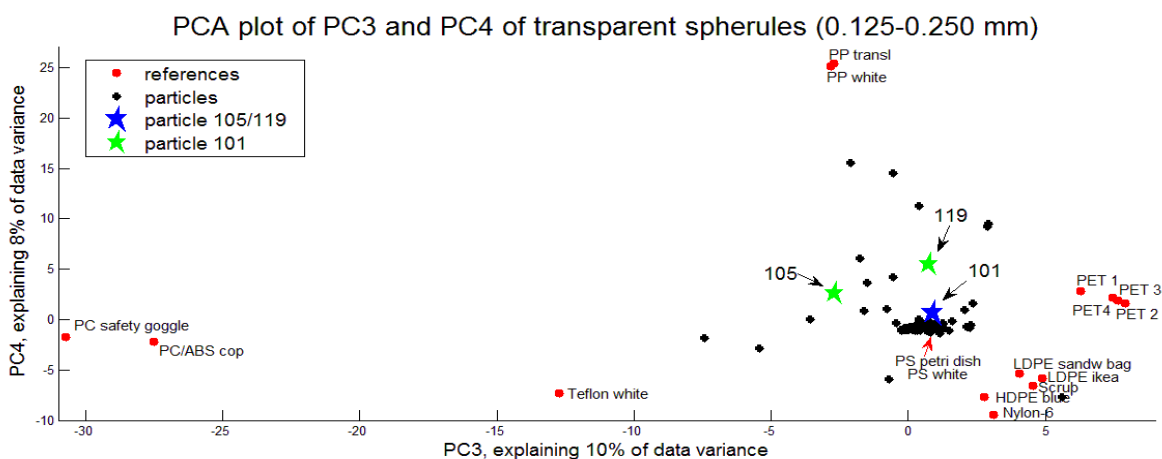

Figure 19. PCA plots of PC3 and PC4 of Raman spectral data on transparent spherules, size range 0.125-0.250 mm. In total 18% of data variance is explained. The polystyrene references are covered by the sample markers. Particles 101 (blue), 105 and 119 (both green) were selected for line plot comparison (figure 20).

With Raman, PS is characterized by two distinctive doublets at 1603 and 1584 cm^{-1} and at 1033 and 1002 cm^{-1} (both ring-mode vibrations). According to Lobo and Bonilla (2003) polystyrene is often copolymerized, leading to additional peaks in the finger print region. To investigate the mutual similarity of the both used PS references and the correspondence to the above peak characteristics, the PS references were line plotted together in figure A13 (appendix 5) .

Most of the samples that are arranged near PS in the PC1 and PC2 PCA plot, are also arranged to PS in the second PCA plot. However, sample 101 seemed distant to PS in the first PCA plot whilst in the PCA plot of PC3 and PC4, similarity to PS is just suggested. A spectral line plot comparison of sample 101 with the PE, PP and PS references (figure 20) suggests similarity to PS indeed. The red arrows point at the expected doublets, while the black arrow points at an unconfirmed broad peak between 1225-1425 cm^{-1}. The latter could be caused by the presence of co-monomers in this specific sample.
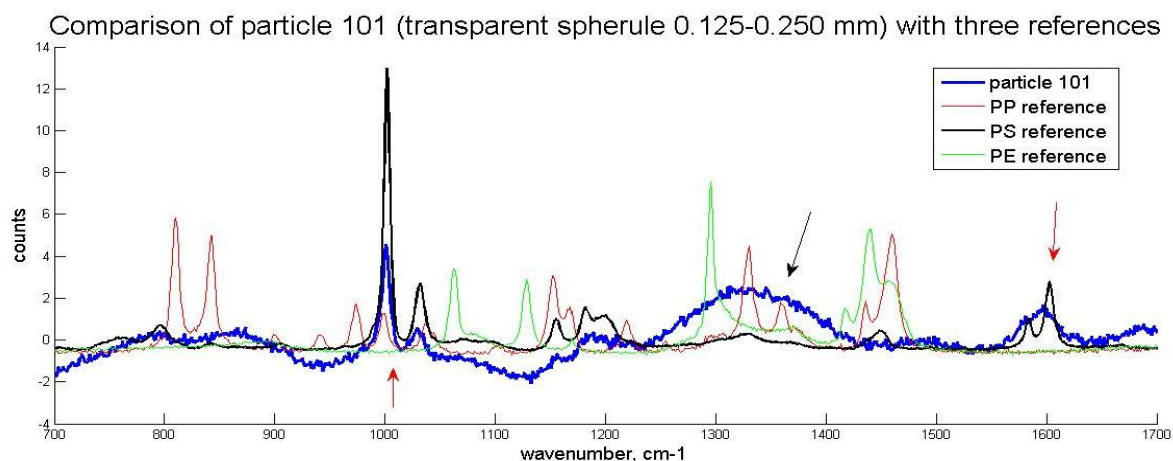
Figure 20. Line plots of the Raman spectra of the selected particle 101 (see figures 18 and 19) with PE, PP and PS references. Laser wavelength: 785 nm. Before plotting, the baseline was removed, and scatter correction was applied to improve peak pronunciation. Because of this, the Y-ax is dimensionless. On the X-as the wavenumbers in cm^{-1}. The red arrows point to characteristic PS peaks. The black arrow points to an unexplained wide peak in the particulate spectrum.

Two outliers, samples that are spread over the diagram instead of being clustered near a reference, have been studied in detail. The Raman spectra of outliers 105 and 119 are line plotted in figure (21). Clearly their distant presence in the PCA plots was caused by noise recording (sample 119, magenta line) and sensor saturation (sample 105, blue line).
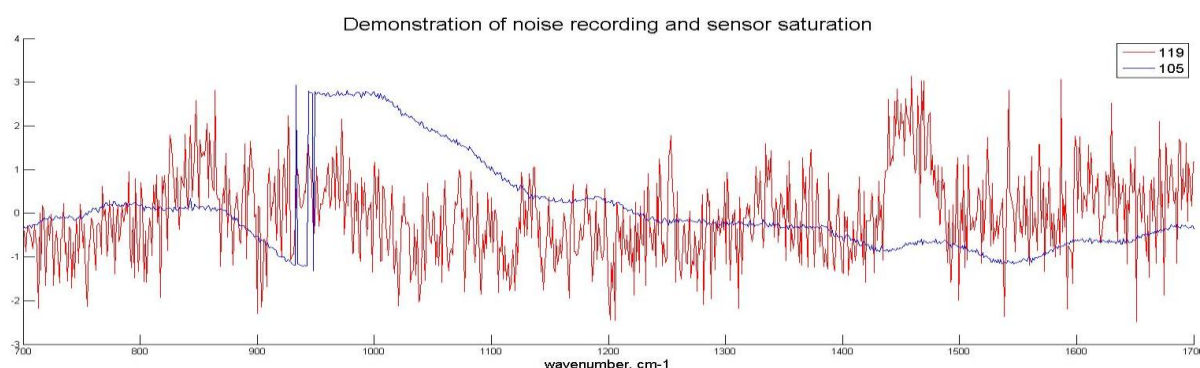

Figure 21. Line plots of the Raman spectra of two transparent spherules from the small size fraction. Noise (119, magenta line) and sensor saturation (105, blue line) are demonstrated. Before plotting, the baseline was removed, and scatter correction was applied to improve peak pronunciation. Because of this, the Y-ax is dimensionless. On the X-as: the wavenumbers in cm^{-1}. Laser wavelength: 785 nm.

Transparent spherules 0.250-5mm

Out of three river Rhine samples, 141 transparent spherules in the larger size range were selected for Raman (table 10). The total number of transparent spherules over these three samples is 154. The sample spectral data was combined with the spectral data of the reference plastics (table 4 on page 29) and organized into one dataset for PCA. The first 16 numbers were attached to the references and the samples were numbered consecutively from here. This means that 16 references plus 141 samples led to 157 projections in the PCA plot.

Table 10. Transparent spherules in the larger size range selected for Raman and PCA.

MP sample	Total transparent spherules in sample	Randomly picked for Raman
L3	72	59
L8	22	22
L17	60	60
Total	**154**	**141**

In figure 22 the PCA plot of PC1 and PC2 is shown, in total expressing 53% of data variance. Figure 22 displays the PCA plot of PC3 and PC4,
explaining an additional 23% of data variance. To study possible temporal variations, each sample series is presented in a different colour.
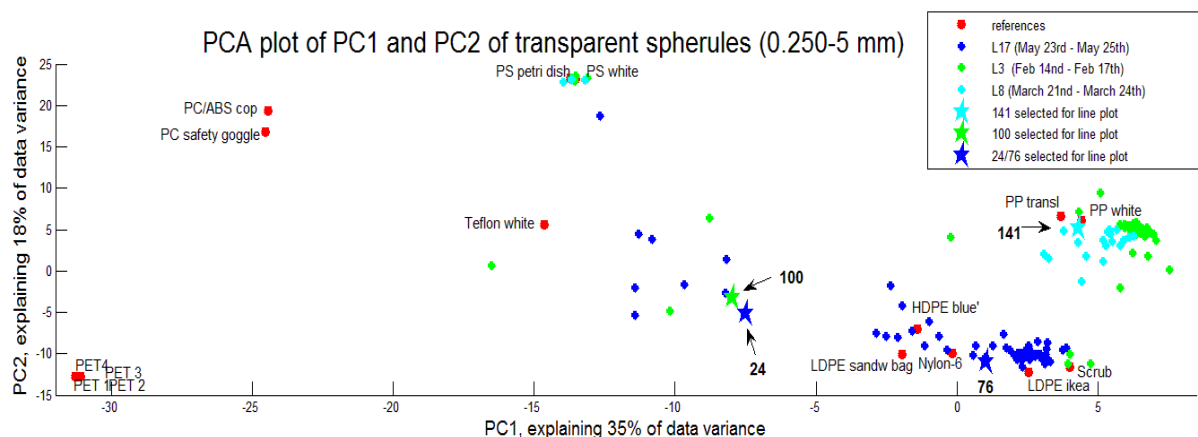
Figure 22. PCA plot of PC1 and PC2 of PCA of Raman spectral data of transparent spherules, size range 0.250-5 mm. In total 53 % of data variance was explained. Each sample is presented in an unique colour. Clusters were formed near PS (top middle), PP (right) and PE based samples (under right corner). Samples 24, 76, 100 and 141 are selected for line plot comparison (see figure 23).

In the PCA plot of PC1 and PC2, multiple clusters were formed: near PS (top, middle), near PP (right) and in between the PE-based references (right below). This suggests that the studied samples comprise multiple polymer types. The PET, PC and Teflon references are distant.

In the PCA plot of PC3 and PC4 also multiple clusters were observed, but they differ referring to the first PCA plot. Here one cluster is formed near PS (top, middle), while the cluster near PE seems to be spreading away from PE. The cluster near PP in the first PCA plot is now projected at some distance to the right, away from any other reference (marked with an ellipse in the PC3 versus PC4 PCA plot).

Based on these observations, the similarity to PP, PE and PS were each further studied in detail.

For the comparison of the three MP samples, each sample is expressed in its own colour. In the PCA plot can be seen that the coloured scats are not equally arranged towards the different references. Temporal variation came in sight and is discussed in detail.
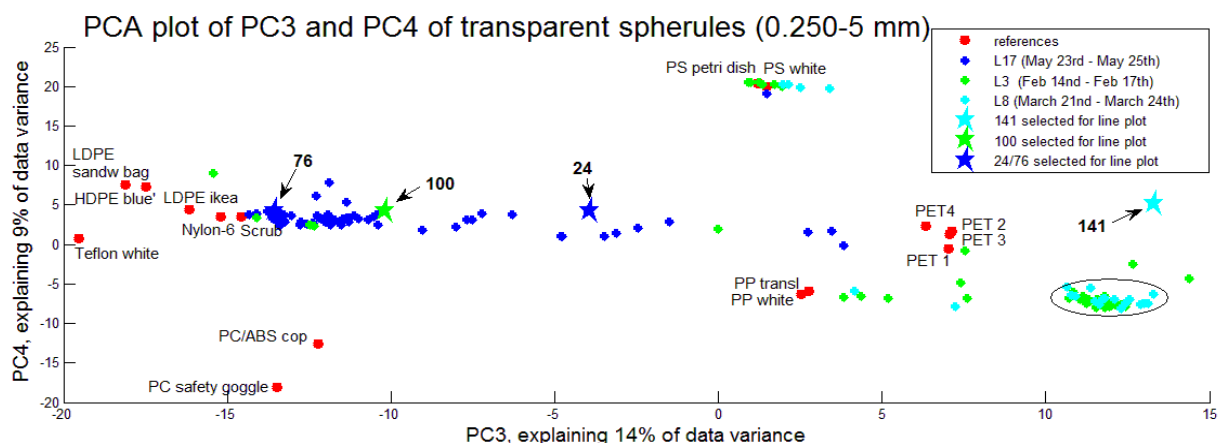
Figure 23. PCA plot of PC3 and PC4 on the large size fraction of the transparent spherules. In total 23 % of data variance is explained. Just like PC1 and PC2 (figure 22), clusters were formed near PS and PE. At the right, a cluster was formed that is not near to any reference. Samples 24, 76, 100 and 141 are selected for line plot comparison (figure 24).

Verifying the polypropylene references
According to Lobo and Bonilla (2013), commercially available polypropylene mostly exists in an isotactic form, with a head-to-tail alignment (this means that each monomer is aligned in the same direction). The both PP references were first verified (see figure A12 in appendix 5). Then only one PP reference is used for identification of the MP samples.

Sample 141 was chosen for further line plot comparison as it is very near to PP in PC1 and PC2, but yet remote to PP in PC3 and PC4. The Raman spectrum of sample 141 was line plotted with the transparent PP reference (figure 24). Both missing and emerging peaks were observed, so an exact determination was not possible. Similarity to PP was not demonstrated.

Figure 24. Line plot comparison the Raman spectra of sample 141, and the transparent PP reference. Laser wavelength: 785 nm. B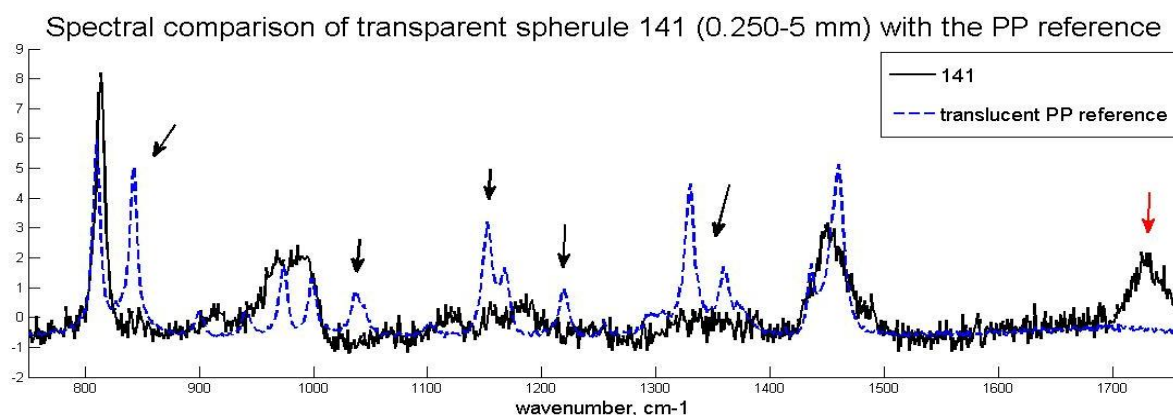efore plotting, the baseline was removed, and scatter correction was applied to improve peak pronunciation. Because of this, the Y-ax is dimensionless. On the X-as the wave length in cm^{-1}. Black arrows point out characteristic PP peaks that are lacking in the spectral image of sample 141. The red arrow marks a peak that seems lacking for the PP reference.

To investigate the similarity of sample 141 to others, three edging samples in the point cloud near PP in the PC1 versus PC2 PCA plot were line plotted together with sample 141 in figure 25. These samples are numbers 98, 109 and 122 (not individually marked in the PCA plots). Besides the observation of differences in spectral quality, all four showed approximate similarity.
Additional individual line plotting showed that the concerned scatter cloud near the PP reference (in PC1 versus PC2) is build up of 55 samples approximate similar to sample 141. This means that a group of 56 out of the studied 141 samples could not be identified. It could not be determined whether this was caused by tactility or the presence of additional functional groups. The features of sample number 122 (figure 25) and the fact that the concerned group was closely arranged to PP in the first PCA plot, suggest that the unclassifiable samples are still PP-based. However, as a proper reference match was not provided, the group of 56 samples were regarded as not classifiable. For only 4 samples a proper match to PP was found.
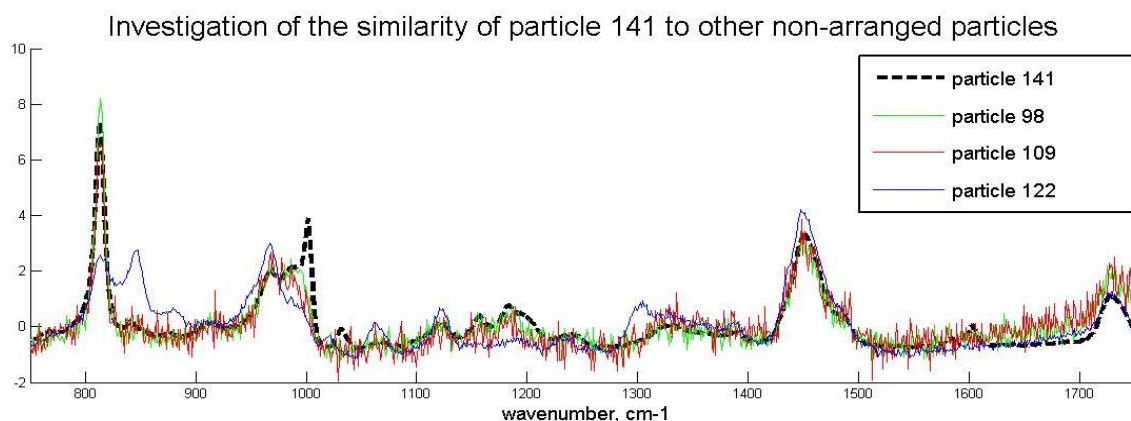

Figure 25. Line plot comparison of the Raman spectra of sample 141 and three random chosen samples in the circled point cloud in PC3 en PC4 (figure 23) Before plotting, the baseline was removed, and scatter correction was applied to improve peak pronunciation. Because of this, the Y-ax is dimensionless. On the X-as the wave length is presented in cm^{-1}. Laser wavelength: 785 nm.

Polyethylene

To determine the similarity to PE, a closer look is taken at three outer edge samples near PE in the scatter clouds of both PCA plots. It concerns the numbers 76, 100 and 24 which were chosen as they are increasingly distant to PE in both PCA plots (see figures 22 and 23). First their spectral data was line plotted with the scrub reference (which is identified as PE) in figure 26. For sample 76, which is closest arranged to PE in the PCA plots, a match can been observed with the bare eye (blue line). Obviously, as the samples are arranged at increasing distant to PE in the PCA plots, the less similarity can be observed. For sample 100, printed in green, multiple additional peaks were observed at 800 cm^{-1} and in between 1300-1400 cm^{-1}. This may be caused by the presence of PP as for that polymer type peaks are expected at these wave lengths.

Apparently for sample 24, which was actually distant to any reference in both PCA plots, severe noise was recorded, that makes identification difficult (red line). Also for other widespread samples in the PCA plots was observed that poor spectral data led to their unflustered projection. Based on individual line plots (not shown), in total 26 samples could not be used for identification. Regarding PE, with individual line plots for 44 samples a proper match to PE could be demonstrated.
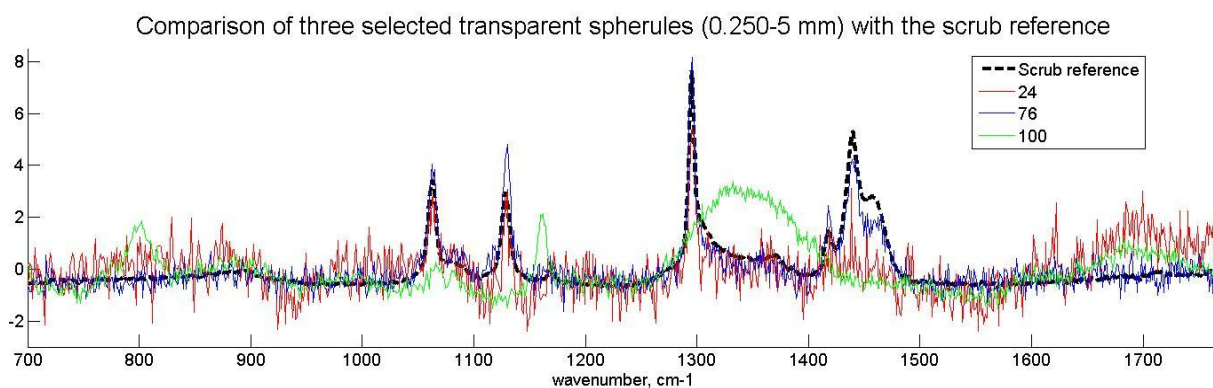
Figure 26. Line plots of Raman spectra of three selected spherules (24, 76 and 100) from the larger fraction and the scrub reference. Before plotting, the baseline was removed, and scatter correction was applied to improve peak pronunciation. Because of this, the Y-ax is dimensionless. On the X-as: the wavenumbers in cm^{-1}. Laser wavelength: 785 um).

Polystyrene

Spectral line plots of the transparent PS reference and all 11 samples ordered near PS in both PCA plots demonstrated great similarity, concluding that PS can be determined with high certainty (figure 27). Also here was observed that the most distant arranged sample displays the largest level of noise recording. As can be seen in the figure, noise is influencing the base line more than the actual peaks.
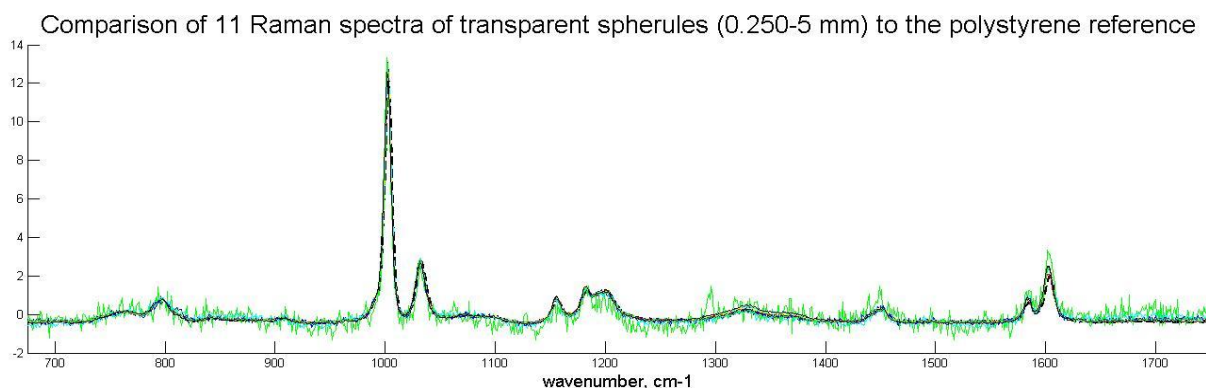
Figure 27. Raman spectra of the transparent PS reference (black plot) and 11 samples that were arranged near to PS in the PCA plots (figures 22 and 23). Before plotting, the baseline was removed, and scatter correction was applied to improve peak pronunciation. Because of this, the Y-ax is dimensionless. On the X-as: the wavenumbers in cm^{-1}. Clear similarity is demonstrated. Laser wavelength: 785 um.

Temporal differences in composition and relative contribution of polymers in MP samples

The three studied samples were obtained on different dates but at just one sample location: Lobith. Colour distinction in the PCA plots in combination with line plot analysis made it possible to determine the relative contribution of transparent spherules over all three samples (table 11).

It must be noted that two out of three samples were split (L8 and L17) and that splitting can lead to differences in MP distribution. Notably sample L17 contained no PP spherules and the yet unknown polymer, while samples L3 and L8 contained nearly to none PE-based spherules. This observation indicated temporal differences in the presence of polymer types in different samples. This also indicates that caution is needed when the spectroscopic results are being extrapolated to full sample levels.

Table 11. Relative distribution of polymer types regarding transparent spherules in the large size range.

MP sample	Total number of transparent spherules studied	PS	PP	PE	No match found	Fail
L3	59	6	3	4	41	5
L8	22	4	1	--	15	2
L17	60	1	--	40	--	19
Total	**141**	**11**	**4**	**44**	**56**	**26**

Conclusions on transparent spherules:
- Applications of transparent spherules in consumer products were not found. An industrial origin is likely, where they become emitted during production, transport or further fabrication.
- Spectral failure (noise recording, microscopic out of focus situations, sensor saturation) is a nuisance to accurately designating polymer types. For both size groups, approximately 18% of the translucent particles studied delivered insufficient spectral data.

Conclusions on the small size fraction (0.125-0.250 mm)
- Based on the PCA, 92 out of 113 transparent spherules were identified as PS and just 1 as PE.
- 20 transparent spherules could not be identified with certainty, as they remained distant from reference particles. Some might be partly polystyrene based and others were not classifiable because of sample failure and noise recording.

Conclusion on the large size fraction (0.250-5 mm)
- Plotting PC3 and PC4 in addition to PC1 and PC2, was shown useful to designate a polymer that was not represented by the used reference set.
- Contrary to the size range 0.125-0.250 mm, and to any of the other observed particle groups, the larger fraction comprises more different types of polymers.
- Contrary to the size range 0.125-0.250 mm, and to any of the other observed MPs particle groups, temporal differences in the presence of polymer types in different samples were observed.
- Temporal variation was demonstrated by highlighting three samples in the PCA plot (figure 22).
- Temporal variation indicates that interpretation errors can occur when the of studied particles are part of (an) unrepresentative sample(s).

6.6 Scrubs

Scrubs are recognized as resilient, ragged, semi-transparent, MPs whose presence in cosmetic products, exfoliants and hand cleansers was reported for decades. An industrial application of scrubs is as air blast media (Derraik, 2002; Fendall & Sewell, 2009). Predominantly PE is used, but for Canada and New Zealand also PS and PP scrubs are reported (Gregory, 1996)

Starting in 2013, large cosmetic fabricants such as Unilever, Proctor&Gamble, l'Oreal, Colgate-Palmolive and Beiersdorf announced they would ban plastic scrubs from their products. However, on April 2nd, 2014, in Wallonia (Belgium) two cosmetic product were bought from which plastic scrubs were derived: 1) *Palmolive Thermal* and 2) *Labell douche gommante.* The presence of PE was listed on both the product labels. The alikeness between river scrub samples and those derived from the exfoliants is demonstrated in figures 28a and b.

Their presence in fresh water suggest insufficient household sewage water treatment or the discharge of unfiltered sewage water. However, also spillage during manufacturing, handling or transport cannot be excluded. Scrubs appeared in both size fractions in all samples studied in both the Meuse and the Rhine. The size distribution was not determined in detail, but microscopic study revealed that most particles remained under 1 mm.

Scrubs may be easily confused with semi-transparent fine sand, as under the light stereomicroscope the both particles look quite similar (see figure 28). Both can be distinguished by squeezing them with tweezers: scrubs are resilient, while sand particles are rigid and grind audibly. Density separation in a saturated NaCl solution (1.2 g/cm^3) will separate both as the density of PE is reported between 0.82-0.97 g/cm^3 and sand at 2.65 g/cm^3 (Hidalgo-Ruz et al., 2012).

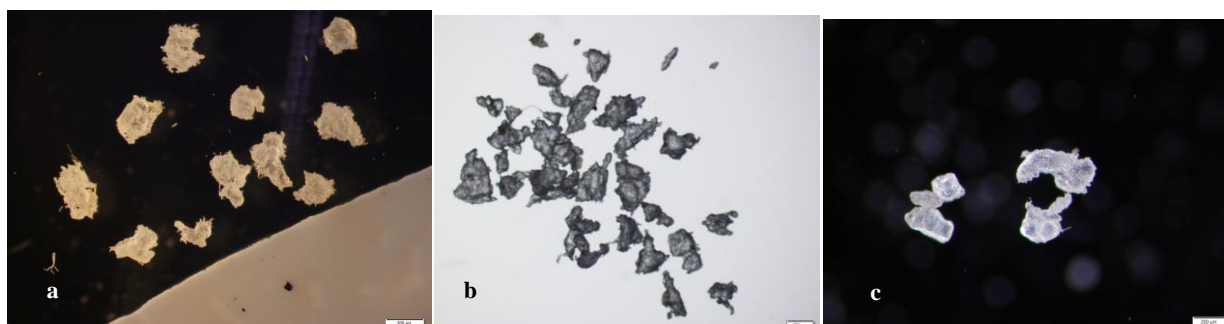Figure 28 Stereomicroscopic images of scrubs to express similarities.
(a) Scrubs extracted from exfoliant Nivea pure impact. Scale bar = 200 µm.
(b) Scrubs derived from L16 >0,250mm. Scale bar = 500 µm
(c) Two translucent river sand grains (left) and two scrubs (right). Scale bar = 200 µm.

Out of one Meuse river sample, 140 scrubs from both size fractions were selected for Raman (table 12). The sample spectral data was combined with the spectral data of the reference plastics (table 4 on page 29) and arranged into one dataset for PCA. The first 16 numbers were attached to the references and the samples were numbered consecutively from here. This means that 16 references plus 140 samples led to 156 projections in the PCA plot.

The PCA plot of PC1 versus PC2 explains 57% of the data variance and is displayed in figure 29. The PCA plot of PC3 and PC4 in figure 30 explains an additional 21% of data variance. Each size fraction is distinguished by a separate colour. This provides the possibility to observe composition variances between the two size fractions.

Table 12. Scrubs from both size fractions in the same sample selected for Raman and PCA.

Sample	Total scrubs in sample	Randomly picked for Raman
E6 (0.125-0.250 mm	170	80
E6 > 0.250 mm	97	60
Total	**267**	**140**

In both PCA plots a tail of samples ranges from the scrub reference towards the PS reference. The colour distinction shows that both size fractions are similarly arranged. Proportionally, as more large size samples (blue) were included into the data set, more of them are closely arranged to PE than the small size fraction (green). Remarkably, in the PCA plots the PE-based references are rather distant to each other as well. A small cluster is formed near PS, and PP, PET and PC are distant. PE, Teflon and PS are discussed further in detail. Three samples from the cluster near PE were selected for line plot analysis: numbers 21, 84 and 142, which are distinctively marked in the PCA plots.

Figure 29. PCA plot of PC1 and PC2 of Raman spectral data of scrub samples from the Meuse sample E6. Both size fractions are displayed in separate colours. The marked particles (21, 84 and 142)were selected for line plot analysis (figure 31).
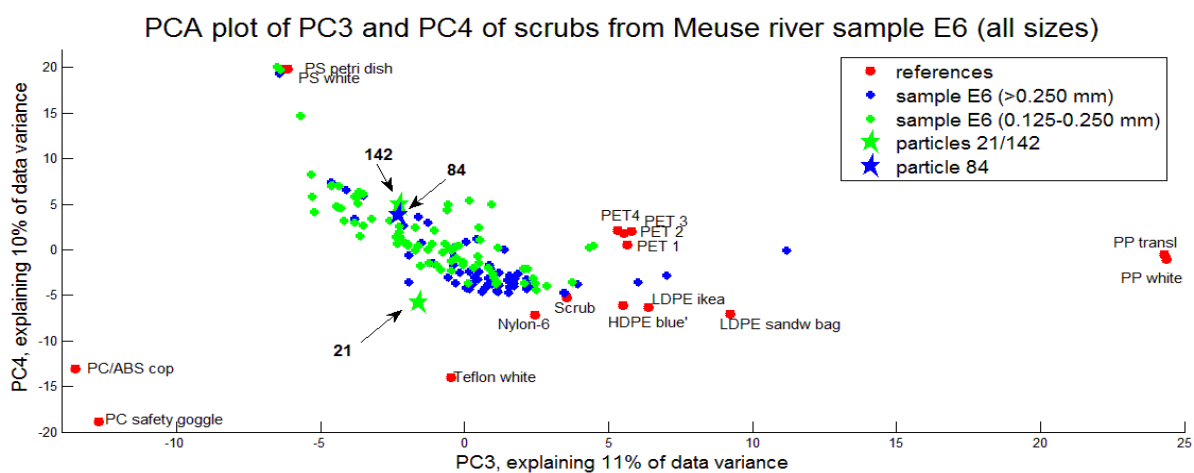
Figure 30. PCA plot of PC3 and PC4 of Raman spectral data of scrubs from Meuse river sample E6. Both size fractions are displayed in separate colours. The marked particles (21, 84 and 142) were selected to line plot analysis (figure 31).

Polyethylene
In both PCA plots, clusters were formed near the scrub reference. The Raman spectral data of the particles 21, 84 and 142 were line plotted together with the scrub reference in figure 31. Particle 142, that is closest arranged to PE, matches the scrub reference best. For particle 84, PE characteristics were still observed, as peaks appeared at the expected wavenumbers, but the accuracy of determination declines as more noise was recorded. Based on this line plot analysis, particle 21 and all specimens at the left of it in the PC1 versus PC2 PCA plot, were rather arbitrarily considered as record failures. This means that out of 140 samples, 122 were designated at PE.

Further line plot analysis on individual samples (not shown) demonstrated a relation between data quality and the distance to a cluster or a certain reference in the PCA plots. Aberrations by means of additional pronounced peaks, for example caused by copolymers or additional functional groups, were not found.

Figure 31. Line plots of Raman spectra of the selected samples 142, 84 and 21 and the scrub reference. Before plotting, the baseline was removed, and scatter correction was applied to improve peak pronunciation. Because of this, the Y-ax is dimensionless. On the X-as: the wavenumber in cm^{-1}. Laser wavelength: 785 um.

Polystyrene and Teflon
In both PCA plots, three samples approach PS and similarity to PS is demonstrated by line plots (not shown). In the PCA plots some samples seem to approach Teflon but in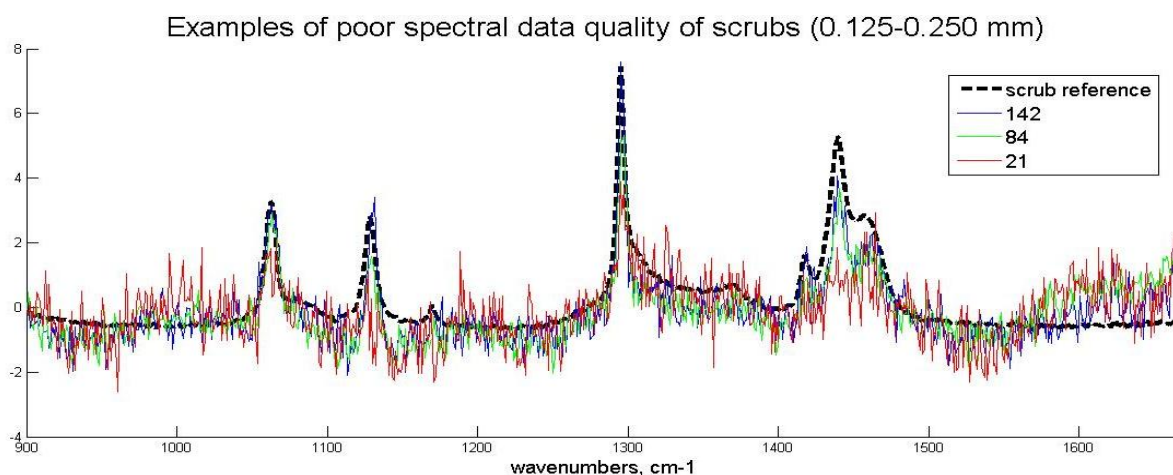dividual line plots demonstrated that their projection was due to poor spectral quality (not shown). No match to Teflon was found.

Conclusions on scrubs (all sizes):
- Scrubs are known to be used in consumer products, such as exfoliants. At the time of river sampling, scrub containing exfoliants were still available in shops in the Meuse river basin.
- Under the stereomicroscope, scrubs and sand can be mutually mistaken, as they look similar.
- PCA and line plots demonstrated that the majority of scrubs matched the PE-based references, whereby the self-derived scrub reference appeared to be closest related.
- Based on line plot analysis, 122 out of 140 particles were designated as PE and 3 as PS. A match to polypropylene (PP) characteristics was not found.
- Spectral data quality of 15 particles was insufficient for visual verification. This equals 10%.
- The Raman spectral data quality appears to be better for the larger size fraction. This is possibly caused due to the microscopic focus.

6.7 Analysis of particles left behind after microscopic study
The above chapters showed that the visually selected particles were of polymeric origin. Hence MPs can be rather accurately selected from river samples. This subsection discusses whether MPs can become overlooked during stereoscopic research.

From the small size fraction of sample B17, 1320 particles were manually identified as polymeric. From the remaining particles on the micro pore filter, a number of 320 remaining particles were randomly selected for Raman. The particle spectral data was combined with the spectral data of the reference plastics (table 4 on page 29) and arranged into one dataset for PCA. The first 16 numbers were attached to the references and the samples were numbered consecutively from here. This means that 16 references plus 320 samples led to 336 projections in the PCA plot.

The PCA plot of PC1 versus PC2 explains a total of 59% (figure 32) and the PCA plot of PC3 and PC4 and additional 23% (figure 33). In total 82% of variance is explained. In the first PCA plot at the right a compact cluster of scatters is formed which is not near to any reference. In fact, all the references are distant, which indicates a far distant nature to the references and most probably not of any polymeric nature. However, at the left a handful of scatters are near to the PE based references and the two PP references.
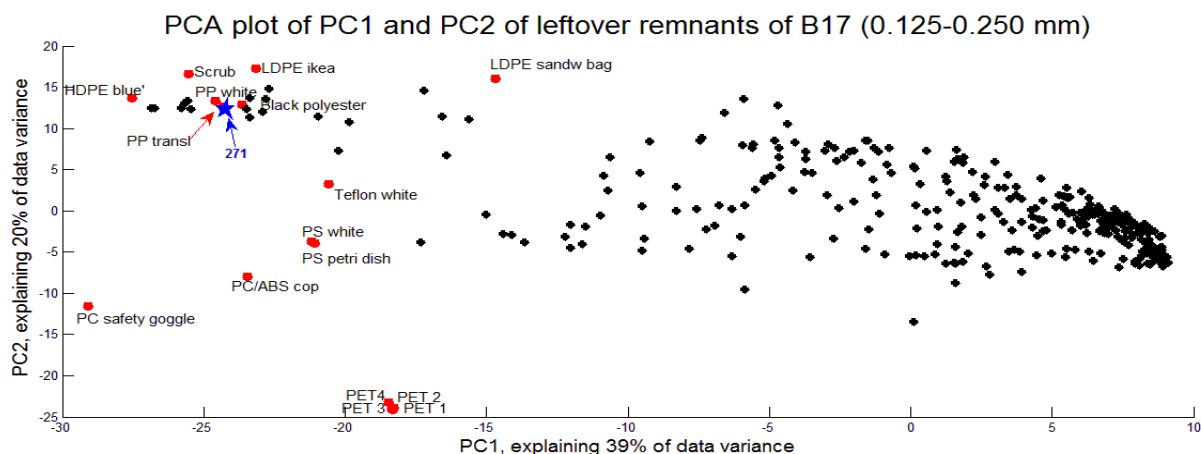
Figure 32. PCA plot of PC1 and PC2 of Raman spectral data of remnants left after microscopic study of Rhine sample B17 (0.125-0.250 mm). Sample 271 is marked for further study (see figure 34).

In the second PCA plot the majority of scatters are concentrated in the middle, where again no references are near. A small tail of samples tends towards PS. Now no samples are approaching PP.
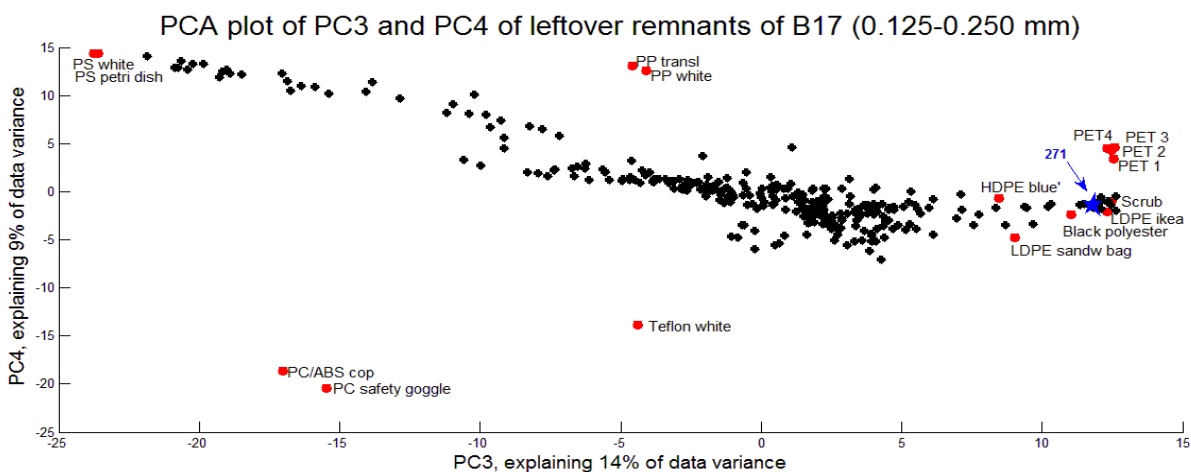
Figure 33. PCA plot of PC3 and PC4 of Raman spectral data of remnants left after microscopic study of Rhine sample B17 (0.125-0.250 mm). Sample 271 is marked for further study (see figure 34)

Sample number 271 is chosen for line plot analysis as it in the first PCA plot is arranged near the transparent PP reference (left above corner), but yet near to PE and distant to PP in the second PCA plot. In figure 34 sample 271 (black solid line) is overlaying the scrub reference (blue, dashed line) and the transparent PP reference (red, dashed line). Obviously, however the first PCA plot suggested otherwise, sample 271 is clearly similar to PE.

A range of individual line plots were made to study the similarity of the samples (not shown in this report). It appeared that the more samples were near to a certain reference, the more similarity was observed towards that reference. At further distances, less signal quality was observed, but also unexplained peaks appeared. This suggests the possible presence of functional groups that are lacking in the reference data set, including biological specimens.

Based on visual judgement of the line plots, at least 20 of the studied 320 samples were regarded to exist of, or comprise, PE. Twenty one samples were regarded to tend to PS. Some caution here is needed, as the styrene functional group, of which yet its ring mode vibrations are considered, can also be present in biotic molecules. Other polymers, such as PET, PC or Teflon were not identified.

Figure 34. Line plots of Raman spectra of sample 271, the PP transparent reference and the scrub reference. Before plotting, the baseline was removed, and scatter correction was applied to improve peak pronunciation. Because of this, the Y-ax is dimensionless. On the X-as: the wavenumbers in cm^{-1}. Laser wavelength: 785 um.

Conclusions on the spectroscopic analysis of leftover remnants of Rhine sample B17:
- Raman spectroscopy in combination with PCA demonstrated that after microscopic study, polymeric particles can still be present in the sample.
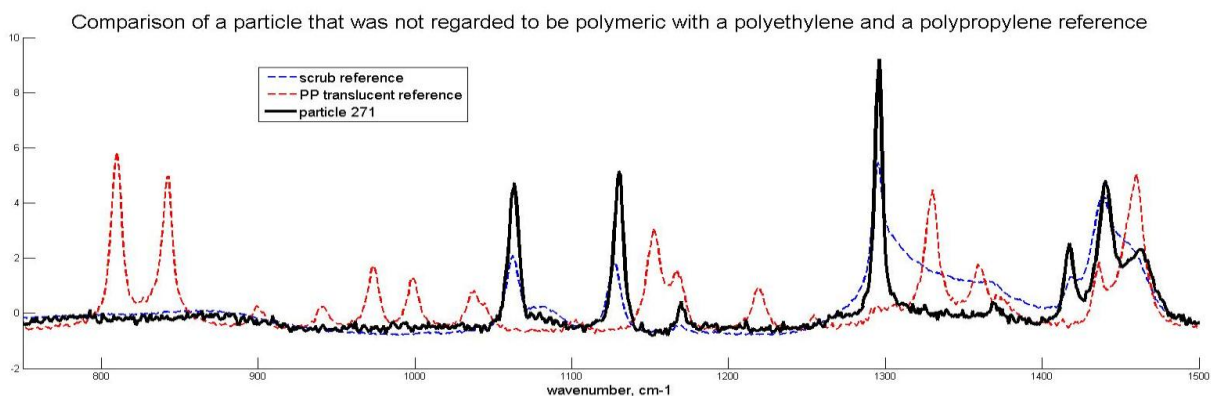- The line plot of particle 271 with the scrub reference and a PP reference learned that additional PC plots (PC3 and further) can be helpful to study similarity of particles.
- It cannot be excluded that the spectral dataset included organic remnants.
- In the case of sample B17, at least 20 out of 320 studied particles were identified as polymeric (approximately 6%). This does not imply that 6% of a full sample is overlooked, as already 1320 MPs were already sorted out from the sample during microscopic study.

6.8 **Discussion on the spectroscopic methods and PCA**

For the identification of MPs several methods are reported, such as FT-IR, Raman, Mass spectrometry and diverse application of Electron microscopy (Rocha-Santos & Duarte, 2015). FT-IR and Raman are seen as reliable methods to determine the factual chemical composition of polymers (Hidalgo-Ruz et al., 2012). This identification is important as visual selection can lead to false identifications (Song et al., 2015), however standardized protocols are yet lacking. Also SEM is reported as a useful tool to eliminate false identifications by studying the surface morphology of particles found in the Laurention lakes. Up to 20% of the selected particles under 1 mm appeared to be fly ash (Eriksen et al., 2013).

In this study on the presence of MP in the rivers Meuse and Rhine it was tried to purify the MP samples as much as possible by extensive laboratory processing and precise stereomicroscopic work. The extensive laboratory processing was needed to eliminate organic remnants and inorganic particles that both are part of the suspension mix of running rivers. It was demonstrated that precise manual selection of MP under the stereomicroscope can help preventing false identification. This was surely the case with the cenospheres and, to a lesser extent, solid fly ash particles, that could not removed beforehand by laboratory processing steps.

On the other hand, spectral analysis and PCA demonstrated that at least 6% of the particles that were not identified as polymeric during visual observation, were afterwards still designated as of polymeric nature. It must be noted that this test was only performed on one of the in total 67 studied MP samples and that is far from representative regarding all the studied sample within this research.

Contrary to FT-IR, with Raman so called map scans could be recorded. This offered the advantage that with one sample preparation, multiple MPs could be studied. FT-IR brought along the necessity to study MPs one by one, which is more time consuming. It occurred however that for one specific group, the white spherules, no useful spectroscopic images could be recorded with Raman, despite the efforts to alter the number of recordings and laser power. Films, probably polyethylene, appeared to be scatter sensitive with Raman spectroscopy and sensor saturation was regularly observed.

The used dataset was obtained from regular consumer products, of which verification took place on the description or resin code prints on the products themselves. A comparison of the reference spectra and examples in literature showed occasional spectral variations, but still similarity was demonstrated based on verification on expected peaks. To avoid self induced variation, for some polymers several different references were included in the reference data set. However, still caution can be needed, because the variations in polymer chemistry are practically inexhaustible. On the other hand, the influence of the probable blue color pigment Copper Phthalocyanine, by mean of new introduced peaks toward the regular Raman PE spectrum, did not seem to disturb the arrangement of the PE-based references as they were all arranged near to each other. Proper laboratorial polymer references are expensive. Even questionable is when a reference is precise: variations in tactility, the presence of functional groups, additives and copolymers would bring forth the necessity to obtain a very large reference set.

Further spectral improvements can make identification more precise, as is demonstrated by Kappler et al. (2015) with improved FT-IR recordings of the chemically closely related polymers Polyethylene terephthalate (PET) and Polybutylene terephthalate (PBT), by using a silicon filter.

Within this study, spectroscopic imaging and PCA showed that poor spectral data recording was observed regularly, which with Raman is expressed as noise recording, scattering and sensor saturation. Other laser power intensities and reputational recordings might help improve, however while making map scans, out of focus situations of the Raman microscope still occur as the MPs differ in shape and dimensions. With FT-IR was observed that both size fractions of the white spherules were sensitive to noise recording that is, despite the background recording beforehand, possibly due to atmospheric influences by H_2O or CO_2 (Shimadzu tutorial, 2015).
Also the influence of present H_2O in the samples themselves cannot be excluded, as polymers can absorb or include water. Using the Fourier Transform Infrared stage, spectral data is obtained by compressing individual particles on the ATR plate. The radiated surface of the white spherules is small: in between 0.05 and 0.28 mm^2, which is noticeably smaller than the ATR plate itself (2 mm^2). All the reference material was obviously larger than the environmental samples. Perhaps in the case of the particulate samples too little infrared radiation was absorbed, indicating that the apparatus' sensitivity is too low for this size range. Also more repetitions could perhaps improve the recordings, but this was not tested within the study. Finally, the environmental samples may have been effected by one or more degradation forces during their stay in the environment. It was not studied in detail whether sample processing, such as hot digestion with H_2O_2, might have influenced the MPs surface on which spectral recording aimed at.

Improvements for FT-IR and Raman can be found in better understanding of the optimal settings, for each polymer group.

To date, the application of PCA to identify large numbers of MP spectral recordings was not reported in literature yet. However, it was demonstrated in this study that PCA offers a useful tool to indentify multiple MP simultaneously. Labeling different samples with different scat colours, provides the ability to study differences in sample compositions mutually within one data set. As the used spectral data was not cleaned beforehand, individual line plots were needed to investigate the nature of outlying scatters and spread out scatter clouds in the PCA plots. The time this required, diminished the time gain of the PCA method. With the large size fraction of the transparent spherules, PCA was able to denote a polymer group that was not present in the dataset.

Improvements for PCA can be found in:
- Data preparation
    - the removal of record failures
    - shorter intervals between background measurements, and
    - auto correction for atmospheric influences during spectroscopy (for example the Shimadzu Atmosphere Correction Scan).
- A larger and more scientifically established reference data set.

6.9 **Blank control**

For 24 hours a clean and empty sieve set up was placed next to the tap at the monitoring station of Bimmen. The sieves were collected and processed as a common sample, what means that possible contents were rinsed into a beaker, that the sample was digested with H_2O_2 under a fume hood and led over a micro pore filter on a vacuum pump. The interim filtration step was not included. The micro pore filter was directly studied under the stereomicroscope. No target MPs nor fibres were observed.

Conclusion:
- Based on this short blank test is concluded that, for as far MPs in the size range 0.125-0.250 mm are concerned, contamination with air borne particles is not likely.

6.10 **Fibres**

Fibres were not the subject of this study but as their presence was observed in almost all studied samples, a short subsection is dedicated to them. Figure 35a shows an example of polymeric fibres that were found in the river Rhine. If a substantial amount of fibres were present, despite their relative high density they ended up entangled at the micro pore filter. This was caused during the laboratory processing, probably during the splitting of samples for which a magnetic stirring bar was used.

Heating up MPs in an acid environment, as was done in the beginning of the research, led to the observation of fibres and other MPs merging with each other (figure 35b).

In a fibre clew, particles from other MP groups were entangled as well, leading the clew to end up floating at the surface during the density separation step. Manual disentangling with two pairs of tweezers was needed to the release target MPs. Spherical particles were not susceptible to become entangled. However, films, scrubs and miscellaneous MPs, were all the more susceptible due to characteristic rough features. Free fibres were observed in the sinking layer during density separation as their density is higher than 1.2 g/cm/cm^3 (Hidalgo-Ruz et al., 2012).

Figure 35. Fibres were regularly observed and they occasionally caused hindrance for microscopic study, such as (a) A clew of polymeric fibres found in the Rhine River (Bad Honnef) holding target MPs. Scale bar = 0.5 mm. (b) A scrub particle and a polymeric fibre molted together. Scale bar = 0.2 mm. Picture taken in pilot phase after HNO3 digestion. (c) Lumps of (suggested) cotton fibres found in Meuse river (sample E14, 0.250-

In the larger fraction of sample E 14 remarkable brownish lumps were found (figure 35c). In the lumps, target MPs and also regular observed polymeric fibres were entangled. The lumps comprised lots of very fine fibres that were too small to be disentangled individually and were obviously much less in diameter than the regularly observed polymeric fibres. The nature of the lumps was not determined within this study. Based on its small diameter it may comprise organic fibres like cotton (cellulose based fibre) or wool (protein based fibre). Remarkably, it was observed that sample E14 was the only sample in this study that contained not any particle in the size range 0.125-0.250mm. It is not known whether this is related to the presence of the described fibre lumps.

6.11 Recognition of fragments obtained from household materials and fresh water fish

To increase the recognition of particles under the stereomicroscope, three polymeric particles were obtained from household materials and studied beforehand. These were:
1) PET fragments, derived from teenage glitter spray (figure 36a).
2) Fragments from expanded insulation foam, probably Polyurethane (PUR) (figure 36b and 36c).
3) Fragments from the scourer sponge used to clean the sieves in between samplings (figure 36d)

Furthermore, to increase the recognition of MPs and to exclude possible organic material to be designated as MPs, the remains of fish were studied in detail. These were:

1) Fish scales, derived from two common fresh water fish species:
   a. Common roach (*Rutilus rutilus*), and
   b. Perch *(Perca fluviatilis)* (figure 36e).
2) Fish eyeballs, isolated from a Cormorant pellet (probably *Phalacrocorax carbo sinensis*) (36f).

The characteristics of the above mentioned specimens, their recognizability and their presence in the MP samples are being discussed.
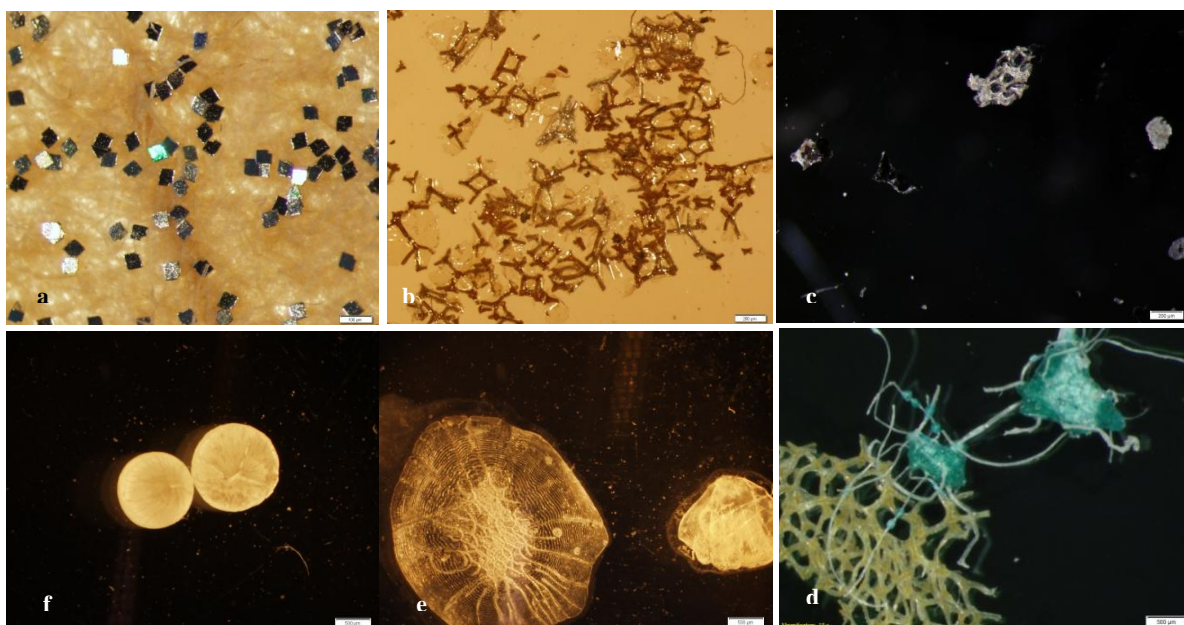
Figure 36. Stereomicroscopic images of several objects studied in detail for increased particle recognition. Clockwise: (a) PET fragments derived from teenage glitter hair spray. (b) Expanded construction insulation foam fragments. (c) Particle similar to expanded construction foam found in the Meuse, sample E8. (d) Details of fragments of the used scouring sponge. (e) Unprocessed fish scales from a Common roach (*Rutilus rutilus*) and (right) a Perch (*Perca fluviatilis*). (f) Unprocessed fish eye balls derived from a cormorant pellet, fish species unknown. Scale bars for a+b = 100 µm, for c = 200 µm and for d,e,f = 500 µm.

PET particles derived from teenage glitter hair spray
First, the presence of PET was verified on the product label. Then, 2 grams of teenage glitter hair spray were dissolved in hot (not boiling) water, filtered over a ø 47 micro pore filter, rinsed with MilliQ and directly studied under the stereomicroscope (figure 36a). PET is reported denser (1.37-1.45 g/cm^3) than saline water (1.2 g/cm^3) and expected to sink along with sediment particles (Hidalgo-Ruz et al., 2012).
The PET flakes deviate strongly from sand particles as they, contrary to sand particles, strongly reflect light. Both these characteristics would help to distinguish them. PET particles like those derived from the teenage glitter hair spray were not found in neither Meuse, nor Rhine samples.

<u>Particles from expanded construction insulation foam</u>
Building construction foam that was exposed to weather conditions for at least five years was crumbled by hand and stored in a Petri dish (figure 36b). Similar particles were occasionally observed in both size fractions of the MP samples, however they mostly occurred in the small size range (figure 36c). It was difficult to pick suchlike particles up with tweezers, as the fragments crumbled easily. If they occurred, their number was relatively low: estimated 1-5 particles per sample. One exception was formed by sample B6, size fraction 0.125-0.250 mm, where several tens of these particles appeared. Their identity was visually conformed but not verified with spectral analysis.

<u>Fragments from the scouring sponge used to clean the sieves in between samplings</u>
In this study a double layered scouring sponge was used for cleaning the sieves. The two layers comprise a yellow, soft squeezable bed with a green scouring layer on top. Scourer and sponge fragments were pulled out with a pair of tweezers and studied under stereo microscope (figure 36d). The main idea behind this was to avoid scourer fragments – that are of polymeric origin - to become erroneously considered as MPs derived from the rivers. Obviously the sieves were duly rinsed before following sampling period and no scourer fragments were derived from the rivers.

<u>Fish scales.</u>
In fresh water systems, fish scales could been expected to part of the mix of suspended matter and to end up the sieve beds. To increase distinctiveness, fish scales were obtained by scraping them off a freshly caught Perch and Common roach. The scales were not rinsed but directly digested with H_2O_2 on a Schott electrical heating plate for four hours (exact temperature could not be determined). The scales were affected at the edges but were not crumbling. The features of fish scales – either digested or not digested – were not recognized in any sample but it must be stressed that there was no focus on identifying them separately.

<u>Fish eyeballs</u>
Before Raman pointed out the polymeric nature of the white spherules, a Cormorant pellet researcher at Rijkswaterstaat suggested that they might be fish eyeballs. Two eyeballs were isolated by hand from a random Cormorant pellet (probably *Phalacrocorax carbo sinensis*) and directly studied under the stereomicroscope.
The eyeballs are identifiable because of their external characteristics and the glass-like appearance. With a pair of tweezers, the eyeball could not be compressed. Just as with the fish scales, fish eyeballs were not found separately in the samples.

Conclusions:
- PET particles like those derived from the teenage glitter hair spray were not found in the rivers.
- Fragments similar to those self derived from the scourer that was used for the sieve cleansing were not observed in this study. This indicates that self contamination did not occur.
- Fragments similar to those self derived from a piece of expanded isolation foam, were regularly observed. Their occurrence varied between samples, on average between 1-5 particles per m^3.
- Remnants from fish, i.e. fish eyeballs and fish scales, that possibly could be mistaken for MPs, were not observed. It is unknown whether they were not sampled or just digested during processing.

6.12 Cenospheres
Microscopic study revealed particles that had an approximately similar appearance to transparent spherules, and, to a lesser extent, to white spherules (figure 37). These so called *cenospheres* ('hollow spheres') can be described as brownish or grayish, spherical, hollow, translucent aluminosilicate particles. As silicates are not Raman active in the polymer finger print region, their nature was not verified with Raman. However, a commercial supplier of cenospheres (PMS BV), was able to verify them as cenospheres.
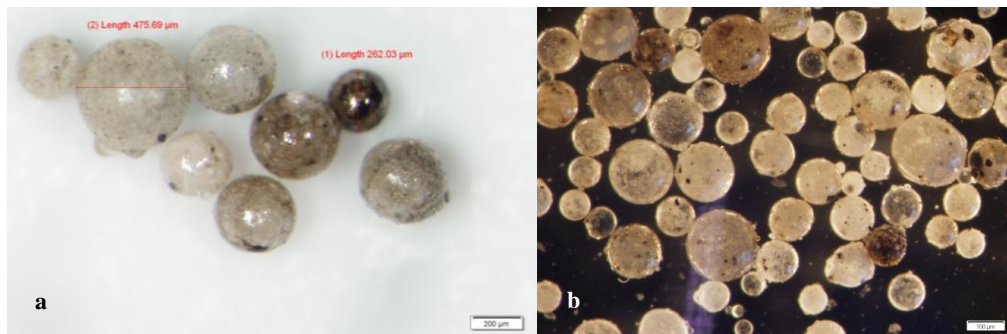
Figure 37 Examples of cenospheres from (a) The Rhine river (scale bar=0.2 mm), and
(b) from supplier PMS BV (scale bar=0.1 mm)

Similarities of cenospheres to MPs are:
- Spherical form.
- Comparable size range (50 µm to approx 500 µm).
- No obvious effects of H_2O_2 digestion.
- Floating on plain ultra pure water.
- Translucent under light microscope.

Differences of cenospheres to MPs are:
- Rigid, but hollow.
- Shattered by exerted tweezers pressure.
- Ability to scratch a plastic Petri dish.
- Electron microscopic imaging reveal irregular surface.

Origin of cenospheres
Cenospheres are part of fly ash that is initiated in coal fired energy plants. Fly ash also contains
magnetic beads and solid beads, both of which are much denser than saturated saline water.
Cenospheres comprise less than a 0,5% of the total fly ash distribution (Li, Xu, Feng & Shang,
2014).

Cenospheres are recovered in large scale open air float/sink processes (Blissett & Rowson, 2012).
They are referred to as inert and applied as lightweight filler in road and building construction
industries. They are also used as soil amelioration, with the aim to raise pH levels and increase soil
texture, as reported by Blissett and Rowson (2012).

Cenospheres were identified by pinching them with squeezers, if they imploded and crumbled into
pieces leaving half shells or less. They were found in both Meuse and Rhine river samples,
predominantly in the smaller size range. Not all samples contained cenospheres and their abundance
fluctuated (section 7.10). It is not known in detail how the cenospheres end up in fresh water
systems. They could become lost during recovery, transport or appliance, such as run-off from
farmlands after amelioration. According to PMS BV (personal communication), can it not be excluded
that cenospheres escape through the flue gas treatment system at the coal fired power plants.

Their composition varies widely based on the circumstances and place where they are originated
from. Major contributors are SiO_2 (29-65%), Al_2O_3 (17-35%), Fe_2O_3 (3-19%), CaO (0-33%), MgO
(0-7%) and K_2O (0-5%). Smaller contributors are TiO_2, P_2O_5 and BaO. The size distribution of
cenospheres is reported from 1 micron up to 500 microns (Ghosal & Self, 1995).

Fly ash particles may contain environmentally sensitive elements. Izquierdo and Querol (2012)
reviewed over 90 studies on the leaching behavior of 34 elements out of fly ash and concluded that
overall these elements are not easily released to the environment, but that acidity as well as
alkalinity play a role in their leaching behavior.

Cenospheres are included in this report for two reasons:

1) Accuracy of MP determination.
   Improved sample clarity and better light conditions have revealed the presence of cenospheres in the filtrate. Due to the wide range of densities, the removal of cenospheres from the sample was difficult. In the laboratory density separation step, cenospheres will float just like other MPs in the saline solution and end up at the cellulose microscopic filter.
   During microscopic study of the samples, the distinction whether a particle was polymeric or not, was made by applying the destructive and time-consuming method of squeezing them. If a particle grinded and imploded, than it was not polymeric. Their similarity and distribution may jeopardize the accuracy of MP determination and number count. The abundance of cenospheres was recorded in a few occasions, what is discussed in section 7.10.

2) Possible similar risks of cenosphere ingestion as of microplastics ingestion.
   MPs are reported to be ingested by various species of marine life. MPs are attributed to cause gastro-internal blockages to marine organisms and their internal presence can cause adverse effects. The carriage of hydrophobic pollutants by ingested MPs may be of additional concern.

Considering:
- that cenospheres are also present in the fresh water column,
- that their appearance is comparable to MPs,
- that they were found in the same size range as MPs,
- that their distribution in fresh waters may be comparable to MPs,
- that they are just like MPs designated as inert,
- that they may possibly leach harmful elements under changing pH conditions,
- that from uptake till excretion pH conditions in the gastro-intestinal tract can change.

Gave idea to the thought that, regarding the adverse effects or the putative harm of MPs to marine life, similar concerns may be applicable to cenospheres. Up to date, no studies on the ingestion of cenospheres by marine life were found.

Conclusions on cenospheres:
- Cenospheres were found in both rivers.
- Cenospheres are Aluminosilicate particles, not polymeric.
- Cenospheres originate from the combustion of coal, probably in power plants, and may contain pollutants that may be released under changing pH conditions.
- Their emission routes to the rivers are yet unknown.
- Cenospheres may be mistaken for white or transparent spherules.

6.13 Tiny silicate fragments

In the residue layer of the small size fraction of Rhine samples, very thin, fragile, translucent sheet-formed fragments were found. Depending on the light conditions, also a glance was observed. Its fragility makes it impossible to pick them up with tweezers as they crumble away (figure 38).

It was thought that these fragments might be PET flakes, To study this in detail, with the Raman setup, spectra were recorded from an air dried sediment sample of Rhine sample B8. The spectral data did not show any similarity to PET. It must be noted that Raman images were derived in the polymer finger print region and that clues to non-polymeric bonds, for example mineral bonds, were not studied in detail.

Figure 38. Scanning Electron Microscopic image of a tiny silicate fragment. Magnification: 400 times.

Prof. dr W. (Wim) van Westrenen, professor at the department of Life Sciences, Faculty of Earth And Life Sciences, VU University Amsterdam, studied the sediment sample briefly under a polarization microscope and confirmed – for at least a part of the fragments – a silicate nature. This was based on his trained eye and the fact that the colour of particles changed as a result of switching from lane-polarized light to cross-polarized light. It must be noticed that crystalline polymers could also be detected with the same set up, as was demonstrated with some transparent spherules. However, given the fact that Raman did not provide a polymer match, it can be assumed that the fragments were not of polymeric origin indeed.
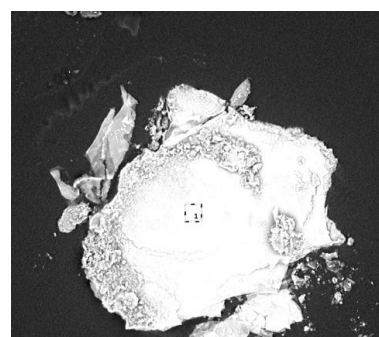
6.14 Pumps possibly generating microplastics

Contrary to the other designated groups, the so called miscellaneous MPs are generally diverse in both colour and size. However, occasionally multiple similar particles were observed within the same single sample. In the larger fraction of sample B5, similar particles were found twice (figures 39 a, b and c). This observation raised the interest to know where these similar particles stemmed from. It is important to bear in mind that the amount of river water passing by the monitoring stations is considerably larger than the amount taken in: approximately 30 m^3 per hour versus hundreds of thousands m^3 (Meuse) or several millions m^3 (Rhine) per hour. This indicates that either many similar particles are present in the river water column during the sampling period, or that they originate from larger plastic parts and become generated in the sampling or laboratory process.
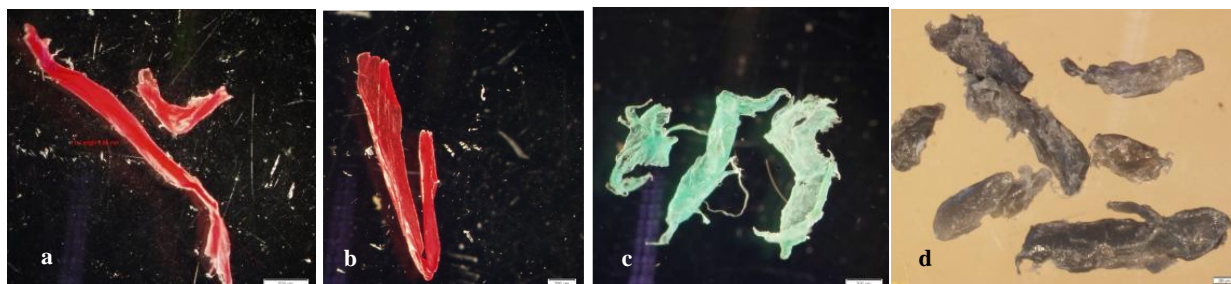
Figure 39. Stereoscopic images of similar particles found within a single sample.
(a,b,c) Three red and three green fragments found at Bimmen in the larger size fraction of sample B5.
(d) Grey fragments found at Eijsden in sample E4. Scale bar for a = 0.5 mm, for b, c and d = 0.2 mm.

Suggested is that the similar particles stem from either the same source or the same origin by one of the following processes:

1) Multiple similar particles were present in a plume passing by the monitoring stations.
   Such a plume may originate from an emission upstream. Fragments from waste treatment or (traffic) incidents may run down to the rivers. An inquiry at Dutch water boards learned that pumps in sewage systems may damage present plastic fragments. It was also suggested that the large turbines in the electricity power plant at Lixhe may be able to shred plastic litter into smaller fragments and that this results in a plume of similar MPs passing by the monitoring station at Eijsden.

2) The inlet pumps themselves generate MPs by shredding larger plastic particles along with the water intake process. At Eijsden and Lobith centrifugal pumps were taking water in, while at Bimmen and Bad Honnef eccentric screw pumps are installed. An inquiry at the monitoring stations learned that centrifugal pumps may be able to shred plastic parts but that it is considered unlikely that eccentric screw pumps are able to do so.

The idea that fragments are generated during the laboratory processing is not likely as not any mechanical processing was included in the laboratory processing. With a view to accuracy and certainty for a future monitoring program more knowledge on the origin of MPs and the possible risk of self induced MP generation is required.

6.15 Possible damage of sonication to microplastics

During studying the small size fraction of sample L17 it was noticed that some white spherules appeared to show different characteristics from those in earlier non-sonicated samples. Their resistance to tweezer pinching seemed to decline, which manifested itself in particles easily falling apart. It appeared that this sample was sonicated to remove coal fragments.

To investigate whether sonication could damage sample MPs, two white spherules from the sonicated sample were randomly selected for electron microscopic imaging. A third white spherule was handpicked from a part of the same MP sample that equally processed, but not sonicated. Figure 40a displays the white spherule that was not part of the sonication process. However not perfectly smooth, the particle displays a globular form. Figures 40b and 40c display two white spherules that were isolated from a sonicated part of the same MP sample. Obviously, the particles surfaces show external deterioration and the shapes are less spherical. The two particles in question were not measured before and after the test, so the actual size reduction cannot be determined.
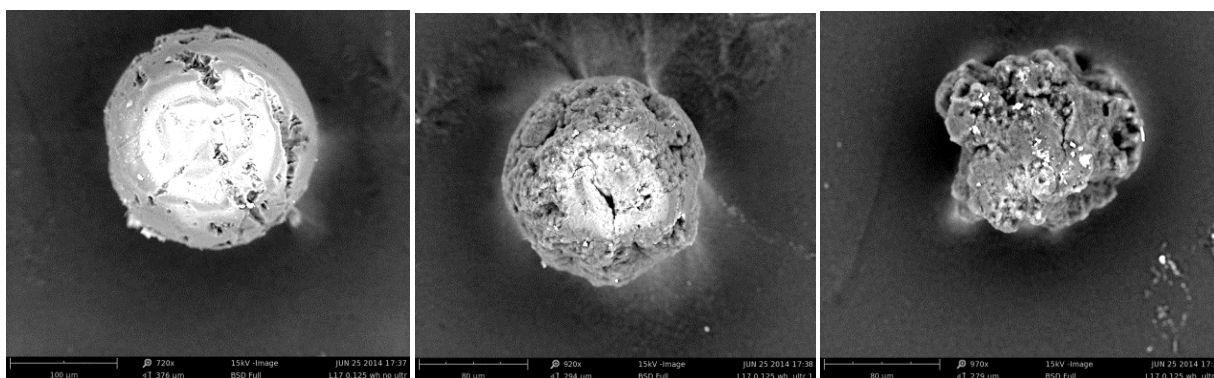
Figure 40. Scanning electron microscopic images showing the observed effects of sonication to white spherules (sample L 17, 125-250 µm). Images created by a Phenom SEM (800 07334/PW-100-017).
(a) White spherule derived from a non-sonicated part of the sample. Scale bar = 100 µm.
(b) and (c) Particles each derived from a sonicated part of the sample. Scale bar = 80µm.

Sonication test with reference plastics

To probe whether sonication could also possibly affect other target MPs, one set of reference plastics as described in appendix 4 was placed in a 150 ml PFA beaker. Added were 2 unprocessed white spherules, 2 transparent spherules and 2 scrubs from the large size fraction of sample B5. The beaker was filled up with MilliQ to 100 ml, and the suspension was sonicated for 20 minutes at 20 kHz, without pulsation, on a Branson 5510 ultrasonic cleaner. After this, the contents were filtered over a cellulose micro pore filter and studied under a stereomicroscope. Both the PE sheets from the set of reference plastics were not found back. With the stereomicroscope, also no external effects to the white spherules were observed. The reference plastics were not weighed for and afterwards the test, but possibly the high frequent sound energy could have affected other plastics as well. This test was performed once.

The precise mechanism to the harmful effect of sonication is not known in detail. The first observation demonstrated that the white spherules were affected, but in the second observation this was not clearly determined. It must be noted that in the first case it concerned specimens from the small size fraction, while in the second case larger specimens from the large size fraction were selected. Similarity in polymer type between the two specimens can be debated. Finally, it could be that other particles in the suspension, such as the coal fragments, collide with the white spherules can cause damage to them this way.

Conclusion on sonication:
- Sonication may damage polymers with weak molecular bonds, such as films and white spherules.
- Sonication may possibly lead to size reduction and hence particle loss during interim filtration
- As a result of the above, sonication may affect MP sample weight determination.

7. Quantitative results

7.1 Introduction to the quantitative results

During microscopic study, the particles were identified based on their external features. Isolated particles were individually counted and, after completion, measured per group. These counts and weights were used as input for this chapter. The quantitative data, i.e. the particle numbers and the sample concentration levels, are presented and discussed here. As the method of laboratory processing might have influenced the quantitative results, the accuracy of the applied sample splitting and uncertainties regarding sample weighings are discussed first.

7.2 Accuracy of sample splitting

For faster processing, samples were split into parts. A challenge that was encountered is to create a method based on which representative sample parts can be obtained. This appeared to be difficult as the particulate matter can vary per sample, by means of specific gravity, shape, size and abundance. Besides MPs also inorganic particles and organic remains are present. The only suggested method was to stir a solution and to use a pipette to obtain weight divided parts from this solution.

Splitting samples by this method, and succeeding extrapolation of recorded data up to full sample levels, might cause uncertainty that influences data precision. To determine the accuracy of the laboratory processing, four tests were performed that are discussed in this subsection.
If not denoted otherwise, the materials used comprise a 10 ml pipette with an enlarged pipette point opening, a regular balance (Sartorius L420S) a microbalance (Mettler Toledo MX5) and an IKA Big Squid stirring device. MilliQ was added from newly obtained wash bottles that were only used for this study. All tests were performed under a fume hood.

7.2.1 Pipette test

The accuracy of the pipette and the manual accuracy were determined with the following test: 100 ml of milliQ at room temperature was poured into a 250 ml glass beaker. One clean and dry PFA 100 ml measuring cup was placed onto the microbalance and set to zero. First an amount of 7 ml was pipetted and discarded into the sink. After this, aliquots of 7 ml were pipetted from the beaker into the PFA cup. In between weights were recorded. After a repetition of 10 times, the deviation of the pipette was determined at 0.04%.

7.2.2 Splitting sample B5 (0.250-5 mm)

Red preprocessed microspheres (further: red spherules) were used to test the accuracy of laboratory processing. The polymer is polystyrene divinylbenzene (PSDVB), its density is reported for 1.06g/cm^3. The weight of an individual red sphere was determined by successively weighing 10 spheres on a microbalance and is set to 0.0160 mg.

An amount of 1.840 mg red spherules were placed on top of the sieves of sample B5, just before sample collection. This particular sample was chosen as no sediment or organic material were visibly present that could possibly influence the weight distribution during splitting. Due to the known regular size of the red beads, 310 μm, all of them were expected to remain on the 0.250 mm sieve and hence only to appear in the large size fraction. The sample was further treated as a common sample and after the digestion step split into 2 parts, following this procedure:

A magnetic stirring bar was placed in a clean PFA 200 ml beaker and placed onto a balance. The balance was set to zero. The sample was rinsed with MilliQ directly into the beaker and filled up to a total weight of 70 grams. The beaker was placed on a magnetic stirring device and a small vortex was obtained. A 100 ml glass beaker was placed on the balance. The scale was set to zero. Using a pipette, 35 grams were extracted from the suspension in the 200 ml PFA beaker, in steps of 7 ml. The pipette point was set to one third of the volume and halfway the vortex and the beaker wall. In the last step 6.2 mg was needed to complete the 35 grams. This method resulted in 2 samples of each 35 grams: part 1 (the pipetted part) and part 2 (the residue in the beaker).

Both halves were separately washed with MilliQ over ultra pore cellulose filters and the filters were directly observed under a stereomicroscope. The materials used, i.e. pipette point, stirring bar and beakers, were washed above a new cellulose micro pore filter on a vacuum pump to see whether any red spherules remained on them. Also the soil sieve beds of this sample were inspected under the stereo microscope. In table 13a (top) the observed number of particles are shown and in table 13b (bottom) the associated weights. It appeared that in the residue part, 4 out of 7 groups showed

larger numbers. With reference to the weight contribution, at all times, larger weights were recorded in the residue part.

For films and scrubs it was observed that however the pipetted part contained more particles, the associated weights were less than in the residue part. This suggests that within one sample, smaller films and smaller scrubs are more prone to being pipetted, than larger films and larger scrubs, causing an higher weight contribution with less particles. The largest difference in particle distribution was observed for the transparent spheres and the scrubs: both 39% versus 61%, however each in opposite parts.

From the pre-added 1.84 mg of red spherules, just 1.50 mg were recovered. Apparently, during sample collection, laboratory processing and/or microscopy study, 18% was lost. The recovery rate was for this reason set to 82%. No remaining particles were found on the materials used.

Table 13. The results of splitting sample B5 (0.250-5 mm), on which a known amount of red spherules were deliberately added. After splitting the sample into halves, both parts were studied under the stereomicroscope. (a, above): Particle numbers and (b, under) the associated weights . Yellow marking point out the highest particle number and highest weight.

(a) Particle numbers	Red spherules		White Spherules		Transparent spherules		Films		Other		Scrubs	
Pipetted part	42	45%	33	40%	13	39%	212	53%	41	44%	58	61%
Residue part	52	55%	49	60%	30	61%	189	47%	53	56%	37	39%
Total number	94		82		43		401		94		95	

(b) Weights (mg)	Red spherules		White spherules		Transparent spherules		Films		Other		Scrubs	
Pipetted part	0.60	40%	1.01	46%	0.48	28%	4.82	41%	1.71	46%	1.19	47%
Residue part	0.90	60%	1.18	54%	1.23	72%	6.82	59%	2.01	54%	1.33	53%
Total weights	1.50		2.19		1.71		11.64		3.72		2.52	

Conclusions:
- This test showed that splitting samples on a weight basis can introduce uncertainty on both number and weight determination.
- Equal abundances over the parts were not achieved for any of the particle groups. The scrubs deviated the most : 61 % of the scrubs were pipetted, while 39 % remained in the beaker.
- Equal weight distributions were not achieved for any of the particle groups. The transparent spherules deviated most: 28 mass% was found in the pipetted half, en 72 mass% in the remaining part in the beaker.
- After splitting was observed that the particle distribution and weight distribution do not have to be related. Larger numbers of films and scrubs in the pipetted half contributed to less weights.
- 18 mass % of the pre-added red spherules were lost during sample collection, laboratory processing and/or microscopic study. This indicates that there is risk that other particle groups become lost during processing and that this influenced particle and MP weight concentration calculations.

7.2.3 Splitting a suspension of only red spherules
Because of the diverging results of splitting sample B5 (previous section), two different pipetting strategies were tested.

A) A magnetic stirring bar was placed in a clean and dry PFA 100 ml beaker and placed on a balance. The balance was then set to zero. A clean and empty 150 ml PFA beaker was filled with 7.675 mg pre-weighed red spherules and filled up with milliQ to a total of 40 grams. The beaker was placed on a magnetic stirring device. Stirring started and the rotation was increased until a small vortex appeared: approximately down to four-fifth below the surface. Three aliquots of 10 ml were pipetted at a depth of one third under the surface and halfway between the vortex and the beaker wall. The fourth aliquot consisted of the remaining layer in the beaker. Each part was led over a cellulose micro pore filter on a vacuum filtration pump.

The results of this test are displayed in table 14a (left). Obviously, the three pipetted parts contained similar amount of red spherules, while the leftover part in the beaker contained twice the amount of one pipette part. The particle distribution is approximately 1:1:1:2.

B) As A), but now an amount of 6.722 mg red microspheres were weighed and also a deeper vortex was achieved: down to one-third below the surface. Parts were pipetted at different and randomly chosen depths. The results of this test are presented in table 14b (right). Here a distribution that approaches 1:1:1:1 was obtained.

Table 14. The results of two different sample splitting approaches. Known amounts of red spherules were brought in suspension in two beakers on stirring devices. In each beaker a different vortex was achieved. Three times an amount of 10ml was pipetted from each beaker. 'Rest' regards the remaining part in the beaker. For each part the red spherules were filtered and weighed separately.

	First strategy: Small vortex in the beaker, only one pipette depth. Added: 7.675 mg red spherules.		Second strategy: Deeper vortex in the beaker and different pipette depths. Added: 6.722 mg red spherules.	
	Recovered (mg)	Recovered %	Recovered (mg)	Recovered (%)
Pipette I	1.47	19	1.45	22
Pipette II	1.29	17	1.64	24
Pipette III	1.48	19	1.55	23
Rest	2.90	38	1.56	23
Total Recovered	**7.14**	**93**	**6.20**	**92**

Conclusions:
- A combination of a deeper vortex and random varying pipette depths led to a better contribution of particles over the four parts than a small vortex and just one stationary pipette depth.
- The total recovery rate was not improved by using a different pipette strategy, in both cases 7 to 8% of red spheres were lost during laboratory processing and/or microscopic study.

In this study, the samples were split according to the second strategy: a vortex down to one third of the surface and different pipette depths.

7.3 Weight deviations of stored samples over time
To investigate possible weight deviations over time, sample L4 was measured again on the same microbalance, 3 months after the initial sample completion. The Eppendorf tubes in which the MPs were stored were not touched and not opened in between.

Table 15 presents the initial empty Eppendorf tube weight and results of both weighings. Obviously, the second weighing resulted in decreasing weights for all particle groups, but the decline rate differs between them. The largest decline was observed for the white spherules in the large size fraction (36%).
For the large size fraction of the miscellaneous group, which appeared to be the heaviest group within the sample, just a decline of 0.4% was reported.

Remarkably, for the white spherules in the small size fraction, the second full weight was less than the original empty tube weight (yellow markings in table 15). It must be noted that the samples in question are very light compared to the tube weights. The fact that all second weights were less than the first series, suggests that the microbalance consequently measured less. This may be caused by microbalance movements or a recalibration in between the two measurements.

Also suggested is that a part of the weight decline could be caused by water loss. The white spherules were earlier discussed with regard to the retention of water in its rather open internal structure (section 6.2), but actually all polymers absorb water when immersed. Depending on the polymer type, weight increase from nil to 1.2% are reported (Curbell plastics, 2015).
PP, of which the Eppendorf tube is made, is known to have low water permeability compared to other polymers (Dyrstad, Veggeland & Thomassen, 1999). It was not studied in detail, but whether three months of storage were sufficient for water to diffuse through the tube wall is doubtful; also the closure of the tube lid can be debated.

Table 15. Re-measurement of all distinguished MP particle groups in sample L4, 3 months after initial weighing. Per MP group is shown: 1) the empty Eppendorf tubes weights, 2) the first weighing on March 21st , 2015 and 3) the determined weights per MP group. The right part of the table shows 4) the second measurements at July 22nd, 2015, 5) the difference between the measurements and 6) the ratio of the decline. The yellow markings denotes a second measurement that was less than the original empty tube weight.

Group	First weighing of sample L4			Second weighing of sample L4		
	Empty Eppendorf tube (mg)	Tube weight after sample completion on March 21st 2015 (mg)	Sample weight (mg)	Tube weight on July 22nd, 2015 (mg)	Differences between tube weights (mg)	Difference to original weights (%)
Large size fraction						
White spheres (0.250-5 mm)	998.976	999.145	$1.7.10^{-1}$	999.083	$-6.2.10^{-2}$	36%
Films (0.250-5 mm)	1003.716	1004.607	$0.9.10^{-1}$	1004.533	$-7.4.10^{-2}$	8.2%
Miscellaneous (0.250-5 mm)	1022.934	1026.133	3.2	1026.120	$-1.3.10^{-2}$	0.4%
Transp. spheres (0.250-5 mm)	985.678	986.304	$6.3.10^{-1}$	986.200	$-1.0.10^{-2}$	1.6%
Small size fraction						
White spheres (0.125-0.250 mm)	997.055	997.127	$7.0.10^{-2}$	997.020	$-1.1.10^{-1}$	-
Films (0.125-0.250 mm)	999.009	999.157	$1.5.10^{-1}$	999.128	$-3.1.10^{-2}$	21%
Miscellaneous (0.125-0.250 mm)	1007.003	1007.841	$8.4.10^{-1}$	1007.761	$-8.0.10^{-2}$	9.5%
Transp. spheres (125-250m)	999.017	999.240	$2.2.10^{-1}$	999.226	$-1.4.10^{-2}$	6.4%

Conclusions:
- Re-measuring sample L4 showed that weight deviations can occur over time. The deviations are not equally large over the associated MP groups.
- It must be noted that the sample weights are small compared to the empty tube weights and that temporal influences, such as humidity, or a moved microbalance could have contributed to the deviations.
- Possibly not all groups were full air dried when initially weighed. Retaining water could have escaped from the Eppendorf storage tubes over time, resulting in weight loss.

7.4 Microplastic concentrations in the Meuse

MPs are suspended matter that comprise different densities, shapes and volumes. Due to this, the particle concentrations and MP weight concentrations can differ when succeeding sample series are being studied. Both are addressed in this subsection. The concentrations of particles in a volume can be expressed in two ways:
- The number of MP per unit of volume : MP particle concentration (MPs/m^3).
- The weight of MP per unit of volume : MP weight concentration (mg/m^3).

7.4.1 Microplastic particle concentrations in the Meuse

In figure 41 the MP particle concentrations of nine fully processed Meuse samples are presented against the primary Y-axis. The red columns represent the large size fraction and blue columns represent the small size fraction. The samples are arranged on the x-axis based on increasing river discharge. The least recorded average river discharge was 78 m^3/s and the largest 463 m^3/s.

In all cases more small size fraction MP (in blue) were found than larger fraction MP(in red), except for the least and the highest river discharge levels. Leaving these two aside, from 1.4 up to 3.1 times more MP from the small fraction were found than from the larger fraction.

Sample E14, that showed large lumps of thin fibres (section 6.10) and which did not contain any MP in the small size range, belongs to the least recorded discharge (78 m3/s). Sample E4 (463m3/s) is the only fully processed sample where the discharge rate exceeded the power plant capacity and water was released over the dam. The MP particle concentration could not be related to river discharge.

7.4.2 Microplastic MP weight concentrations in the Meuse

Per individual sample series, all recorded weights of all distinguished MP groups were consolidated into one total sample weight. These aggregated weights were used to calculate the MP weight

concentrations per sample. The MP weight concentrations are marked with a black dash and presented against the secondary y-axis in figure 41. Observed MP weight concentrations range from 0.03 mg/m^3 (or µg/l) to 0.38 mg/m^3, but remained in 5 out of 9 samples below 0.10 mg/m^3. The MP particle concentration could not be related to river discharge.

7.4.3 Abundance and distribution of microplastics in the Meuse

In the river Meuse, no spherules were found. For this reason, only films and miscellaneous MPs were initially recorded. However, in addition to this, in some samples scrubs were designated as individual group. Sheets were at all times least abundant in both the small size fraction (0%-12,5%) and the large size fraction (2.5%-24.3%). Based on the samples where scrubs were separately recorded, their relative abundance was calculated for 37.9% - 43.6% in the small size fraction and 25.4%-40.1% (in the large size fraction). Taking only the samples where scrubs were separately recorded into account, the abundance of miscellaneous MP was calculated between 53.3%-56.5% for the small size range and 57%-69% for the larger fraction, indicating that scrubs formed a relative large share of the miscellaneous group.
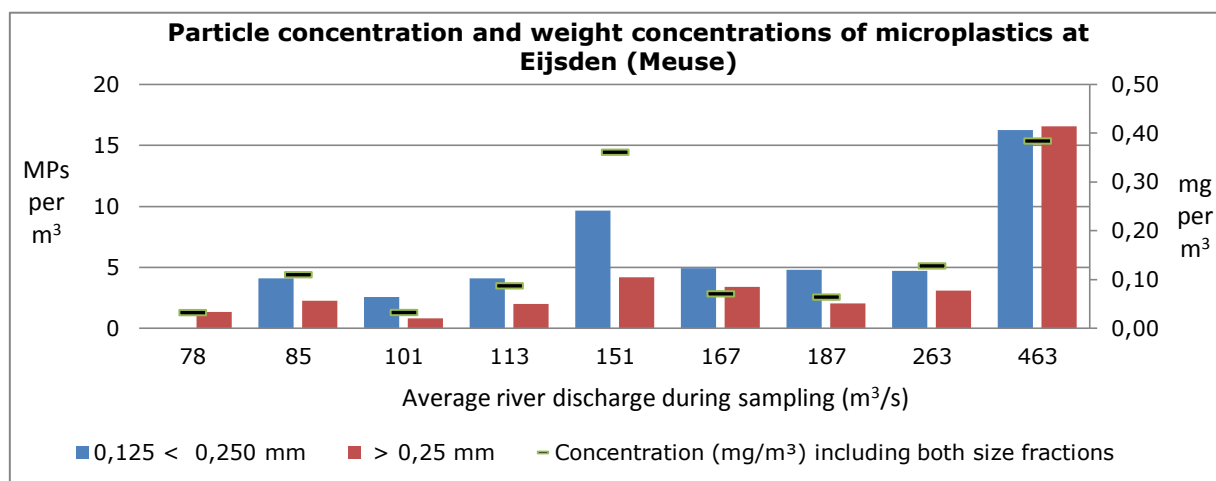

Figure 41. The MP particle and weight concentrations of 9 fully processed samples from the river Meuse. The river discharges are increasingly arranged on the X-axis, and represent from left to right: samples E14, E12, E11, E10, E15, E8. E7, E6, E4. On the primary Y-axis: MP particle concentrations for either size fraction. On the secondary Y-axis: the full sample MP weight concentrations, marked with a black dash . Sample E14 (78m^3/s) was fully processed, but contained no particles in the small size range.

7.5 The effects of turbidity on sampling in the Meuse

Regarding the Meuse river, the highest discharges were observed in the first four sampling weeks. After this, the discharge rate dropped gradually to remain around 100 m^3/s. Samples E1 (517 m^3/s) and E3 (630 m^3/s) were aborted as the whole sieve stack flooded. For sample E2 (505 m^3/s), the bottom sieve (0.125 mm) clogged. For the river Meuse, turbidy is a factor to be taken into account. The risk of flooding filters is due when the tap flow rate exceeds the rate of water seeping through the sieves. A declined tap flow rate decreases the risk of sample failure.

The samples that flooded were excluded from this research as most likely MPs were lost with the flooding water. It has not been studied in detail which kind of particle matter, organic or inorganic, was primarily causing the clogging risks. The volumes of MPs derived from successfully processed river samples are small; all MPs from any studied sample could be stored in one 2 ml Eppendorf tube. The same is observed for the volume of inorganic material (sand). The volumes of organic matter, however, could even in the successfully processed samples vary from nil up to an estimated amount of 50 ml. For this reason it is suggested that organic matter contributes most to the risk of clogging sieves.

7.6 Annual load of microplastics by the Meuse

High uncertainty has to be dealt with as it comes to calculating the annual load of MPs to the seas and much more data is needed to make a trustful approximation. Within this study, no correlation between river discharge and MPs concentrations in the river Meuse was found. As neither the upstream emission sources, nor their relative contribution to the river Meuse are known, it cannot be concluded whether higher river discharges lead to dilution. However the sampling took place at a weekly basis and endured for 72 hours each, only 9 samples were successfully carried out, of which mostly in the spring season. It must be reminded that polymeric fibres were not included and possibly very light dense MPs were not derived from the river. Also, the representativeness of the (sole) monitoring station at Eijsden is not known in detail.

The nine observed fully processed samples come to an average MP weight concentration of 0.14 mg/m^3 for MPs in the size range 0.125-5 mm, excluding fibres and other possibly untraced polymers. Just imagining that this approaches a yearly averaged concentration for the observed groups, then considering an annual discharge at Eijsden of about $7.4x10^9$ m^3, the load of the river Meuse would be in the order of 1 ton per year.

The number of observed MPs differ widely between individual samples. Over the nine observed fully processed samples, on average 5.7 MP per m^3 were found for the small size range and 4.0 per m^3 for the large size range. Referring to the probable risks induced by ingesting MPs by marine animals, theoretically, the two groups may comprise 70.10^9 and 29.10^9 MPs, yet excluding fibres and other possibly not traced polymers, that could become available to marine life on a yearly basis.

Conclusions for the Meuse:
- In 7 out of 9 samples, small size microplastics were more abundant than the larger size fraction microplastics.
- Miscellaneous MP, comprising the groups other and scrubs, were at all times more abundant than sheets.
- No correlation between river discharge and MP particle concentrations can be concluded so far. Yet 7 out of 9 samples were derived at river discharges under 200 m^3/s, which is not representative on an annual basis. Too little data is available for regression analysis.
- Higher turbidity levels resulted in clogging filters. Declined tap flow rates can reduce the risk of clogging.
- For estimating a annual load of MPs for the river Meuse, more data has to be acquired.

7.7 Microplastic concentrations in the river Rhine

MPs are suspended matter that comprise different densities, shapes and volumes. Due to this, the particle concentrations and MP weight concentrations can differ when succeeding sample series are being studied. Both are addressed in this subsection. The concentrations of particles in a volume can be expressed in two ways:
- The number of MPs per unit of volume : MP particle concentration (MPs/m^3)
- The weight of MPs per unit of volume : MP weight concentration (mg/m^3)

The MP particle concentrations are discussed first, followed by a closer look at the abundance and distribution of MP over the associated Rhine samples. Finally, the MP weight concentrations are being discussed.

7.7.1 Microplastic particle concentrations in the Rhine

The MP particle concentration for both Lobith and Bimmen are presented in figure 42. Triangles indicate the large size fraction and dots represent the small size fraction, while green represents Bimmen and red represents Lobith. The river discharge is line plotted in black along the secondary Y-as to interpret variations over time. A correlation between river discharge and MPs abundance was not observed for any of the monitoring stations.

Taking both Lobith and Bimmen into account, the upper and under limit regarding MP particle concentrations in the Rhine are set as follows:
- Small size fraction   : between 20.5 and 50.4 MPs per m^3 (on average 37.0, σ: 12.7).
- Large size fraction   : between   5.5 and 23.9 MPs per m^3 (on average 18.1, σ: 5.1).
- Whole sample   : between 26.0 and 71.1 MPs per m^3 (on average 52.3, σ: 13.0).

At Lobith mostly more MPs per m^3 were found than at Bimmen, except for the large size fractions of series 3, 5 and 12, and the small size fractions of series 8 and 14.

At all times more small size, than large size fraction MP were recorded within the same sample:
- At Lobith   : 2.2 till 5.9 times more (on average 3.4 times, σ: 1.2).
- At Bimmen   : 2.5 till 7.6 times more (on average 4.4 times, σ: 1.8).
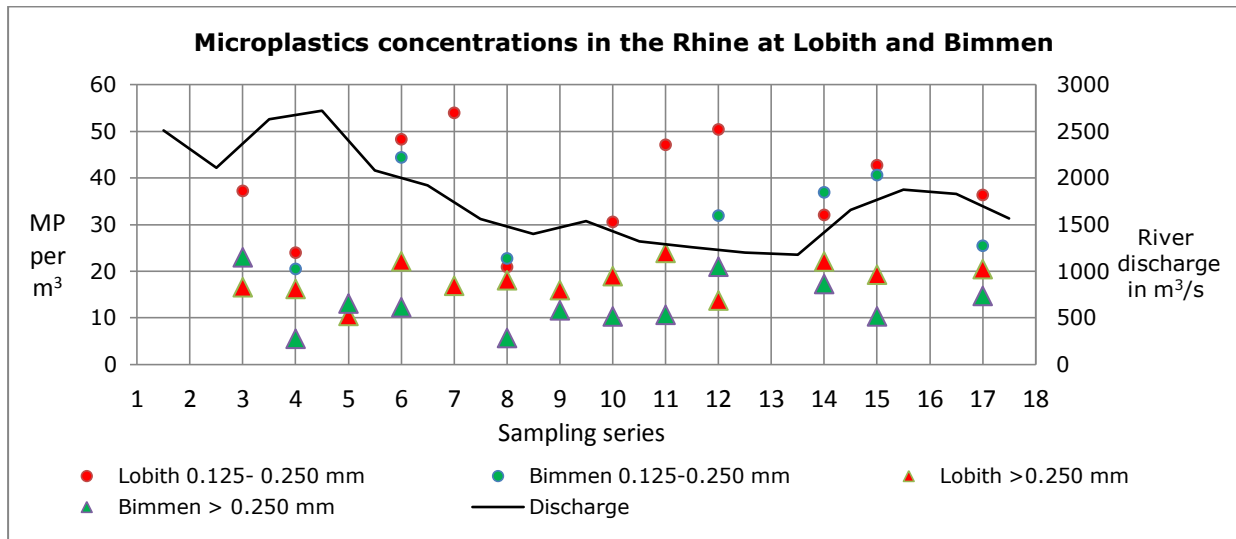

Figure 42. The observed MP particle concentration in the Rhine. The sampling series on the X-axis can be read for both Lobith and Bimmen. Green represents Bimmen and red represents Lobith. Triangles represent the large size fraction and dots represent the small size fraction. The river discharge is line plotted along the secondary y-axis to interpret possible variations over time. Sample series 1 and 2 were not divided in size fractions and hence taken out of account. Samples 13 and 16 were not processed.

Regarding the Rhine, initially four groups of MPs were distinguished: films, white spherules, transparent spherules and miscellaneous MPs. In total 18 small size fraction samples and 25 large size fraction samples were processed. Scrubs were separately recorded in 7 (small size fraction) and 11 (large size fraction) occasions. Both the abundance and the relative distribution of MP groups were studied in detail.

7.7.2 Abundance and distribution of microplastics (0.125-0.250 mm) in the Rhine

The abundance stands for the total of MP of all distinguished groups together; it is a measure of all MPs that were found in one sample. In figure 43, the abundance of MPs in the small size fraction (0.125-0.250 mm) of the Rhine samples is presented. All distinguished groups are presented in stack columns. In the cases where scrubs were not recorded as a separate group (orange), their numbers are added to the miscellaneous group (green). The samples are arranged increasingly on river discharge, ranging from 1180 m^3/s till 2721 m^3/s.

Regarding the abundance, i.e. the aggregated total of all MPs in one sample, no correlation to the river discharge was found. Regarding the distinguished MP groups, it was noticed that their individual contribution differed per sample. To study this in detail, in figure 44 the samples are displayed along the Y-axis as 100% stack columns. The samples are here arranged increasingly on river discharge as well.
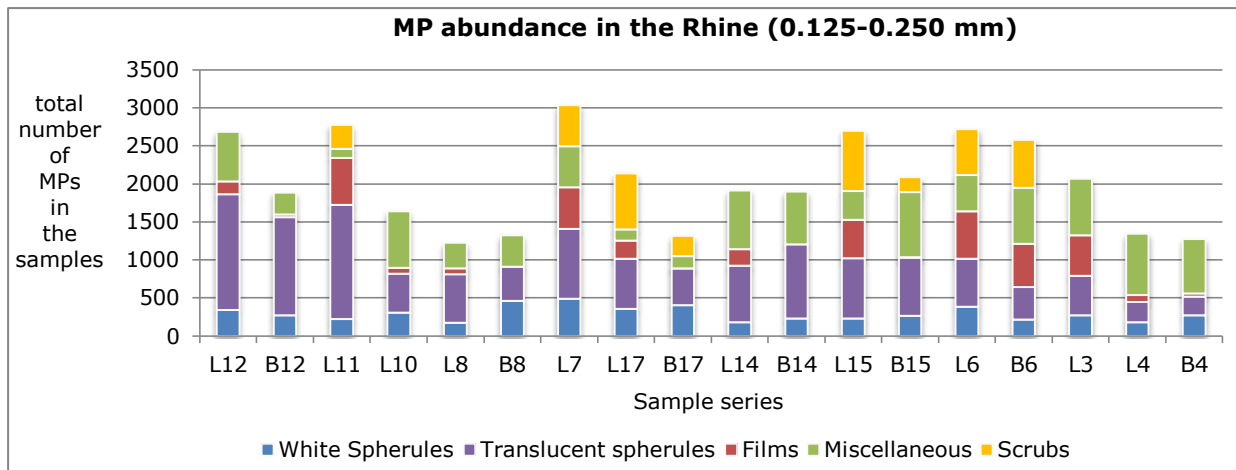
Figure 43. Abundance of MPs found in the Rhine in both Lobith and Bimmen samples. Here the small size fraction is presented. MP groups are plotted in different colours. The associated number of particles per sample are presented along the Y-axis, while the sample series are arranged based on increasing river discharge. Scrubs are regarded as miscellaneous MPs if not recorded separately.
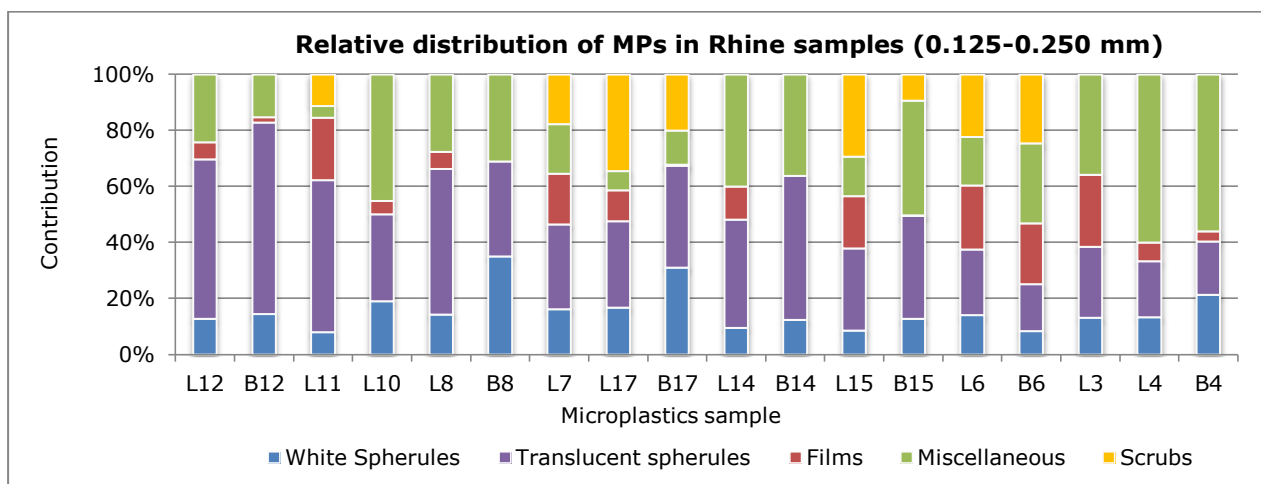

Figure 44. Relative distribution of MPs in the Rhine. Here the small size fraction is presented. The samples are arranged on increasing river discharge. Each MP group is plotted in a different colour. Scrubs were regarded as miscellaneous MPs if not recorded separately.

All five MP groups were found in Rhine MP samples, except for films that were not present in the small size fractions of Bimmen samples B8 and B14. As can be seen in figure 44, the relative contribution of the individual groups can differ widely. The relative contribution of the miscellaneous group (4%-60%) showed the largest differences in abundance, followed by transparent spherules (17%-68%), white spherules (9%-35%) and films (nil-26%). If recorded separately, the scrubs contributed for 9%-34%.

7.7.3 Abundance and distribution of microplastics (0.250-5 mm) in the Rhine
Regarding the large size fraction (0.250-5 mm), the abundance of MPs is presented in figure 45. All distinguished groups are presented in stack columns. In the cases where scrubs were not recorded as a separate group (orange), their numbers are added to the miscellaneous group (green). The samples are arranged increasingly on river discharge, ranging from 1180 m^3/s till 2721 m^3/s.

Regarding the abundance, i.e. the aggregated total of all MPs in one sample, no correlation to the river discharge was found. Regarding the distinguished MP groups, it was noticed that their individual contribution differed per sample. To study this in detail, in figure 46 the samples are displayed along the Y-axis as 100% stack columns. The samples are again increasingly arranged on river discharge.
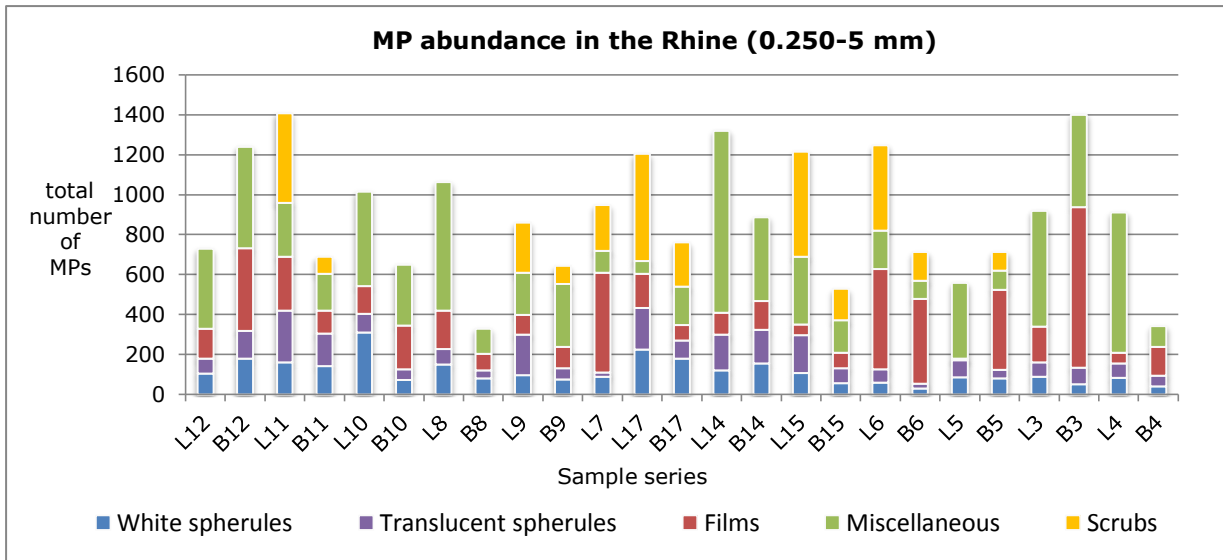
Figure 45. Abundance of MPs found in the Rhine in both Lobith and Bimmen samples. Here the large size fraction is presented. MP groups are plotted in different colours. The associated number of particles per sample are presented along the Y-axis, while the sample series are arranged based on increasing river discharge. Scrubs were regarded as miscellaneous MPs if not recorded separately.
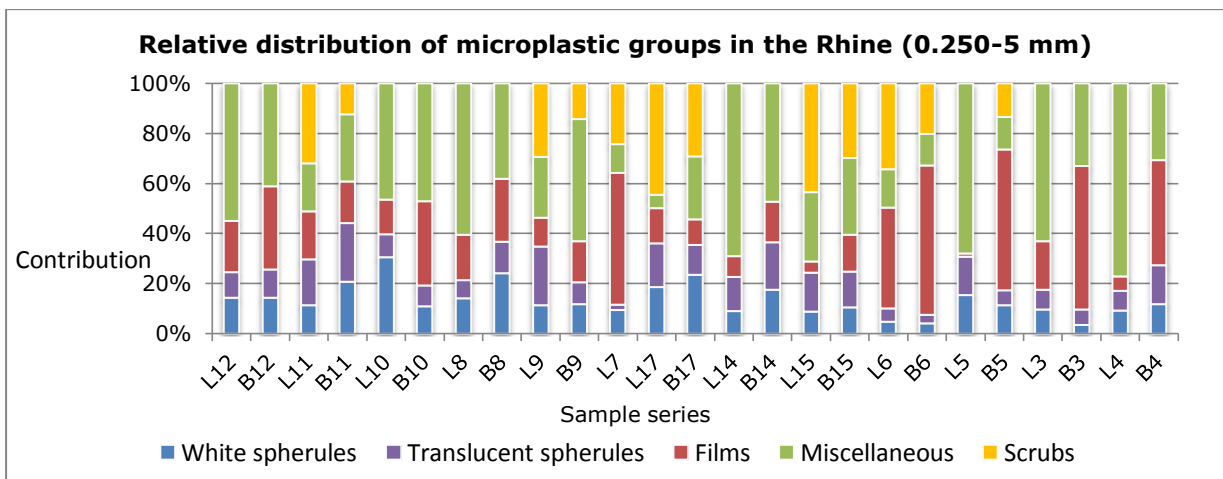

Figure 46. The relative distribution of microplastics groups found in the Rhine. Here the large size fraction is presented. The samples are arranged on increasing river discharge. Each MP group is plotted in a different colour. Scrubs were regarded as miscellaneous MPs if not recorded separately.

Regarding the large size fraction, at all times were the five different MP groups observed. However, their relative distribution within single samples differ widely (figure 46). The relative contribution of the films showed the largest differences in abundance (4-60%), followed by the miscellaneous group (26%-77%), white spherules (4%-31%) and transparent spherules (2%-24%). If recorded separately, the scrubs contributed for 12%-44%.

7.7.4 Microplastics concentrations versus Rhine discharge: an applied regression analysis

This subsection discusses possible temporal variances between successive samples. For a secure comparison, only fully processed Rhine samples were taken into account: 11 Lobith samples and 8 Bimmen samples.

The numbers found in both size fractions of each distinguished group were, per sample, summarized. The numbers of scrubs were added to the miscellaneous group. Figure 47 displays for each distinguished group, the total of particles as a function to the discharge rate. All four groups display a wide spread of scatters. The difference between the least and the highest number ranges from a factor 4 (white spherules) up to a factor 13 (films). The spherules seem to point out that the more the discharge rate increases, the more the numbers are closer arranged to the trendline).

For the spherules the trendlines are downwards. This could suggest that higher discharges lead to dilution of MP concentrations. For the miscellaneous MP, however, the relation seems just opposite. In total 19 observations were included. Considering the uncertainties regarding the sources, the emission intensities and the mixing mechanisms in rivers (see chapter 8), can for none of the four groups be concluded whether a relation between particle numbers and river discharge exists. More samples would be required, including a number of samples between 2000 and 2600 m^3/s, which are now lacking. This could either support the interpretation or just have a straightening effect on the trend lines.
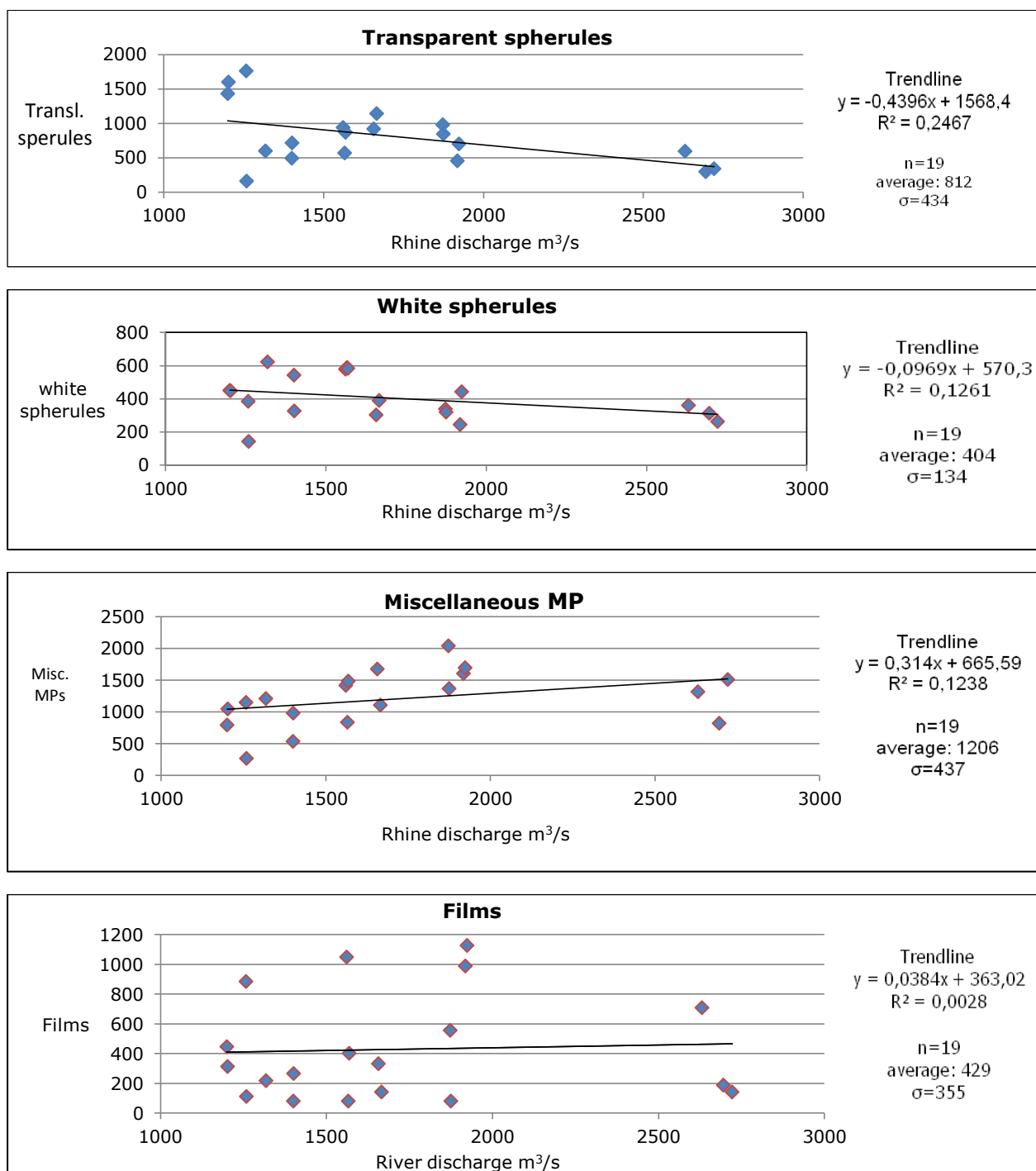
Figure 47. The total number of particles as a function to the river discharge. Each plot displays an individual distinguished group. From top till bottom: transparent spherules, white spherules, miscellaneous MP and films. The trendlines are given, as well as the trendline equation, the number of values included, the overall averaged number of particles and the associated standard deviation . For all groups 19 observations were included in the scatter plot. The samples were arranged based on increasing river discharge on the X-axis.

A closer look is taken at the spherical parts derived from the river Rhine, whose alignment is not influenced by their shape. In figure 48 both white and transparent spherules of both size fractions are presented with stack columns along the primary Y-axis. In this figure only fully processed samples were included. The river discharge is line plotted along the secondary Y-axis (in black).

Obviously, the small fraction of transparent spheres show remarkable peaks at L11, L12 and B12 (in blue). The larger transparent spheres (purple) do not show similar deviations. A correlation to the river discharge was not found. It must be noted that for the other distinguished MP groups also temporal variations were observed that could not be related to the discharge rate. Suggested is that the variations were caused by discontinuous emissions, rather than differences in river discharge or possible dilution effects.

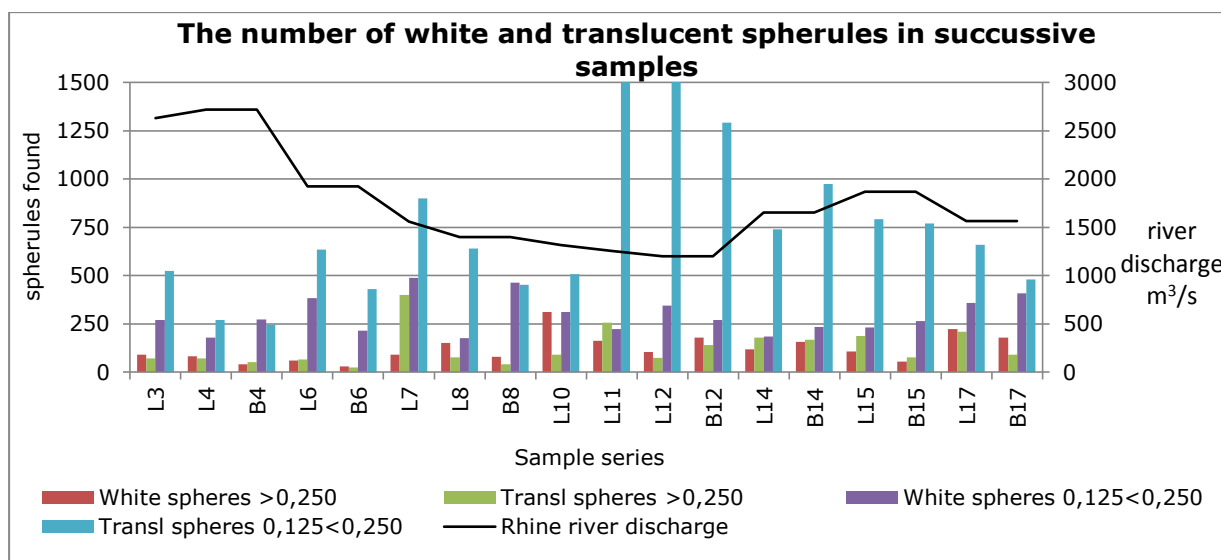Figure 48. The total number of white and transparent spheres found in both size fractions of Rhine samples. The Rhine discharge is line plotted along the secondary y-axis. Stack columns in four colours represent both size fractions of both particle groups. Notice the peaks at L11, L12 and B12.

Samples series 4, 6, 8, 12, 12, 15 and 17 were successful at both Lobith and Bimmen, what makes mutual comparison possible. In many, but not all cases, more particles per distinguished group were found at Lobith than at Bimmen. Regarding full samples, on average, 1.7 times more particles were recorded at Lobith than at Bimmen, with a maximum of 3.2 times.

7.7.5 Microplastic weight concentrations in the Rhine

The MP particle concentrations were calculated by aggregating all recorded weights in each individual sample and dividing it through by the recorded cubic meters of sieved river water. Between Lobith and Bimmen differences were observed, that are discussed here below.

At Lobith full sample MP weight concentrations range from 0.22 to 1.05 mg/m^3 and at Bimmen from 0.29 to 0.70 mg/m^3. Regarding only the small size fraction, observed concentrations at Lobith ranged from 0.05 mg/m^3 to 0.21 mg/m^3 (on average 0.13 mg/m^3, σ: 0.05). At Bimmen, for the small size fraction 0.08-0.18 mg/m^3 was found (on average 0.11 mg/m^3, σ 0.04).

Regarding only the larger fraction, at Lobith 0.16-0.92 mg/m^3 (on average 0.52 mg/m^3, σ: 0.20) and at Bimmen 0.21-0.70 mg/m^3 (on average 0.42 mg/m^3, σ: 0.11) was found.

Here under a closer look is taken at the weight distribution in Rhine samples. In figure 48 the calculated concentrations for the small size fraction and the large size fraction are presented in stack columns. The small size fraction is presented in red and the large fraction in green. The sample series are arranged increasingly based on river discharge. However the large fraction features less particles, due to their larger size range (0.250-5 mm), their weights contribute more at all times. The larger size fraction contributed to 50% up to 90% of the total sample weight.

It was noticed that the contribution of both fractions differs over time, however no correlation between river discharge and MP weight concentrations was found.
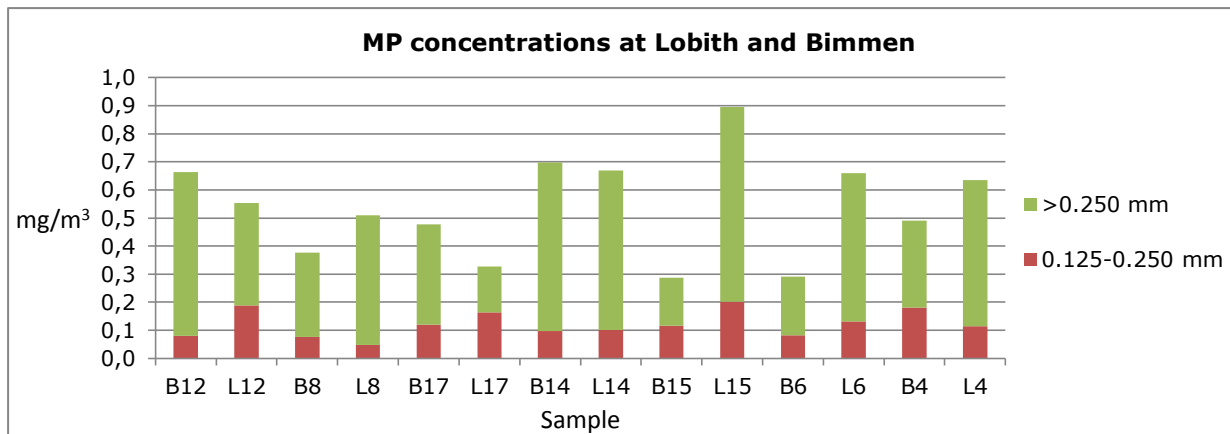
Figure 49. Microplastic concentrations of seven Rhine samples, which are arranged on increasing river discharges. The average over the these samples read for Lobith 0.65 mg/m^3 (σ: 0.23). For Bimmen 0.47 mg/m^3 (σ: 0.17).

7.7.6 Bad Honnef

The monitoring station of Bad Honnef is located approximately 49 km past the influx point of the Moselle river, but lies prior to tributaries as the Lippe, the Emscher and the Ruhr (see figure 51 at page 65). The distance between Bad Honnef and Lobith/Bimmen is approximately 221 km. The sole sample at Bad Honnef revealed all distinguished particle groups, in both size fractions, except for one: white spherules, that were not found in the size range 0.125-0.250 mm.

At Bad Honnef 9.5 particles in the small size range and 5.4 particles in the large size range per m^3 river water were found, which for each is near to 50% of the least recorded amount of particles at Lobith/Bimmen. Regarding the MP weight concentrations, the MPs found in the small size fraction amount for 0.05 mg/m^3 and in the large size fraction for 0.17 mg/m^3. This brings the total sample weight on 0.22 mg/m^3, which is recorded also for Lobith once, but not at the similar date. All other recordings at Lobith and Bimmen show higher weights.

The larger MP particle concentrations and MP weight concentrations suggest that upstream of Bad Honnef, MPs are emitted to the Rhine. The Ruhr region district lies upstream and is more densely populated than the Moselle river basin. Also, the Ruhr region is known for its extensive industrial enterprises. Personal communication with personnel at the Bad Honnef station learned that the river Moselle fluxes in upstream of Bad Honnef, but at the opposite bank. For sediment is known that the distance between the Moselle and Bad Honnef is too small to get a homogeneous mixture at Bad Honnef. Therefore it cannot be excluded that MPs are emitted to the Rhine by the Moselle, without detecting them at Bad Honnef. It must be stressed that the emission sources and emission mechanisms are not known and that further research is required.

7.8 Annual load of microplastics by the Rhine

As the sampling in the Meuse and Rhine were synchronized, the same considerations are at stake: for accurately determining a rivers load, preferably more data should be acquired, taking account all four seasons in one year. Excluding the group of fibres and averaging the full sample concentrations at Lobith and Bimmen of the observed seven fully processed samples, a concentration of 0.56 mg/m^3 is calculated. Just imagining that this approaches a yearly averaged concentration for the observed groups, then considering an annual discharge at Lobith of about 72.5x10^9 m^3, the load of the river Rhine would be in the order of 40 ton per year.

The number of present particles differs widely between individual samples. Over seven observed fully processed samples, on average 56 particles per m^3 were found at Lobith and 44 at Bimmen. Referring to the probable risks induced by ingesting MPs by marine animals, theoretically, in between 3.2 .10^{12} and 4.1. 10^{12} particles, yet excluding fibres and other possibly not traced polymers, could become available to marine life on a yearly basis.

Conclusions for the Rhine:
- MPs in the small size fraction (0.125-0.250 mm), were at all times more abundant than MP in the larger size fraction (0.250-5 mm).
- At Lobith at all times higher MP particle concentrations were observed, except for 2 small size fraction and 3 large size fraction measurements.
- All distinguished groups were found in all Lobith and Bimmen samples, except for sheets that were not found in 2 out of 18 small size fraction Bimmen samples.
- The relative contribution of MPs groups varied between samples. Transparent spherules (0.125-0.250) showed large temporal variations that are uncorrelated to river discharge.
- For estimating a annual load of MPs for the river Meuse, more data has to be acquired.

7.9 The effects of turbidity on sampling in the Rhine

At Lobith, no samples failed. At Bimmen, the bottom sieve (0.125 mm) clogged five times: At sample B1 (2224 m^3/s), B3 (2677 m^3/s), B9 (1538 m^3/s), B10 (1317 m^3/s) and B11 (1259 m^3/s). There seems no correlation with river discharge and clogging risk. Possibly external factors were of influence, but it is not known which.

It is observed that at Bimmen ships can pass by at a relative short distance from the inlet pipe (figure 49) and also local turbulence was noticed within the groyne at Bimmen. Both could possibly lead to whirling sediment, what can be considered as a local increase of turbidity at the inlet point. The turbidity levels that were recorded in this study were deducted from Lobith, so local fluctuations at Bimmen would not have been noticed.

Figure 50. Ships can pass by at short distance to the water inlet at Bimmen, which is at the viewpoint of the photographer.

The samples that flooded were excluded from this research as most likely MPs were lost with the flooding water. It has not been studied in detail which kind of particle matter, organic or inorganic, was primarily causing the clogging risks. The volumes of MPs derived from successfully processed river samples are small; all MPs from any studied sample could be stored in one 2 ml Eppendorf tube. The same is observed for the volume of inorganic material (sand). The volumes of organic matter, however, could even in the successfully processed samples vary from nil up to an estimated amount of 50 ml. For this reason it is suggested that organic matter contributes most to the risk of clogging sieves.

7.10 The abundance of cenospheres

Cenospheres were observed in samples from both rivers, but mostly found in the small size fraction (0.125 – 0.250 mm). In seven MP samples the cenospheres were recorded. For the Meuse, the cenosphere particle concentrations varied between 3.1 till 12.1 spheres per m^3 and for the Rhine between 2.2 till 11.9 per m^3. The abundance of cenospheres was compared to the abundance of the distinguished MP groups, in the same samples (table 14). Conclusively, regarding the small size fraction, cenospheres can contribute equally to the mix of particulate matter as some of the designated groups of MPs.

Table 16. Comparison of the cenospheres particle concentrations with the particle concentrations of the distinguished microplastics groups within the same samples. White and transparent spherules were not found in the Meuse leading to empty table cells.

Sample	River	Number of particles per m^3 river water (0.125-0.250 mm)				
		Cenospheres	White Spherules	Transparent spherules	Scrubs	Miscellaneous MP
E6	Meuse	3.4			3.6	0.9
E10	Meuse	3.4			2.6	1.4
E11	Meuse	3.1			n.r.	2.4
E15	Meuse	12.1			n.r.	9.4
L6	Rhine	11.9	8.2	13.6	13.0	10.1
B6	Rhine	2.2	4.6	9.2	13.6	15.8
L11	Rhine	3.6	4.8	32.2	6.7	2.6

8. Representativeness of the monitoring stations

8.1 The characteristics of the rivers Meuse and Rhine
The rivers Meuse and Rhine both have unique characteristics, which are discussed in this section.

The river Meuse
The river Meuse rises in France and runs through Wallonia, and enters the Netherlands at Eijsden. The foreign river basin district area of the Meuse comprise about 28,300 km², of which 12.276 km² in Wallonia (DLW, 2012). The upstream distance to Eijsden is approximately 600 kilometers. The yearly average discharge at Eijsden is 236 m^3/s. The river discharge can vary significantly within short time intervals. This is caused by two factors:

1) The Meuse is a rain river that is highly dependent on, and influenced by, rain fall. In winter and spring the river rises, while in summertime the banks often nearly run dry. Most rainfall occurs in the French and Belgian Ardennes, where the rocky surface allows little water to be stored, resulting in quick discharge intervals at times of rainfall (Bakker, Klaver, Jansen, Joziasse & Van der Meulen, 2008) .

2) At Lixhe in Wallonia, just 4,5 kilometers upstream of Eijsden, a hydroelectric power plant dam influences the flow rate powerfully and causes translatory waves (Gerretsen, 1982). The plant comprises 4 individual switchable turbines, each letting 85 m^3/s river water pass through. As the river water supply is low, EDF, the power plant operator, can choose to store water behind the dam for later use, resulting in low river discharge downstream, including at Eijsden. Discharge levels less than 10 m^3/s can swell up to over 200 m^3/s back and forth within one day (e.g. May 6th, 2014, own retrieved data). When exceeding the capacity of the power plant, river water is released over the full width of the dam. Incidental discharge rates up till 3000 m^3 per second have been reported (V&W, VROM en LNV, 2009). , but were not recorded during this study's time path.

The river Rhine
The Rhine is a glacier river that rises in the Swiss Alps. Its tributaries are all – just like the river Meuse - rain rivers. In between Basel and just prior to Karlsruhe, the river Rhine forms the French-German border. Above Dusseldorf a large urban and industrial area is passed by: the Rhine-Ruhr region. The Rhine itself runs through part of it; three tributaries drain the north part (the Lippe), the middle (the Emscher) and the south part (the Ruhr) of the Ruhr region (figure 51). These tributaries run into the Rhine at the right river bank.

Figure 51. The drainage of the Ruhr region. The Rhine (left) and three of its tributaries (from above: Lippe, Emscher and Ruhr) run through the densely populated and highly industrialize Ruhr region district. Source: https://en.wikipedia.org/wiki/Ruhr .

In between its origin and the Dutch border, the Rhine basin covers about 170.000 km^2 and is populated by about 58 million people (IKSR, 2005). Its length to Lobith is approximately 1170 kilometers. The average annual discharge at Lobith and Bimmen is 2,300 m^3 per second; roughly 10 times larger than the Meuse at Eijsden, but is generally less dynamic. River discharge details of the Rhine at Lobith/Bimmen within the time path of this study can be found in appendix 6.

8.2 Turbidity and river discharge: an applied regression analysis
One of the research questions in this thesis deals with a possible relations between the abundance of MPs of either turbidity or river discharge. Dr. G. Stroomberg (Rijkswaterstaat) informed that in the past regularly a relationship between turbidity and river discharge was found. However, sediment transport can be dynamic. For both the rivers it is known that in times of low discharge, suspended matter accumulates in so called sediments reservoirs or sediment stocks (Asselman, 1999; Doomen et al., 2008). At times of higher discharge, river floor sediment and/or river (fore)bank sediment are taken up again and transported downstream. After an enduring high-discharge interval, an effect called sediment depletion can occur. Altogether, sediment transport is influenced by river dynamics.

To investigate whether turbidy and discharge were related with this study's time path, regression analysis is applied on the data of both rivers (appendix 6). Regression analysis showed that for both rivers turbidity and river discharge were highly correlated. It suffices to use either one of them. For further reading it should be noted that the discharge rate was chosen to present abundance and composition data.

8.3 Hydrological influences on the dispersion of pollutants and suspended matter

For specifically Lobith and Bimmen, Van Mazijk (1986) studied the representativeness of the two opposite monitoring stations. His study was based on the emission of well known chlorine (Cl-) concentrations to the Rhine by the upstream tributaries Ruhr, Emscher and Lippe, and refers a concept called mixing length. This is the distance needed to completely mix an emitted substance, across the transverse length of the river. At Lobith and Bimmen a concentration of a substance would be representative, if the concentration is more or less equal to the average concentration of this substance over the cross section of the river.

Based on the rather well known chlorine emissions and several cross section samples, Van Mazijk (1986) concluded that just prior to Lobith and Bimmen, till 3000 m^3/s discharge, the mixing length is at least 90 kilometers long. In other words: under 3000 m^3/s, a shore based emission of Chlorine takes at least 90 kilometers to become homogeneously mixed over the cross section of the river. Based on this observation, a closer look was taken at the tributaries of the river Rhine prior to Lobith and Bimmen. Table 17 presents 7 of them, including their influx bank and their average contribution. The contributing rivers Lippe, Emscher and Ruhr are within shorter distance than 90 km to the monitoring stations at Lobith and Bimmen and could – for Chorine – result in an uncompleted mixture when passing by the both stations.

Table 17. Seven tributaries to the river Rhine upstream to Lobith and Bimmen that could possibly emit MPs to the Rhine. The Lippe, the Emscher and the Ruhr are within shorter distance than 90 kilometers. Sources: Van Mazijk (1986), http://de.wikipedia.org/wiki/Rhein, retrieved on January 12th, 2015 and personal communication Bad Honnef monitoring station.

Tributary (*or monitoring station*)	Distance to Lobith/ Bimmen in Rhine km	Influx bank (*or location*)	Average contribution to the river Rhine (m^3/s)
Lippe	47.5	Right	45 (m^3/s)
Emscher	67.5	Right	16 (m^3/s)
Ruhr	82.5	Right	81 (m^3/s)
Erft	132.5	Left	17 (m^3/s)
Wupper	159.5	Right	17 (m^3/s)
Sieg	203	Right	53 (m^3/s)
(Monitoring station at *Bad Honnef)*	*221.5*	(Right)	---
Moselle	270.5	Left	328 (m^3/s)

Within the time frame of this study, the river Rhine reached discharge levels above 3000 m^3/s only on 5 out of 137 days. Assuming that the mechanisms to mix MPs can be compared to those to mix the chlorine-ion, then MPs emitted by the Lippe, the Emscher and/or the Ruhr may not be a homogeneously mixed at Lobith and Bimmen and differences in MPs concentration levels may occur. It must be stressed that it is not known whether and to what extent the behaviour of MPs is similar to that of a soluble ion.

Regarding the Rhine, multiple studies were carried out on the transport and mixture of suspended matter and pollutions (Van Mazijk, 1986, 2002; Van Mazijk & Veling, 2005). It is concluded that groyne fields affect the behaviour of suspended matter and pollutions as they act as 'dead zones' in the current, for which the interaction with the main stream is not yet fully understood. The number of groynes, the dimensions of groyne fields, the river discharge, varying river depths and the river width-depth rato are all influencing factors to the exchange of suspended matter and pollutions. It must be noted that both the intakes of Lobith and Bimmen are situated in a groyne. Spills in a river show a skewness in observed concentrations over the cross section, until full mixture downstream is achieved. The skewness can be persisted or enlarged by tributaries, confluences and morphological variations. This may also apply to emissions and observed concentrations of MPs.

Appendix 7 shows a river contour map of the Rhine including a cross section at Lobith. Depending on the actual discharge rate, the river's width is approximately 330 meters. The river floor is a gradual

slope starting at a depth of approximately 6 meters at Lobith till its deepest point in the concave bank at the Bimmen side of approximately 9 meters. The river flow velocity is usually larger at the concave side than the convex side. The discharge rates to calculate the MP concentrations were derived from a gauge at Lobith and for the calculations it was assumed that the river discharge at Lobith and Bimmen were equal. It was also assumed that the river flow velocity over the cross section was equal as well, which in reality probably is not the case, regarding the differences in river depth and the influences of the earlier discussed groynes.

Meuse
Previous research on the representativeness of the Eijsden monitoring station was not found. As the monitoring station at Eijsden is a pontoon located at the right river bank, it is according to Van Mazijk (1986) per definition not representative, as it is unknown what the simultaneous concentrations are over the cross section of the river. In the part of the Meuse where the Eijsden monitoring station is located, professional shipping is prohibited and groynes are absent, so groyne influences are not expected. Within the time path of this study, at almost all times the Meuse river water was led through the turbines of the Lixhe power plant. It is believed that the internal forces of the turbines to the water lead to a homogeneous mixture, but it is yet unknown whether the MPs become dispersed afterwards due to gravitational mechanisms. Also differences in the river flow velocity might lead to varying concentration calculations as is explained below.

Appendix 8 shows a contour map of the river Meuse where the pontoon is located. The river's width is, depending on actual discharge rates, approximately 180 meters. Over the cross section, the river depth varies. An island midstream in front of the pontoon separates the stream. A little to the south, the right river bank is shallow while at the left bank, which is opposite to the monitoring station at Eijsden, the channel is continued. Differences in river depth can influence the river flow velocity, and thus discharge rate, at this very location. The discharge rates to calculate the MP concentrations were derived from a gauge at Sint Pieter, Maastricht, which is approximately 5 kilometer downstream of Eijsden. For the calculation it is assumed that the river discharge at Sint Pieter and Eijsden were equal. Also is assumed that the river flow velocity over the cross section was equal as well, which in reality probably is not the case.

For the sake of certainty, sampling should, preferably, be done continuously . However, for practical reasons, the sampling series were set to 3 working days. This means that during this study for about 43% of the time, river water was tested. Referring to the chlorine-ion studied by Van Mazijk (1986) prolonged sampling for at least 24 hours to level temporal concentration abnormalities were proposed. The 72 hour sampling in this study met this requirement. In relation to the Chlorine-ion, Van Mazijk (1986) recommended to average the measured concentrations at Lobith and Bimmen as this leads to a deviation of maximal 10%, to a concentration measured at either Lobith or Bimmen. However, regarding the MP particle concentrations, this expectation was scarcely met (see chapter 7). Contrary to the Chlorine-ion, of which the emission loads and emission spot were well known, the emission loads and emissions spots of MPs are not known.

The dynamics related to sediment transport are complex. In the river Elbro (Catalonia, Spain) is found that the pattern of organic suspended matter differed from (the denser) inorganic suspended matter. Also differences were found in the transport ratios over the cross section of the river (Rovira, Alcaraz & Ibanez, 2012). The Elbro can just slightly be compared to either the Meuse or the Rhine as the characteristics in terms of discharge, channel width, river bed elevation and river depth.

8.4 **The representativeness of the water intake**
The behaviour of MPs in the river water column is yet largely unknown (Eerkes-Medrano et al., 2015). As is briefly discussed in the previous subsection, physical forces in the water are of great influence on their presence and behaviour in the water column. In calm waters, dense particles could sink and less dense particles could rise. In a current river, random water forces are expected to contribute to a continuously suspended phase, but for what range of MP densities or MP shapes this is applicable, is not known.
In salt water studies, the density-rising effect of bio-fouling is reported (Wright et al., 2013) but it may be debatable if the length of stay in the river is enduring enough to let bio-organisms grow on MP surfaces. Suspended MPs could be trapped and buried by denser particles, like sand, on the river bed or river banks, and re-suspended at times of higher discharge.

In this study, river water was taken in at a depth of 80 centimeters beneath the water surface. Questioned is whether this may lead to selective sampling, as denser particles may pass by beneath,

and less dense particle may pass above this point. In this subsection a closer look is taken at the components of the suspended matter. The density of MPs is reported from 0.8 to 1.4 g/cm^3, while the most dense compound of suspended matter, sand, is reported at 2.65 g/cm^3 (Hidalgo-Ruz et al., 2012). The density of organic debris is not known, but visual observation in the laboratory points out that the major part is denser than water. Sand was not observed in all MP samples. Organic debris was at all times except for 5 occasions, observed.

Approximating the density under limit
Cenospheres and scrubs from a Palmolive exfoliant were used to investigate the density lower limit of sampled particles. To extract the scrubs, 25 ml of Palmolive Thermal was brought in a 250 ml glass beaker, filled with hot water (65° C), stirred and rinsed with hot tap water over a 125 μm metal cloth sieve for one minute. The scrubs were taken from sieve bed using a spatula. The similarity of Palmolive scrubs and scrubs found in both rivers, was verified with Raman.
Due to the destructive method used to identify cenospheres, no self derived sample material was available from the rivers Meuse and Rhine. The used cenospheres were offered by supplier PMS BV, which conveys the spheres from electrical power plants in Rumania. It is for this test assumed that density and particle size distribution are similar to those derived from the rivers.

Four tubes were filled with each one spatula scoop of cenospheres and four tubes were filled with each one spatula scoop of scrubs. Then the tubes were filled with four different liquids with descending density and left to rest for one hour before further study. The liquids were milliQ, Ethyl Acetate, Methanol and Petroleum Benzene (table 18).

Table 18. Four liquids used to study the dispersion of scrubs and cenospheres.

Liquid	Density	Density source	UN identification code
MilliQ	1.00 g/cm^3		
Ethyl acetate (EA)	0.90 g/cm^3	Bottle	UN 1173
Methanol (METH)	0.79 g/cm^3	Bottle	UN 1230
Petroleum Benzene (PB)	0.65 g/cm^3	Bottle	UN 1268

Figure 52 shows the result of the immersion. The four tubes on the left contained scrubs, the four tubes on the right contained cenospheres. All scrubs float on MilliQ, but sink in Ethyl acetate and the other liquids. Obviously, scrub density was in between 0.90 g/cm^3 and 1.00 g/cm^3, which corresponds to the density reported in literature: 0.92-0.97 g/cm^3 (Hidalgo-Ruz et al., 2012).
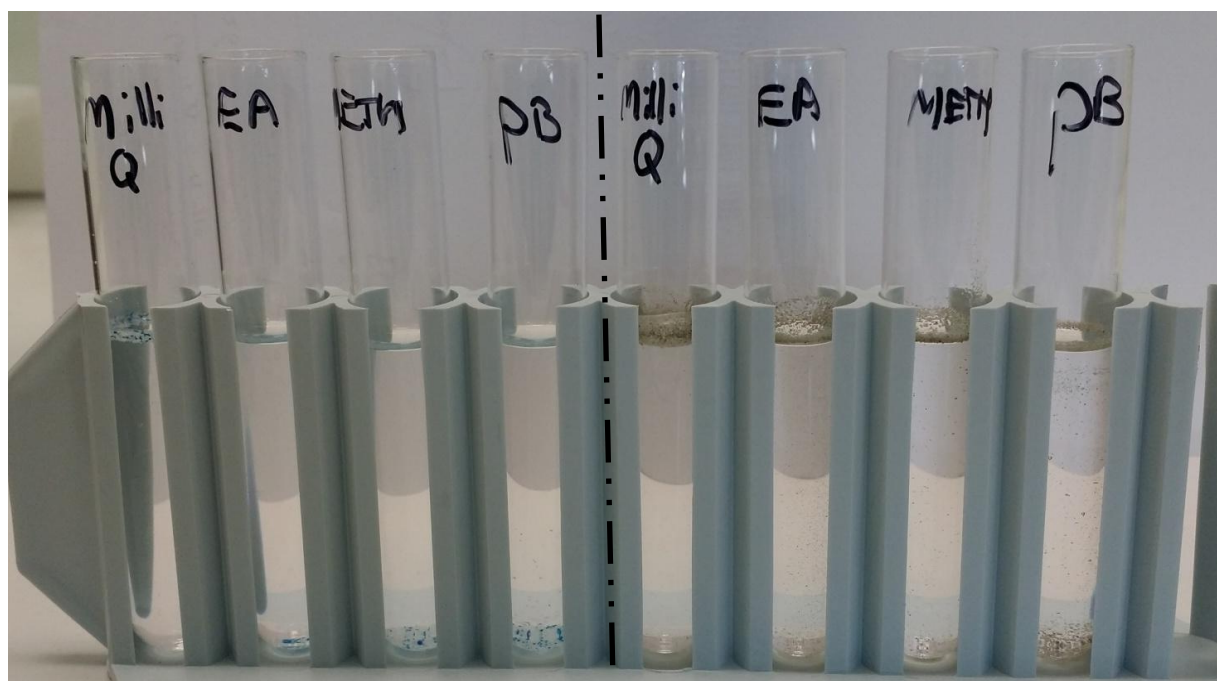

Figure 52. Density test with scrubs and cenospheres in four different dense liquids. The four tubes on the left contained blue and white coloured scrubs, the right four tubes contained the grayish cenospheres. For both: from left to right: MiliQ, Ethyl acetate, Ethanol and Petroleum benzene.

The cenospheres, however, dispersed in all four media. Obviously the density of the cenospheres ranges from less dense than Petroleum Benzene (<0.65 g/cm^3), till denser than MilliQ (>1.00 g/cm^3). Cenospheres have an aluminosilicate shell that encloses entrapped flue gas. Aspects like particle size, the shell's thickness and the amount of gas entrapped, influence the inorganic-gas ratio and hence also the particle densit

The absence of expected MPs
The Dutch based independent foundation Waste Free Waters carried out frequent measurements in the Meuse and incidentally in the Rhine. The method of sampling is based on a water sampler with a mesh of 3.2 mm, that is towed by a boat. The sampler skims the upper 10 centimeters of the water column and simultaneously samples at a depth of 20-70 cm directly underneath. By this method, a distinction can be made between floating particles and suspended particles. Based on the personal communication with G. Tweehuysen from Waste Free Waters and (yet) unpublished results, it is assumed that in the upper size range, not all MPs are sampled at the monitoring stations. This assumption is reinforced based on two examples:

1) Extremely little dense materials, for example expanded plastics like EPS, were not found at all within this study. Expanded plastics in the upper micro size range, however, were observed in the samples of the Waste Free Waters sampler and their presence is reported in shore sediment samples in the Rhine-Mainz area (Klein et al., 2015). Apparently, they are not passing by at a depth of 80 cm beneath the surface. Assumed is that the upward forces of expanded plastics prevent them to becoming suspended again, resulting in a predominantly floating phase of little dense MPs.
2) Pellets, which can be regarded as flattened spherulic particles and reported as granular precursors for the plastic industries were reported in the current of the Danube river (Lechner et al., 2014). EPS and pellets were also abserved in shore sediment samples of the Rhine-Mainz area (Klein et al., 2015). Two examples are specifically known to be carried by the Main: blue pellets and silver pellets. None of these were observed in the present study.

Conclusions on the representativeness of the monitoring stations:
- According to Van Mazijk (1986) is any shore based monitoring station, including Eijsden, not representative.
- The observations of Van Mazijk regarding concentrations of the Chlorine-ion over the cross section of the Rhine near to Lobith and Bimmen, were not reflected by the measured MP concentrations at Lobith and Bimmen. This could be due to other mixing characteristics but also other (fluctuating) emission characteristics.
- Based on the presence of cenospheres in the river samples, the lower density limit of particles derived from the rivers is set to 0.65 g/cm^3, but could possibly be less. It is however not certain whether the used cenospheres are similar to those present in the rivers. The upper density limit of particles is set to 2.65 g/cm^3 based on the density of sand reported in literature. Also, cenospheres and/or sand grains were not at all times observed.
- Extremely light dense polymers, such as expanded polystyrene, were not observed at all.
- Plastic pallets in the size range 0,63-5 mm were not sampled, while their presence is observed in the Rhine.
- More knowledge is required on
  o the emission sources of MPs,
  o their emission intensities, and,
  o the behaviour of MPs in the water column in general.

9. Discussion

The general aim for this MSc. project was to develop guidance for a probable future monitoring program using the stationary monitoring stations in the rivers Meuse and Rhine. For this, an in-depth study on the abundance and composition of microplastics in the Dutch parts of the European rivers Meuse and Rhine was carried out. Several challenges were encountered that were not, or just briefly reported in literature and at some point the research was like pioneering. This study is one of the first, if not the first, that includes an extending series of synchronized samples, collected at exactly the same locations and using the same method, in two running European rivers. Insights were gathered on all distinguished steps: sampling, sample collection, laboratory processing, sample splitting, stereoscopic analysis, concentration determination, spectroscopy, and processing large amounts of spectral data simultaneously with PCA.

A method to monitor microplastics in the running rivers is established, but also suggestions for method developments and further research are proposed. Altogether, the insights gathered within this study are expected to contribute to a further professionalization of microplastics research and standardization of microplastics monitoring.

MP particle concentrations
However rivers are more and more seen as transport vectors for MPs to the seas, research on their loads of MPs is scarce and fragmentary. Besides, a comparison of MP concentrations can be difficult as 1) the reported size limits can vary, 2) the used nomenclature can differ and 3) the concentrations can be differently reported. In a recent review, Eerkes-Medrano et al. (2015) summarize 12 studies in fresh waters worldwide, of which six addressing sediment samples. Just two concerned European rivers: the Danube (Lechner et al., 2014) and the Tamar (Sadri & Thompson, 2014), whose methods were both based on surface water sampling.

Considering all the uncertainties encountered in this study, an estimation of concentrations was made based on averaging the concentrations of all fully succeeded samples. With reference to the size range of 0.125-5 mm and excluding any fibres, an average particle concentration of 56 MPs/m^3 (σ: 12,31) was calculated for the Rhine at Lobith/Bimmen, and 9.7 MPs/m^3 (σ: 9,34) for the Meuse at Eijsden. The highest recorded value was found at Lobith: 71.1 MPs/m^3. The MP particle concentrations between the synchronized samples at Lobith an Bimmen, both in the Rhine, could differ widely. This also accounts for the relative contribution of MPs within the samples. Uncertainties that arose during this study, such as the loss of MPs during processing or the probable damage to MPs of some processing steps, was not discussed in literature before. This could indicate that the reported concentrations, among those in this study, are regularly underestimated.

Regarding the Danube, in 2010 and 2012 samples were taken to a depth of 50 cm using stationary driftnets with a mesh size of 0.5 mm. Macroplastics were sampled as well, as the inlet frame formed an upper limit of approximately 5 cm. Distinguished were spherules, pellets, flakes and a group of others. For 2010 were reported 937.6 (σ: 8543.8) MPs/1000 m^3 and for 2012 55.1 (σ: 75.4) MPs/1000 m^3. Compared to the most polluted river in the present study, the Rhine, these concentrations are 60 to 1000 times smaller. The high standard deviation reported over 2010 indicates that incidental peak levels were recorded. The highest concentration seen in 2010 was 141,647 MP/1000m^3, which is about twice the highest level found in the Rhine and two-and-a-halve times its average. While interpreting these figures, it must be noted that a negative correlation exists with mesh. In the Rhine, 65-70% of the MPs were observed in the size fraction 0.125-0.250 mm. If the negative correlation also applies for the Danube, than with similar under and upper limits less differences in abundance would be expected.

The surface of the Tamar was sampled with a neuston net to a depth of 50 cm. In the size range 0.3 mm-5 mm, an average concentration of 0.028 MPs/m^3 was found. This is, compared to only the large size fraction in this study, 142 times less than for the Meuse and between 4620-6445 times less than for the Rhine. The river characteristics of the Tamar differ from the Rhine and the Meuse: it is a short river in Cornwall, in the South-West of England, just under 100 km long. Along this river only one large conglomeration is situated: the city of Plymouth.

Regarding the Meuse, MPs were subject to two bachelor theses of which the results of the most recent one was professionally published (Kroes et al., 2014; Van Paassen, 2010). Although their presence was confirmed, in both MP particle concentrations and MP weight concentrations were not taken into account.

Separator sediment
In October 2013, Brandsma, Nijssen, Van Velzen and Leslie (2013) studied suspended matter that was derived with sediment separators at each of the three monitoring stations at Eijsden, Lobith and Bimmen. Density separators are centrifuge-like stages whose separation process is based on centrifugal force. Water is taken in with the same pump system as used for this study, led through the separator and forcing suspended particles to the sides, while the water is released at the bottom. The amount of water that was taken in for this study, was recorded, and the amount of retrieved sediment, was weighed. Based on these figures, the number of observed MPs can be converted into particle concentration approximations and compared with the own retrieved data.

Brandsma et al. (2013) took two size fractions into account: 0.01-0.3 mm and 0.3–5 mm, and distinguished fibres, foils and spherules. Based on full samples, the highest numbers were found at Lobith (4520-5280 MPs/kg d.w.; average: 4900, σ:540) followed by Bimmen (1420-1970 MP/kg d.w.; average:1700 σ: 390) and Eijsden (1030-1760 MPs/kg d.w.; average: 1400, σ: 520). This hierarchy is accordingly to the results of the present study. Lobith figures ranged 2.8 times higher than Bimmen, a situation that in the present study was only met twice: (2.8 and 3.2 times). The contribution of spherules in the larger fraction of the separator sediment (>0.300 mm) was estimated at 10.7 (Lobith) and 3.7 (Bimmen) spherules/m^3. In the present study, including both white and transparent spherules (0.250-5 mm), at Lobith on average 4.4 spherules/m^3 (σ: 2.1) were calculated, and at Bimmen 3.4 spherules/m^3 (σ: 2.0).

In the separator sediment samples, foils were only observed at Eijsden, while miscellaneous MPs, scrubs and cenospheres were not reported. Contrarily, in the present study, foils were at almost all occasions found: on average at Lobith 12.8 times and at Bimmen 5.7 times more than at Eijsden. The differences could be caused by overlooking them in the samples, but due to their distinctive nature it is more likely, that they were not present in the samples indeed. The actual process of the separation process is not figured out, but suggested is that it is based on density separation. The PE-based miscellaneous MPs, films and scrubs, which are less dense than water, and a part of the cenospheres, could then have passed through. Fibres, such as Polyamide (PA) or the PS transparent spherules, are reported denser than water (Hidalgo-Ruz et al., 2012). In the separator sediment derived at Eijsden, also spherules were observed. In the present study, however, they were not observed at all, suggesting that another particle could have been mistaken for a polymeric spherule. For a proper comparison, a new study on the retrieval of MPs using both methods, preferably simultaneously carried out and preferably using the same laboratory steps, is required. The accuracy of the sediment separator at Bimmen could be easily investigated as the outflow of the separator can be sampled with a soil sieve set up.

Klein et al. (2015) studied shore sediment samples in the Rhine-Mainz area. Two size fractions were taken into account: 0.63–5 mm, meanwhile distinguishing fragments, spheres, and fibres. Foils and pellets were not reported separately, but their presence was noticed. Reported particle concentrations read 228−3763 MPs/kg d.w. along the river Rhine, and 786−1368 MPs/kg d.w for the river Main. In Rhine estuary sediment samples, an average particle concentration of 3300 (σ: 420) MPs/kg d.w. was reported (Leslie, Van Velzen & Vethaak, 2013). The figures for the Rhine tend not to differ widely. The river Main, which is based on discharge rates approximately one-tenth of the Rhine, was reported to contribute to an significant emission to the Rhine (Klein et al., 2015).

River loads
Lechner et al. (2014) estimated the load of the Danube to the Black sea on 7.5 g per 1000 m^3, which is 13.4 times larger than the estimation for the Rhine (0.56 g per 1000 m^3) and 53.6 times larger than the Meuse (0.14 g per 1000m^3). The size limits for the Danube study (0.5 mm-5 cm) yielded less smaller MPs than the present study, but it yielded also macroplastics, which due to their larger volume contribute to higher weight calculations. As a result: less particles but yet larger weights per unit of volume. A factual comparison could be best made based on corresponding methods.

MP composition
The rivers Meuse and Rhine differ with regard to abundance of microplastics. Besides incidental occasions, at all times were films, scrubs and miscellaneous MPs observed, in both size fractions of both rivers. Additionally, in the Rhine, at all times also white and transparent spherules were found in both size fractions. Spectroscopic analysis identified predominantly polyethylene in the Meuse samples, as these only comprised films, scrubs and miscellaneous MPs. Based on 4% of the total number of MPs being studied spectroscopically, 98% of the Meuse MPs consist of PE. Miscellaneous MPs were most abundant, followed by scrubs. Based on the samples where scrubs were separately recorded, their relative abundance was calculated for 37.9%-43.6% in the small size fraction and

25.4%-40.1% in the large size fraction. Films were at all times least abundant in both the small size fraction (0%-12,5%) and the large size fraction (2.5%-24.3%).

Due to the variation in the distribution of particles in Rhine samples, is it difficult to establish a hierarchal order. The results reflect the distribution at that particular moment. Regarding the large size fraction, the relative contribution of the films showed the largest differences (4-60%), followed by the miscellaneous group (26%-77%), white spherules (4%-31%) and transparent spherules (2%-24%). If recorded separately, the scrubs contributed for 12%-44%. For the small size fraction, the miscellaneous group (4%-60%) showed the largest differences in abundance, followed by transparent spherules (17%-68%), white spherules (9%-35%) and films (nil-26%). If recorded separately, the scrubs contributed for 9%-34%.

Based on numerical classification, in Rhine samples, in the small size range, PE (49%) and PS (51%) were observed. The presence of PP was negligible. In the large size fraction more variation was seen: PE (69%), PS (17.5%), a yet unknown polymer (13%) and PP (0.5%). For the river Tamar, PE (40%), PS (25%) and PP (19%) were reported. For the Rhine-Mainz area PS (15%), PE (23%), PP 15%, PA (2%) and others (6%). It must be noted that in the latter also fibres were taken into account which influence the figures of abundance and contribution. Furthermore, in the sediment samples also expanded polymers and pellets larger than 0.7 mm were observed, which both were lacking in the soil sieve samples derived at the monitoring stations.

Based on weight contribution, for the small size fraction of the Rhine, PE and PS account for respectively 53% and 46%. For the large size fraction: PE (83%), PS (11%), PP (1%) and the unknown polymer for 3.5%. For specifically the Rhine, only 0.5% of all yielded particles were subject for spectroscopic analysis.
Nonetheless, apparently, the rivers pollutions seems not reflected by the European plastics demand. The European demand over 2012 accounted for PE: 29,5%, PP: 18,8%, PVC 10,7%, PS: 7,4, PET: 6,5%. PUR and a group of plastics referred as 'others', such as Teflon and ABS accounted for 19,8% (Plastics Europe, 2013). PET, PC, ABS and Teflon were not observed in the Meuse and Rhine, nor were they reported by the others.

MP sources
The sole sample at Bad Honnef learned that all designated MP groups were seen, except for the white spherules who were just scarcely present. Furthermore, Klein et al. (2015) showed the presence of MPs further upstream of Bad Honnef, in the rivers Rhine and Main. The MP particle concentration at Bad Honnef was half of the least recorded, and one fifth of the average at Lobith and Bimmen. This could indicate the presence of upstream emission sources, for example in or near the high densely populated and industrialized Ruhr area. However, it must be noted that the sampling depth at Bad Honnef (approximately -3 m) is unequal to both Lobith and Bimmen (constant -0.80 m). It was discussed in section 8.4 that MPs can be unevenly distributed over the water column and that more study is required to understand mixing mechanisms.
The observation that at Lobith at almost all times, higher concentrations were recorded than at Bimmen, suggest that right river bank emissions are not yet non-homogeneously mixed at the cross section of Lobith-Bimmen. The Ruhr area, partly drained by the Rhine itself and partly drained by the three tributaries Lippe, Emscher and Ruhr, is situated at the right river bank. A comparison with earlier studies on the transport and mixture of sediment and pollutants, shortly upstream of Lobith and Bimmen did not deliver evidence for this (sections 8.3 and 8.4).

The applications of films and miscellaneous MPs in consumer products is not known, it is therefore believed that they originate from larger plastics and hence have to be considered as secondary plastics. The precise mechanisms how they come into existence is not known, but acknowledged are light degradation by UV-radiation, chemical degradation, mechanical degradation, thermal degradation and biotic degradation (Beyler & Hirschler, 2001; Eubeler et al., 2010; Lucas et al., 2008).

White and transparent spherules are believed to be primary MPs, for which applications in consumer products was not found. The spherules are therefore thought to be half-fabricates that, just like the larger pellets (Klein et al., 2015; Lechner et al., 2014), are lost during their initial fabrication, handling, transport or manufacturing into end products. Regarding the white spherules, it is believed that these are pre-fabricates for the ultimate production of expanded foam, in this case expanded polystyrene (EPS) that is commonly used as packaging material or for construction isolation purposes (Raps et al., 2015). It is however difficult to point out specific sources. In a recent study the application of unexpanded PS spherules for water filtration is proposed (Schöntag & Sens, 2014).

The scrubs are known for their application in consumer products like exfoliants, scrub crèmes and facial cleaners (Fendall & Sewell, 2009). Personal communication with G. Tweehuysen from the Dutch independent foundation Waste Free Waters learned that scrubs are often made by shredding larger PE fragments or beads into the desired scrub size. If this is applied in a poorly contained fabrication process, emission from here could be due, but also transport or further handling may lead to emissions. Another yet reasonable route is via domestic waste water. Starting in 2013, large cosmetic fabricants like Unilever, Proctor&Gamble, l'Oreal, Colgate-Palmolive and Beiersdorf announced to ban scrubs from their products. For a Unilever product, Palmolive thermal, it was observed in 2014 that the former present PE based scrubs were replaced with silicon particles.

In the basin of the Rhine, 96% of the households in 2005 were connected to sewage water treatments plants, and a part of the remaining 4% is expected to have an individual treatment facility. Large industrial companies have their own waste water treatment facilities (IKSR, 2005). For the basin of the Meuse, at least in the Walloon part, 87% of the households were connected to collective sewage water treatment plants in 2008. The number of individual and industrial waste water treatment facilities in the Meuse are less well-known. Arising from the European Water Framework Directive, Walloon policy makers plan to increase water treatment capacity (DLW, 2012). The fact that more households become connected to sewage water treatment plants, and the fact that less PE particles are applied in consumer products, enforce the thought that the abundance of scrubs will decline over time. If not, probably other emission sources than sewage systems may come in view.

Monitoring stations as a basis for a future monitoring program
A monitoring program based on repeating measurements requires a stationary monitoring set up. All three monitoring stations met this requirement. The floating monitoring stations at Eijsden and Bimmen are, however, not fully equipped for further sample processing steps like the removal of organic debris, the removal of coal, density separation and stereomicroscopic study. Accurate weight determination is hindered by the movements of the (floating) pontoons. The used spectroscopic setups require extending investments. In conclusion, sampling can be carried out at the monitoring stations, however the laboratory processing, the quantitative research and the qualitative research can be best performed at central dedicated laboratories, such as the central laboratory of Rijkswaterstaat in Lelystad.

MPs are part of the mix of suspended matter in rivers. Studies on sediment transport and pollution dispersal in the Rhine learned that river dynamics are complex and partly understood, especially for MPs (section 8.3 and 8.4). Conclusively, three knowledge gaps are distinguished: 1) the location of the MP emission sources, 2) their emission densities and 3) the factual behaviour of microplastics, including their mixing mechanisms in running rivers. More research on these three aspects is required.

Studies on MPs, especially in running rivers, are scarce and fragmentary. With only a few studies in rivers carried out, a clear picture on the global abundance and varying compositions cannot be formed. The need to monitor and to build up comprehensive datasets on the abundance and composition is repeatedly stressed (Eerkes-Medrano et al., 2015; Ryan, Moore, van Franeker & Moloney, 2009; Wagner et al., 2014) and supported by the author of this report. The present study demonstrated that with the soil sieve method, multiple groups of microplastics can be distinguished, analyzed, characterized and – if desired – measured and weighed. The insights and data retrieved in this study form a basis for a monitoring program.

The use of the soil sieve set up in future monitoring program
To level off incidental emission peaks, it was chosen to sample for relative long periods of time. As a result of this, often more particles were obtained than could be accurately processed. Sample splitting can lead to an unequal distribution and even a probable loss of MPs, what can ultimately influence abundance and concentration calculations. A balance between accuracy of MP determination and time efficiency has to be found. For this, more knowledge on short interval temporal fluctuations is needed. The risks of clogging meshes is apparently a general factor for river sampling. In the Meuse it was encountered before (personal communication Waste Free Waters) and reported for amongst others the Californian rivers (Moore, Lattin & Zellers, 2005). The sediment separators are not prone to these risks, but as previously discussed, they might introduce selectiveness based on MP density. On the other hand, they may be a more useful tool for distinguishing fibres. Furthermore, it is likely that the water intake is not representative for extreme dense MPs and rounded particles above approximately 0.7 mm, as is already discussed in chapter 8.

For all the distinguished method components, which are sampling, sample collection, laboratory processing, sample splitting, microscopic study and spectroscopic analysis, was shown that the accurate determination of MPs abundance and composition is prone to uncertainty. These uncertainties were already discussed in the associated method chapters (see sections 2.5, 3.9, 4.4, 6.8). The boundaries of these uncertainties were not in depth determined, but merely investigated based on simple tests. Further research is required to accurately determine these uncertainties.

Bioavailability and harm of MPs to aquatic life
Adverse effects to aquatic life is gradually more reported. It is noted that studies on the uptake, the transfer and the effects of MPs are conducted under laboratory conditions. MP particle concentrations to which the animals are exposed are reported for amongst others 395 mg MP/l (Hall, Berry, Rintoul & Hoogenboom, 2015) or 300 spheres/ml (Kaposi et al., 2014). The concentration used by Hall et al. (2015) exceeds 7.10^5 times the recorded average weight concentration of those found at Lobith/Bimmen. The recorded spheres in the small size fraction (0.125-0.250 mm) were averaged on 18.4 spherules/m^3, which means that concentration of Kaposi et al. (2014) exceeds the realistic particle concentration $1.6 .10^7$ times. In laboratory studies mostly one particular particle is chosen, commonly spherules, comprising one specific polymer type. In fact, studies on MPs, among which the present study, demonstrate ranges of particle sizes, shapes and different polymers. It could be questioned whether the apparent researches on the harm of microplastics should more focus on 1) realistic MP concentrations and 2) realistic MP mixes.

10. Conclusions

Regarding the first research question: *"Is it possible to quantitatively determine microplastic concentrations in rivers? Which factors are involved?"*, can be concluded that it is possible to determine microplastic concentrations in rivers but that it yet must be acknowledged that uncertainty is a crucial factor to be taken into account. River sampling brings forth the risk of clogging meshes, laboratory processing brings forth the risk of losing microplastics and inaccurate microscopic study may lead microplastics being overlooked. Also false identifications can occur as inorganic particles such as sand grains and cenospheres might be mistaken for microplastics. Finally the representativeness of the water intake is debatable.

Regarding the second research question: *Are the present monitoring locations at Lobith, Bimmen and Eijsden suitable when it comes to quantitatively and qualitatively measuring microplastics? Under what conditions can they be included in a future monitoring program?",* can be concluded that this study demonstrated that a series of comparable samples, obtained from the three stationary locations can deliver good insights on the abundance and composition of microplastics in the rivers Meuse and Rhine. The soil sieve method can be easily set up by the monitoring stations personnel and does not require any particular special equipment that other sampling methods do, such as a towing boat. More research is required on the representativeness of the river water intake to validate the abundance of microplastics in the studied size range. Their behaviour within the complex dynamics of running rivers is largely unknown, what also applies for the Meuse and Rhine. The used method is probably not suitable for the determination of fibres, extreme light dense microplastics and granular particles in the upper size range.

Regarding the third research question: *"Do the rivers Meuse and Rhine differ with regard to the abundance and composition of microplastics? Is it possible to point out sources?"*, can be concluded that, as far as the retrieved particles are concerned, the Meuse and Rhine differ with regard to both the abundance and composition of microplastics. In the Rhine, on average, approximately 6 times more particles per unit of volume were found than in the Meuse but that just a 4 times higher concentration was calculated for the Rhine. Given the size range of 0.125-5 mm, averaged concentrations of 0.14 mg or 9.7 microplastics per m^3 were calculated for the Meuse, and 0.56 mg or 56 microplastics per m^3 for the Rhine.

In both rivers, virtually at all times and in both size fractions, scrubs, films and miscellaneous microplastics were observed, whereas in the Rhine also opaque white and transparent microplastics were found. Films, scrubs and the majority of the miscellaneous microplastics were identified as polyethylene. The white spherules in the Rhine were verified as polystyrene, just as the transparent spherules under 0.250 mm. For the larger transparent spherules, temporal variations in composition were observed comprising polyethylene, polypropylene and polystyrene. Also a yet unidentifiable polymer was noted in this group. Sewage systems, the run-off from land and spillage during transport or manufacturing are reported as contributing emission sources for microplastics, but with the so far available data is it not possible to relate emissions or concentrations to these sources.

Regarding the fourth research question: *"What is the temporal variation in abundance and composition of microplastics in river water?"*, can be concluded that, as far as the retrieved particles are concerned, in all samples and in both size fractions, except for accidental occasions, three (Meuse) and five (Rhine) groups of microplastics were detected. Their relative distribution varied widely. Temporal differences in composition were specifically observed for the large size range of the transparent spherules.

Regarding the fifth and last research question: *"Is there a relationship between the abundance and composition of microplastics on one hand, and discharge and turbidity of the river water on the other"*, can be concluded that regarding both rivers no conclusive evidence is found on relationships between turbidy levels or discharge rates, and presence and abundance of microplastics. More research is needed to determine whether the differences are due to discontinue emissions or due to incomplete mixing over the river cross section.

11. Suggestions for further research

1) As a result of this study, several groups of MPs were identified and a basis for a dataset was formed. To obtain the ability to monitor MP abundances and compositions over time, it is suggested to build further on this database, taking the distinguished groups into account.

2) This study demonstrated that with the same method, at Bad Honnef, upstream of Lobith and Bimmen, similar MP were observed. Possibly similar, but also probably different MP were recently reported for the Rhine-Mainz area, yet more upstream. It is suggested for Rijkwaterstaat to cooperate with the LANUV, and perhaps other Landesämter, to investigate the gaps of knowledge on the abundance and composition of MP in upstream section of the Rhine, including its contributing rivers. The outcomes can be used to complete the dataset and it could also increase the possibility to point out sources.

3) In this study sample series endured for 72 hours that, in many cases, yielded so many particles that the samples had to be split. Splitting samples induced uncertainty, which jeopardizes the accurate determination of microplastic abundances. However, shorter sampling duration could lead to overlooking temporal abnormalities. It is suggested to investigate this, by taking a series of samples at shorter intervals, for example 24 hours each, on each monitoring station. It is expected to contribute in finding a balance between accuracy and time efficiency.

4) At all monitoring stations, sediment separators are used to extract suspended matter from the river water. At Bimmen, the outlet pipe for the sediment separator happens to be the outlet pipe used for the present study on microplastics. It is proposed to use the sieve set up to filter the effluent that is released by the sediment separator, to investigate whether MPs pass through when they are operated.

5) In addition to 4), it is suggested that extreme little dense particles and floating granular particles up to 5 mm are not taken in at the monitoring stations. Meanwhile, in the Danube it is suggested that surface sampling leads to the exclusion of smaller MPs that pass by beneath. Possible a bias is acknowledged and it would not differ whether the soil sieves or the separators are being used. To designate differences in the water column near the water intake spot, it is suggested to develop a method to sample different layers in the column simultaneously. A suggested idea is to use 1) the Waste Free Waters sampler to sample to a depth of 70 cm, 2 the sieve set up used in this study and 3) a submergible pump combined with a sieve set up. Furthermore, cross section samplings are preferred to investigate the possible skewness in the abundance and composition of microplastics over the rivers width.

6) At all distinguished method components, which are sampling, sample collection, laboratory processing, sample splitting, microscopic study and spectroscopy, could uncertainties be addressed. However test were carried out to investigate these uncertainties, it was beyond the scope of this study these uncertainties in detail. Further research on these aspects is required

   - Laboratory processing steps showed that MPs can become lost and that splitting samples can lead to uneven parts. It could be investigated further whether the methods can be optimized to minimize these risks.

   - It was concluded that both the spectroscopic analysis and the PCA could be improved. It is suggested to perform the PCA again on 1) new improved spectral data in combination with 2) an larger data set containing more and also other polymer types than used in this study, preferably made available by polymer suppliers to be ascertained of genuine polymer references. Furthermore, it could be investigated whether MPs can be directly analysed on the micro pore filter with spectroscopic equipment, without manually isolating them.

   - Density separation might have caused dense MPs to end up with sand particles and being overlooked during microscopic study. The suspended mix was not studied spectroscopically. It is suggested to perform a Raman map scan on them in combination with PCA to investigate whether and to what extent particles might have been overlooked.

12. Glossary and abbreviations

σ	:	Small letter sigma (Greek alphabet). Stands for standard deviation.
Abundance	:	In this research: the number of microplastics of all distinguished varieties.
Aluminosilicate	:	Minerals composed of predominantly aluminum, silicon and oxygen.
Aqua regia	:	A reactive mixture of HCl and HNO_3, in this study in a volume ratio of 1:3.
Concave bank	:	The outside bend of a river.
Convex bank	:	The inside bend of a river.
Copolymer	:	Two or more different monomers united into one polymeric macromolecule.
Cross section	:	In this study: a section orthogonal to the two rivers banks.
Demersal	:	Near to the seabed or riverbed.
Discharage	:	See: river discharge.
D.w.	:	Dry weight.
Elastomer	:	A generic name for polymers (both natural and manmade) that exhibit
	:	rubberlike elasticity. When stretching or pinching forces are removed, they recover their original shape and dimension.
Fingerprint region	:	A range of frequencies in infrared spectroscopy where energy gets absorbed by chemical bonds and on which determination can take place. Different molecules require different regions. For polymer analysis with Raman infrared spectroscopy, a fingerprint region between wavenumbers 1769- 672 cm^{-1} was chosen. For FT-IR a full range spectrum between 4000-400 cm^{-1} was used.
FT-IR	:	Fourier Transform Infra Red Spectroscopy.
Groyne	:	A dam-like structure in the river to decrease the river flow at the shore sides. In between the groynes at both banks, the flow rate is increased, preventing suspended mater to deposit, which is in favour of shipping.
Gyre	:	A circular current in oceans, in which floating debris gets trapped.
LANUV	:	Landesamt für Natur, Umwelt und Verbraucherschutz Nordrhein-Westfalen, Germany
Mixing length	:	The distance needed to completely mix a substance after emission across the transverse length of a river.
Monomer	:	A molecule which can be polymerized to contribute to a polymer chain.
MP	:	Abbreviation for microplastic (singular).
MPs	:	Abbreviation for microplastics (plural).
NTU	:	Formazine Nephelometric Turbidity Units, a measure of clarity of a liquid medium, based on the scattering of light by suspended matter in that liquid.
Opaque	:	Not allowing light to pass through (except for to a depth of some microns).
Particle concentration	:	The number of MP particles per unit of volume, such as MP per m^3. See also MP weight concentration.
PC	:	Principal Component, a calculated variable in a dataset. The PC holding the largest variance is called PC1, the second is called PC2, and further on. (It is also a designation of the polymer Polycarbonate).
PCA	:	Principal Components Analysis; a statistical procedure.
PCA plot	:	A two-dimensional scatter plot used to display two different principal
	:	components from a Principal Components Analysis (PCA).
Pelagic	:	In the water column but neither near to the floor nor to the surface.
Polymer	:	A long macromolecule build up from repeating units called monomers.
Record failure	:	Spectroscopic image which spectral information is influenced severely due to noise recording, scattering and/or sensor saturation.
Resin code	:	Symbol printed on plastics or product labels to identify the polymer type. The codes are internally acknowledges for recycling purposes.
River discharge	:	The volume of water passing by a river cross section per unit per time (for example cubic meters per second (m^3/s).

Rhine kilometer	:	Rhine kilometers are customary for shipping navigation on the Rhine. It stated the upstream distance to the city of Konstanz (Germany).
Sample collection	:	Method by which the microplastic samples were taken from the sieves.
Sample failure	:	Situation whereby a microplastic sample could not be taken into account, for example due to flooding sieves.
Scrub	:	A rough particle added to exfoliants such as facial cleansers.
SEM	:	Scanning Electron Microscope (also: Scanning Electron Microscopy).
Skewness	:	Asymmetry from the normal distribution in a set of data, in this study related to concentration levels of pollutions.
Spectroscopy	:	The study of the interaction between matter and electromagnetic radiation.
Spectrum	:	(*Latin:*) Image.
Synthetic	:	Manmade.
Target MP	:	Microplastics in the size range of this study's scope.
Thermo setting	:	Synthetic polymer that melts on warming and then becomes an infusible solid. Examples are Bakelite, polyesters, polyamides and polyurethanes.
Translucent	:	Transmitting light but diffusing light to prevent clear vision through the material.
Transparent	:	Able to see through the material.
Weight concentration	:	The determined weight per unit of volume, such as mg/m^3 or µg/l. See also particle concentration.
Wavenumber	:	A unit of frequency, expressing the number of electromagnetic radiation waves in a unit distance (here: centimeter).

Polymers:
ABS	: Acrylonitrile butadiene styrene
EBA	: Ethylene-butyl acrylate
EPS	: Expanded polystyrene
EVA	: Ethylene-vinyl acetate
LDPE	: Low-density polyethylene
LLDPE	: Linear low-density polyethylene
PA	: Polyamide
PC	: Polycarbonate
PE	: Polyethylene
PET	: Polyethylene terephthalate
PFA	: Perfluoroalkoxy alkane. A polymer with comparable properties as PTFE
PP	: Polypropylene
PS	: Polystyrene
PSDVB	: Polystyrene divinylbenzene
PTFE	: Polytetrafluorethylene, a polymer commonly known as Teflon
PVC	: Polyvinylchloride
PUR	: Polyurethane

13. References

Andrady, A. L. (2011). Microplastics in the marine environment. *Marine Pollution Bulletin, 62*(8), 1596-1605. doi: 10.1016/j.marpolbul.2011.05.030.

Andrianov, A. K. & Payne, L. G. (1998). Polymeric carriers for oral uptake of microparticulates. *Advanced Drug Delivery Reviews, 34*(2-3), 155-170.

Arthur, C., Baker, J. & Bamford, H. (2009). *Proceedings of the International Research Workshop on the Occurrence, Effects and Fate of Microplastic Marine Debris.* Paper presented at the Sept 9-11, 2008. NOAA Technical Memorandum NOS-OR&R-30.

Asselman, N. E. M. (1999). Suspended sediment dynamics in a large drainage basin: the River Rhine. *Hydrological Processes, 13*, 1437-1450.

Barnes, R. J., Dhanoa, M. S. & Lister, S. J. (1989). Standard Normal Variate Transformation and De-trending of Near-Infrared Diffuse Reflectance Spectra. *Applied Spectroscopy, 43*, 772-777.

Besseling, E., Wang, B., Lurling, M. & Koelmans, A. A. (2014). Nanoplastic Affects Growth of *S. obliquus* and Reproduction of *D. magna*. *Environmental Science & Technology, 48*(20), 12336-12343. doi: 10.1021/es503001d.

Beyler, C. L. & Hirschler, M. M. (2001). Thermal Decomposition of Polymers. In P. J. DiNenno (Ed.), *SFPE Handbook of Fire Protection Engineering* (3rd ed., pp. 101-111). Quincy, MA: NFPA.

Bhattacharya, P., Lin, S., Turner, J. P. & Ke, P. C. (2010). Physical Adsorption of Charged Plastic Nanoparticles Affects Algal Photosynthesis. *The Journal of Physical Chemistry C, 114*(39), 16556-16561. doi: 10.1021/jp1054759.

Blissett, R. S. & Rowson, N. A. (2012). A review of the multi-component utilisation of coal fly ash. *Fuel, 97*, 1-23. doi: 10.1016/j.fuel.2012.03.024.

Brandsma, S. H., Nijssen, P., Van Velzen, M. J. M. & Leslie, H. A. (2013). Microplastics in river suspended particulate matter and sewage treatment plants. Amsterdam: Institute for Environmental Studies.

Carpenter, E. J., Anderson, S. J., Harvey, G. R., Miklas, H. P. & Peck, B. B. (1972). Polystyrene spherules in coastal waters. *Science, 178*(4062), 749-750.

Chen, Z., Hay, J. N. & Jenkins, M. J. (2012). FTIR spectroscopic analysis of poly(ethylene terephthalate) on crystallization. *European Polymer Journal, 48*(9), 1586-1610. doi: 10.1016/j.eurpolymj.2012.06.006.

Claessens, M., De Meester, S., Van Landuyt, L., De Clerck, K. & Janssen, C. R. (2011). Occurrence and distribution of microplastics in marine sediments along the Belgian coast. *Marine Pollution Bulletin, 62*(10), 2199-2204. doi: 10.1016/j.marpolbul.2011.06.030.

Claessens, M., Van Cauwenberghe, L., Vandegehuchte, M. B. & Janssen, C. R. (2013). New techniques for the detection of microplastics in sediments and field collected organisms. *Marine Pollution Bulletin, 70*(1-2), 227-233. doi: 10.1016/j.marpolbul.2013.03.009.

Cole, M., Lindeque, P., Halsband, C. & Galloway, T. S. (2011). Microplastics as contaminants in the marine environment: a review. *Marine Pollution Bulletin, 62*(12), 2588-2597. doi: 10.1016/j.marpolbul.2011.09.025.

Derraik, J. G. B. (2002). The pollution of the marine environment by plastic debris: a review. *Marine Pollution Bulletin, 44*(9), 842-852.

Department of V&W, VROM and LNV. (2009). *Stroomgebiedsbeheerplan Rijn 2009-2015 [River basin management plan for the Rhine 2009-2015]*. The Hague, Netherlands: Author.

Department of V&W, VROM and LNV. (2009). *Stroomgebiedsbeheerplan Maas 2009-2015 [River basin management plan for the Meuse 2009-2015]*. The Hague, Netherlands: Author.

Directive 2008/56/EC (Marine Strategy Framework Directive) (2008).

DLW. (2012). *Waalse stroomgebiedbeheerplannen [Walloon river basin management plans]*. (D/2012/11802/37 - SPW-DGARNE-DEE-DESu). Jambes, Belgium: Departement Leefmilieu en Water.

Doomen, A. M. C., Wijma, E., Zwolsman, J. J. G. & Middelkoop, H. (2008). Predicting suspended sediment concentrations in the Meuse river using a supply-based rating curve. *Hydrological Processes, 22*(12), 1846-1856. doi: 10.1002/hyp.6767.

Dyrstad, K., Veggeland, J. & Thomassen, C. (1999). A multivariate method to predict the water vapour diffusion rate through polypropylene packaging. *International Journal of Pharmaceutics, 188*(1),105-109. doi: 10.1016/s0378-5173(99)00210-0.

Eerkes-Medrano, D., Thompson, R. C. & Aldridge, D. C. (2015). Microplastics in freshwater systems: A review of the emerging threats, identification of knowledge gaps and prioritisation of research needs. *Water Research, 75*, 63-82. doi: 10.1016/j.watres.2015.02.012.

Eilers, P. H. C. & Boelens, H. F. M. (2005). *Baseline correction with asymmetric least squares smoothing [unpublished manuscript]*. Department of Medical Statistics. Leiden University Medical Centre.

Eriksen, M., Mason, S., Wilson, S., Box, C., Zellers, A., Edwards, W., . . . Amato, S. (2013). Microplastic pollution in the surface waters of the Laurentian Great Lakes. *Marine Pollution Bulletin, 77*(1-2), 177-182. doi: 10.1016/j.marpolbul.2013.10.007.

Espi, E. (2006). PLastic Films for Agricultural Applications. *Journal of Plastic Film and Sheeting, 22*(2), 85-102. doi: 10.1177/8756087906064220.

Eubeler, J. P., Bernhard, M. & Knepper, T. P. (2010). Environmental biodegradation of synthetic polymers II. Biodegradation of different polymer groups. *Trends in Analytical Chemistry, 29*(1), 84-100. doi: 10.1016/j.trac.2009.09.005.

Farrell, P. & Nelson, K. (2013). Trophic level transfer of microplastic: *Mytilus edulis (L.)* to *Carcinus maenas (L.)*. *Environmental Pollution, 177*, 1-3. doi: 10.1016/j.envpol.2013.01.046.

Fendall, L. S. & Sewell, M. A. (2009). Contributing to marine pollution by washing your face: microplastics in facial cleansers. *Marine Pollution Bulletin, 58*(8), 1225-1228. doi: 10.1016/j.marpolbul.2009.04.025.

Foekema, E. M., De Gruijter, C., Mergia, M. T., van Franeker, J. A., Murk, A. J. & Koelmans, A. A. (2013). Plastic in north sea fish. *Environmental Science & Technology, 47*(15), 8818-8824. doi: 10.1021/es400931b.

Galgani, F., Hanke, G., Werner, S. & De Vrees, L. (2013). Marine litter within the European Marine Strategy Framework Directive. *ICES Journal of Marine Science, 70*(6), 1055-1064. doi: 10.1093/icesjms/fst122.

Gall, S. C. & Thompson, R. C. (2015). The impact of debris on marine life. *Marine Pollution Bulletin, 92*(1-2), 170-179. doi: 10.1016/j.marpolbul.2014.12.041.

Gerretsen, J. H. (1982). Translatiegolven ten gevolge van waterkrachtcentrale te Lixhe (B) [Translatory waves caused by hydroelectrical power plant at Lixhe (B)]: Waterloopkundig Laboratorium.

Gregory, M. R. (1996). Plastic 'Scrubbers' in Hand Cleansers: a Further (and Minor) Source for Marine Pollution Identified. *Marine Pollution Bulletin, 21*(12), 867-871. doi: 10.1016/S0025-326X(96)00047-1.

Gulmine, J. V., Janissek, P. R., Heise, H. M. & Akcelrud, L. (2002). Polyethylene characterization by FTIR. *Polymer Testing, 21*, 557-563.

Gulmine, J. V., Janissek, P. R., Heise, H. M. & Akcelrud, L. (2003). Degradation profile of polyethylene after artificial accelerated weathering. *Polymer Degradation and Stability 79*, 385-397.

Habib, D., Locke, D. C. & Cannone, L. J. (1998). Synthetic fibers as indicators of municipal sewage sludge, sludge products, and sewage treatment plants effluents. *Water, Air, and Soil Pollution, 103*, 1-8.

Hall, N. M., Berry, K. L. E., Rintoul, L. & Hoogenboom, M. O. (2015). Microplastic ingestion by scleractinian corals. *Marine Biology, 162*(3), 725-732. doi: 10.1007/s00227-015-2619-7.

Hidalgo-Ruz, V., Gutow, L., Thompson, R. C. & Thiel, M. (2012). Microplastics in the marine environment: a review of the methods used for identification and quantification. *Environmental Science & Technology, 46*(6), 3060-3075. doi: 10.1021/es2031505.

Hussain, N., Jaitley, V. & Florence, A. T. (2001). Recent advances in the understanding of uptake of microparticulates across the gastrointestinal lymphatics. *Advanced Drug Delivery Reviews, 50*(1-2), 107-142.

IKSR. (2005). Internationale Flussgebietseinheit Rhein, Merkmale, Überprüfung der Umweltauswirkungen menschlicher Tätigkeiten und wirtschaftliche Analyse der Wassernutzung. Koblenz, Germany: Internationale Kommission zum Schutz des Rheins (IKSR).

Ivar do Sul, J. A. & Costa, M. F. (2014). The present and future of microplastic pollution in the marine environment. *Environmental Pollution, 185*, 352-364. doi: 10.1016/j.envpol.2013.10.036.

Izquierdo, M. & Querol, X. (2012). Leaching behaviour of elements from coal combustion fly ash: An overview. *International Journal of Coal Geology, 94*, 54-66. doi: 10.1016/j.coal.2011.10.006.

Kaposi, K. L., Mos, B., Kelaher, B. P. & Dworjanyn, S. A. (2014). Ingestion of microplastic has limited impact on a marine larva. *Environmental Science & Technology, 48*(3), 1638-1645. doi: 10.1021/es404295e.

Kappler, A., Windrich, F., Loder, M. G., Malanin, M., Fischer, D., Labrenz, M., . . . Voit, B. (2015). Identification of microplastics by FTIR and Raman microscopy: a novel silicon filter substrate opens the important spectral range below 1300 cm(-1) for FTIR transmission measurements. *Analytical and Bioanalytical Chemistry, 407*(22), 6791-6801. doi: 10.1007/s00216-015-8850-8.

Klein, S., Worch, E. & Knepper, T. P. (2015). Occurrence and Spatial Distribution of Microplastics in River Shore Sediments of the Rhine-Main Area in Germany. [Research Support, Non-U.S.

Gov't]. *Environmental Science & Technology, 49*(10), 6070-6076. doi: 10.1021/acs.est.5b00492.

Kroes, M. J., Tweehuysen, G. & Löhr, A. J. (2014). Plastics in rivieren uitdaging voor waterbeheer [Plastic river litter is a challenge for water managers]. *Land+Water, 1/2* 31-33.

Law, K. L., Moret-Ferguson, S., Maximenko, N. A., Proskurowski, G., Peacock, E. E., Hafner, J. & Reddy, C. M. (2010). Plastic accumulation in the North Atlantic subtropical gyre. *Science, 329*(5996), 1185-1188. doi: 10.1126/science.1192321.

Lechner, A., Keckeis, H., Lumesberger-Loisl, F., Zens, B., Krusch, R., Tritthart, M., . . . Schludermann, E. (2014). The Danube so colourful: a potpourri of plastic litter outnumbers fish larvae in Europe's second largest river. *Environmental Pollution, 188*, 177-181. doi: 10.1016/j.envpol.2014.02.006.

Leslie, H. A., Van der Meulen, M., Kleissen, F. & Vethaak, D. (2011). Microplastic litter in the Dutch marine environment. Delft: Deltares.

Li, H., Xu, D., Feng, S. & Shang, B. (2014). Microstructure and performance of fly ash micro-beads in cementitious material system. *Construction and Building Materials, 52*, 422-427. doi: 10.1016/j.conbuildmat.2013.11.040.

Lobo, H. & Bonilla, J. V. (2003). (Eds). *Handbook Of Plastics Analysis*. New York: Marcel Dekker inc.

Lucas, N., Bienaime, C., Belloy, C., Queneudec, M., Silvestre, F. & Nava-Saucedo, J. E. (2008). Polymer biodegradation: mechanisms and estimation techniques. *Chemosphere, 73*(4), 429-442. doi: 10.1016/j.chemosphere.2008.06.064.

Lusher, A. L., McHugh, M. & Thompson, R. C. (2013). Occurrence of microplastics in the gastrointestinal tract of pelagic and demersal fish from the English Channel. *Marine Pollution Bulletin, 67*(1-2), 94-99. doi: 10.1016/j.marpolbul.2012.11.028.

Mangaraj, S., Goswami, T. K. & Mahajan, P. V. (2009). Applications of Plastic Films for Modified Atmosphere Packaging of Fruits and Vegetables: A Review. *Food Engineering Reviews, 1*(2), 133-158. doi: 10.1007/s12393-009-9007-3.

Moore, C. J. (2008). Synthetic polymers in the marine environment: a rapidly increasing, long-term threat. *Environmental Research, 108*(2), 131-139. doi: 10.1016/j.envres.2008.07.025.

Moore, C. J., Lattin, G. L. & Zellers, A. F. (2005). *Working our way upstream: A snapshot of land-based contributions of plastic and other trash to coastal waters and beaches of Southern California*. Algalita Marine Research Foundation. Long Beach.

Morritt, D., Stefanoudis, P. V., Pearce, D., Crimmen, O. A. & Clark, P. F. (2014). Plastic in the Thames: a river runs through it. *Marine Pollution Bulletin, 78*(1-2), 196-200. doi: 10.1016/j.marpolbul.2013.10.035.

Noren, F. & Naustvoll, F. (2010). Survey of Microscopic Anthropogenic Particles in Skagerrak. Oslo, Norway: Norwegian Environment Agency.

Pham, C. K., Ramirez-Llodra, E., Alt, C. H., Amaro, T., Bergmann, M., Canals, M., . . . Tyler, P. A. (2014). Marine litter distribution and density in European seas, from the shelves to deep basins. *PloS One, 9*(4), e95839. doi: 10.1371/journal.pone.0095839.

Pichel, W. G., Churnside, J. H., Veenstra, T. S., Foley, D. G., Friedman, K. S., Brainard, R. E., . . . Clemente-Colon, P. (2007). Marine debris collects within the North Pacific Subtropical Convergence Zone. *Marine Pollution Bulletin, 54*(8), 1207-1211. doi: 10.1016/j.marpolbul.2007.04.010.

Raps, D., Hossieny, N., Park, C. B. & Altstädt, V. (2015). Past and present developments in polymer bead foams and bead foaming technology. *Polymer, 56*, 5-19. doi: 10.1016/j.polymer.2014.10.078.

Rios, L. M., Moore, C. & Jones, P. R. (2007). Persistent organic pollutants carried by synthetic polymers in the ocean environment. *Marine Pollution Bulletin, 54*(8), 1230-1237. doi: 10.1016/j.marpolbul.2007.03.022.

Rocha-Santos, T. & Duarte, A. C. (2015). A critical overview of the analytical approaches to the occurrence, the fate and the behavior of microplastics in the environment. *Trends in Analytical Chemistry, 65*, 47-53. doi: 10.1016/j.trac.2014.10.011.

Rochman, C. M., Browne, M. A., Halpern, B. S., Hentschel, B. T., Hoh, E., Karapanagioti, H. K., . . . Thompson, R. C. (2013). Policy: Classify plastic waste as hazardous. *Nature, 494*(7436), 169-171. doi: 10.1038/494169a.

Rovira, A., Alcaraz, C. & Ibanez, C. (2012). Spatial and temporal dynamics of suspended load at-a-cross-section: the lowermost Ebro River (Catalonia, Spain). [Research Support, Non-U.S. Gov't]. *Water Research, 46*(11), 3671-3681. doi: 10.1016/j.watres.2012.04.014.

Ryan, P. G., Moore, C. J., van Franeker, J. A. & Moloney, C. L. (2009). Monitoring the abundance of plastic debris in the marine environment. *Philosophical transactions of the Royal Society of London. Series B, Biological sciences, 364*(1526), 1999-2012. doi: 10.1098/rstb.2008.0207.

Sadri, S. S. & Thompson, R. C. (2014). On the quantity and composition of floating plastic debris entering and leaving the Tamar Estuary, Southwest England. [Research Support, Non-U.S. Gov't]. *Marine Pollution Bulletin, 81*(1), 55-60. doi: 10.1016/j.marpolbul.2014.02.020.

Schöntag, J. M. & Sens, M. L. (2014). Characterization of polystyrene granules as granular media filters. *Desalination and Water Treatment, 55*(7), 1712-1724. doi: 10.1080/19443994.2014.928234.

Setala, O., Fleming-Lehtinen, V. & Lehtiniemi, M. (2014). Ingestion and transfer of microplastics in the planktonic food web. *Environmental Pollution, 185*, 77-83. doi: 10.1016/j.envpol.2013.10.013.

Shemouratov, Y. V., Prokhorov, K. A., Nikolaeva, G. Y., Pashinin, P. P., Kovalchuk, A. A., Klyamkina, A. N., . . . Antipov, E. M. (2008). Raman study of ethylene-propylene copolymers and polyethylene-polypropylene reactor blends. *Laser Physics, 18*(5), 554-567. doi: 10.1134/s1054660x08050046.

Song, Y. K., Hong, S. H., Jang, M., Han, G. M., Rani, M., Lee, J. & Shim, W. J. (2015). A comparison of microscopic and spectroscopic identification methods for analysis of microplastics in environmental samples. *Marine Pollution Bulletin, 93*(1-2), 202-209. doi: 10.1016/j.marpolbul.2015.01.015.

Van, A., Rochman, C. M., Flores, E. M., Hill, K. L., Vargas, E., Vargas, S. A. & Hoh, E. (2012). Persistent organic pollutants in plastic marine debris found on beaches in San Diego, California. *Chemosphere, 86*(3), 258-263. doi: 10.1016/j.chemosphere.2011.09.039.

Van Mazijk, A. (1986). *Representativiteit van de monsternamepunten Lobith en Kleve-Bimmen. Lelystad, Netherlands*: RIWA, werkgroep Hydrologie.

Van Mazijk, A. (2002). Modelling the effects of groyne fields on the transport of dissolved matter within the Rhine Alarm-Model. *Journal of Hydrology, 264*(1-4), 213–229. doi: 10.1016/S0022-1694(02)00077-X.

Van Mazijk, A. & Veling, E. J. M. (2005). Tracer experiments in the Rhine Basin: evaluation of the skewness of observed concentration distributions. *Journal of Hydrology, 307*(1-4), 60-78. doi: 10.1016/j.jhydrol.2004.09.022.

Van Paassen, J. (2010). *Plastic afval in rivieren. Onderzoek naar hoeveelheid en samenstelling [Plastic litter in rivers. A study on abundance and composition]. .* (Bsc thesis), Utrecht.

Verschoor, A., De Poorter, L., Roex, E. & Bellert, B. (2014). *Inventarisatie en prioritering van bronnen en emissies van microplastics*. (2014-0110). Bilthoven, Netherlands: Rijksinstituut voor Volksgezondheid en Milieu [The National Institute for Public Health and the Environment] (RIVM).

Von Moos, N., Burkhardt-Holm, P. & Kohler, A. (2012). Uptake and effects of microplastics on cells and tissue of the blue mussel *Mytilus edulis L*. after an experimental exposure. *Environmental Science & Technology, 46*(20), 11327-11335. doi: 10.1021/es302332w.

Wagner, M., Scherer, C., Alvarez-Muñoz, D., Brennholt, N., Bourrain, X., Buchinger, S., . . . Reifferscheid, G. (2014). Microplastics in freshwater ecosystems: what we know and what we need to know. *Environmental Sciences Europe, 26*(1), 12. doi: 10.1186/s12302-014-0012-7.

Wick, P., Malek, A., Manser, P., Meili, D., Maeder-Althaus, X., Diener, L., . . . von Mandach, U. (2010). Barrier capacity of human placenta for nanosized materials. *Environmental Health Perspectives, 118*(3), 432-436. doi: 10.1289/ehp.0901200.

Wright, S. L., Thompson, R. C. & Galloway, T. S. (2013). The physical impacts of microplastics on marine organisms: a review. *Environmental Pollution, 178*, 483-492. doi: 10.1016/j.envpol.2013.02.031.

Appendix references:

Bovill, A. J., McConnell, A. A., Nimmo, J. A. & Smith, W. E. (1986). Resonance Raman spectra of .alpha.-copper phthalocyanine. *The Journal of Physical Chemistry, 90*(4), 569-575 doi: 10.1021/j100276a017.

Claessens, M., Van Cauwenberghe, L., Vandegehuchte, M. B., & Janssen, C. R. (2013). New techniques for the detection of microplastics in sediments and field collected organisms. *Maritime Pollution Bulletin*, *70(1-2),* 227-233. doi: 10.1016/j.marpolbul.2013.03.009.

Davies-Colley, R. J., & Smith, D. G. (2001). Turbidity, suspended sediment and water clarity: a review. *JAWRA Journal of the American Water Resources Association, 37(5),* 1085-1101.

Hidalgo-Ruz, V., Gutow, L., Thompson, R. C., & Thiel, M. (2012). Microplastics in the marine environment: a review of the methods used for identification and quantification. *Environmental Science & Technology, 46(6),* 3060-3075. doi: 10.1021/es2031505.

Michaud, J. P. (1991). *A Citizens' Guide to Understanding and Monitoring Lakes and –Streams.* Washington: Washington State Department of Ecology.

Van Nieuwenhuijzen, A. (2011). Handbook on Particle Separation Processes. London: IWA.

Ozzetti, R. A., De Oliveira Filho, A. P., Schuchardt, U. & Mandelli, D. (2002). Determination of tacticity in polypropylene by FTIR with multivariate calibration. *Journal of Applied Polymer Science, 85(4)*, 734-745. doi: 10.1002/app.10633.

Web based references (including the appendix):

American Chemistry Council, http://plastics.americanchemistry.com/Education-Resources/Hands-onPlastics/Introduction-to-Plastics-Science-Teaching-Resources/History-of-Polymers-Plastics-for-Teachers.html, retrieved at August 16th, 2015.

Curbell plastics, report on the absorption of water by polymers, http://www.curbellplastics.com/technical-resources/pdf/water-absorption-plastics.pdf, retrieved at September 3rd 2015.

Environmental Protection Agency (EPA), http://water.epa.gov/type/rsl/monitoring/vms55.cfm, retrieved at November 2nd, 2014.

Polymer Science Learning Center, http://pslc.ws/, retrieved at August 16th, 2015.

Shimadzu, tutorial, http://www.shimadzu.com/an/ftir/support/faq/1.html, retrieved on October 3rd, 2015).

Wikipedia page of the Ruhr region (in German), https://de.wikipedia.org/wiki/Ruhrgebiet, retrieved at November 15th, 2014 and at February 1st, 2015.

Appendices.

Appendix 1 The locations of the monitoring stations where microplastic samples were taken
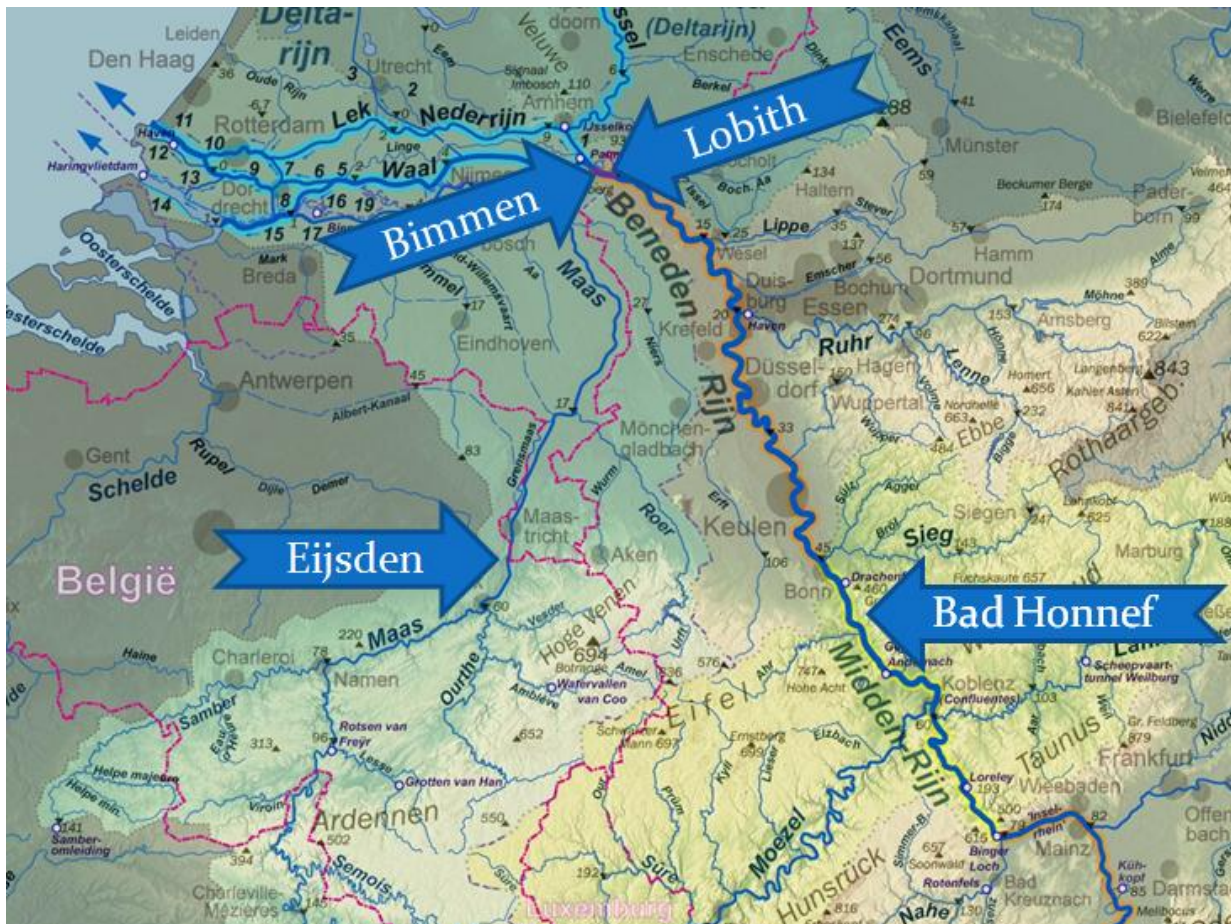

Figure A1. Locations of the monitoring stations where MPs were collected from the Rivers Meuse and Rhine. Eijsden is located at the right bank of the river Meuse. Bimmen is located on the left bank of the river Rhine, while Lobith, and Bad Honnef are located on the right river bank. (Source: https://commons.wikimedia.org/wiki/File:Flusssystemkarte_Rhein_06.jpg (free content, retrieved July 1st, 2015).

Appendix 2 An explanation of the term turbidity

Turbidity is a measure of clarity of a liquid medium. It is measured by letting a light beam pass through a liquid medium and detecting the degree of scattering by undissolved particles in this medium.
Depending of the instruments used, turbidity is reported in different units like Formazine Nephelometric Turbidity Units (NTU), or Jackson turbidity units (JTU) (Michaud, 1991) .

There are several arguments to monitor turbidity levels. The United States Environmental Protection agency (EPA, 2015) sums up that turbidity can lead to:

1) Higher water temperatures and hence declined O_2 level as suspended particles absorb more heat.
2) Reduced photosynthesis due to less light penetrating into the water.
3) Fish gill clogging.
4) Reduced resistance to disease in fish.
5) Lowering growth rates and affecting egg and larval development.

Rijkswaterstaat is primarily interested in turbidity as high turbidity levels can be related to pollution carriage. Pollutants are known to adhere to suspended matter. Higher rates of suspended matter can threaten the water intake for drinking water facilities downstream from Lobith and Eijsden (personal communication, dr. G. Stroomberg, Rijkswaterstaat). Turbidity levels of both the Meuse and Rhine are monitored at Lobith and Eijsden in one hour intervals.

FTU/NTU
Rijkswaterstaat reports in NTU, which is dimensionless. Calibration takes place by a range of standard solutions of Formazine in water. Formazine is a white coloured reaction product of hydrazine sulfate and hexamethylenetetramine. A suspension of 1.25 mg/L hydrazine sulfate and 12.5 mg/L hexamethylenetetramine in water has a turbidity of one NTU (Van Nieuwenhuijzen & Van der Graaf, 2011). Turbidity measurements are carried out by comparing the transmittance of samples with these standards. Figure A2 displays several examples of NTU levels.

According to (Davies-Colley & Smith, 2001), turbidity is not really a scientific measurement but merely a relative index of scattering with reference to an arbitrary standard.
It reaches beyond the scope of this study to discuss the shortcomings of this method in detail. Recording of turbidity values were deducted at the same locations (the monitoring stations) and with the same equipment and automatically derived, without manual adaptations.

Figure A2. Turbidity standards. Picture reprinted with permission of South Fork Instruments, Inc.

Appendix 3 A pilot run to obtain insights in sampling river water with a soil sieve set up

This pilot was run to gain practical insights and experiences for this Master's thesis and it did not intend to obtain scientific trustful data. With respect to the sampling and the laboratory processing, (Hidalgo-Ruz et al., 2012) displayed based on a review of 68 studies on MPs a clear picture of best practice to date and was used as valuable input for both pilot and the actual MSc. project.

In short, sampling in the water stream and processing of samples comprised the following steps:
-   Collection of MPs in a neuston net.
-   Filtration/sieving to determine particle distribution based on their size.
-   Virtual sorting.

For sediment samples, the associated steps were:
-   Bulk sampling (scooping).
-   Density separation to part sand particles (that sink) from possible polymer particles (that float).
-   Filtration/sieving to determine particle distribution based on their size.
-   Visual sorting.

After visual sorting, their nature was occasionally studied with Raman or FT-IR spectroscopy, in order to obtain insights on the possibilities and obstacles of spectroscopic analysis. The presence of organic debris was not addressed by (Hidalgo-Ruz et al., 2012), but the digesting method using H_2O_2 was reported by Claessens, Van Cauwenberghe, Vandegehuchte and Janssen (2013).

Sampling

The pilot was run in the months October and November 2013 at three monitoring locations: Bimmen, Lobith and Eijsden. Metal wire cloth sieves, Ø20 cm and flange height 5 cm were placed under a tap delivering plain river water from a branch of the monitoring stations pump systems. Several mesh sizes, varying from 0,18 mm up to 2.5 mm, were tested at several tap flow rates, different turbidity levels and different sampling time lengths, as displayed in table A1. Just prior and direct after sampling the tap flow rate was determined by measuring the time needed to fill a standard volume.

Table A1. An overview of the sampling pilot run in 2013. Different volumes, flow rates and sampling times were tested at all three locations. * Here the tap flow rate gradually declined, probably due to internal clogging at the occluding parts of the tap. The ball valve in this gauge was replaced prior to the actual sampling.

River	Start	Location (+ sample name)	Sample set-up	Sieve mesh	Depth (m)	Pump of tap flow ra	Durat (h)	Sieved volume (m³)
Meuse	10/10	Eijsden (E1)	Submergible pump at pontoon	0.25 + 1 + 2.5 mm	-3.0	1.9 m³/h		
Meuse	10/10	Eijsden (E2)	Sieves under tap	0.25+ 1 + 2.5 mm	-0.8	0.9 m³/h	1.0	0.9
Meuse	11/10	Eijsden (E3)	Sieves under tap	0.25+ 1 + 2.5 mm	-0.8	1.2 m³/h	72	86
Meuse	18/10	Eijsden (E4)	Sieves under tap	0.25+ 1 + 2.5 mm	-0.8		72	84
Rhine	23/10	Lobith (L1)	Sieves under tap	0.18+ 0.25+ 1 mm	-0.8	*	65.5	16 (est)
Rhine	25/10	Lobith (L2)	Sieves under tap	0.18 mm	-0.8	*	72	22 (est)
Rhine	30/10	Bimmen (B1)	Sieves under tap	0.18 mm	-0.8	3.1 m³/h	4.2	13
Rhine	30/10	Bimmen (B2)	Submergible pump at pontoon	0.18 + 0.25 mm	-0.1	3.3 m³/h	4.5	Failed. Water splashing over the sieve edge.
Meuse	6/11	Eijsden (E5)	Submersible pump middle of river	0.18 + 0.25+ 1,0 mm	-0.1	3.1 m³/h	3.0	Failed. All sieves clogged within 3 hours.
Meuse	6/11	Eijsden (E6)	Submersible pump middle of river	0.18 + 0.25 mm	-3.0	---	---	Failed. Depth not reached due to river current.
Meuse	7/11	Eijsden (E7)	Sieves under tap	0.25 + 0.5 + 1.0 mm.	-0.8	1.2 m³/h	4	9

Cross river sampling

To see whether a mobile pump can be used for, for example, occasional sampling at the longitudinal axis of the river, a test was performed using a 230V Gardena/Husqvarna 6000 submergible pump at Eijsden (figure A3). This type of submersible pump is commonly used to drain ponds or crawl spaces and is developed to let solid parts pass up to 5 mm large without damaging the inner pump parts. To prevent the pump to suck up large parts, the inlet was protected with a mesh (square 8mm).

Figure A3. Pilot sampling in the mid section of the river Meuse (Eijsden) using a submergible pump.
(a, left) Water was directly led over the sieves. Water could run freely through a hole in the hardboard plate.
(b, right) Position of the submergible pump just below water surface.

The submergible pump pilot was not successful. The flow rate was not be alterable, its flow rate of approximately 3 m^3 per hour led to quickly clogging filters and the loss of sampling material. Even more, in a strong river current it turned out to be difficult to bring and keep the submerged pump at the desired depth. Besides, the Rhine is heavily used by professional shipping, which brings along safety issues for prolonged sampling in the mid section of the river.

Laboratory pilot

The material obtained from the sampling pilot were brought in as study objects for the laboratory pilot. Facilities were provided by The Department of Ecological Science, Faculty of Earth And Life Sciences, VU, University Amsterdam.

The contents on all sieves were washed above the sieve with the smallest mesh size. From here, the material was washed with purified water and deposited in 250 ml PE bottles via a glass funnel. The PE bottles are marked with sample location, sample date, amount of water sieved. After this, the PE bottles were brought to the laboratory at Amsterdam by unrefrigerated transport.

Here the samples were shaken, the caps twisted off and the contents were decanted into 250 ml glass beakers. The PE bottles and the caps were washed above the glass beaker three times with pure analytical grade water (MilliQ). This resulted in an aqueous solution. The glass beakers were marked with the sample characteristics and placed on a Schott Electric heating plate in a fume hood. The contents were heated up to approximately 100°C (exact temperature could not be determined) to thicken the sample. When almost all water was evaporated, the sample is digested with hydrogen peroxide (H_2O_2, 35%), by adding aliquots of 10 ml. An aliquot was added as soon as reaction responses faded out. The interval times increased as the available amount of organic matter declined. The number of aliquots depended heavily on the amount of organic material. These numbers were not recorded. As soon as H_2O_2 did not start up any reaction anymore, one aliquot of 7 ml Nitric Acid (HNO_3, 65%) was added. The sample was left on the heating plate for one hour at approximately 100°C. Drying samples were moistened with MilliQ. The digested sample showed a brownish suspension in which some particles could be seen by the naked eye.

The reduced sample was decanted into a 200 ml glass graduated cylinder. The beaker was washed three times above the cylinder with saline water from a wash bottle (NaCl saturated, 1.2 g/cm^3). The graduated cylinder was filled with saline water till 1 cm under the top. The mixture was left to equilibrate for at least one hour. Sediment was allowed to settle, while lighter material was allowed to float.

The top layer was decanted above an electrical vacuum pump and filtered over 47 mm 0.7 μm glass fibre. The pump beaker was duly rinsed with MilliQ to loosen material adsorbed to the pump beaker wall and to wash residues of acid and salt. The brownish layer resulting in a clogging layer on the micro pore filter.

Microscopic study of pilot material.
The glass fibre filters were analyzed under a Leica M8 stereo light microscope. Particles were manually isolated from the filter by a pair of pointy tweezers and transferred to a Petri dish. Particles were ordered on physical characteristics, like shape, size, colour and translucency. Particles that were not resistant to the tweezers pinch were not isolated.

Based on physical characteristics three groups were sorted out:
1. Films   : Thin, foldable but yet hardly tearable transparent sheets
2. Spherules   : Spherical particles.
3. Other   : Particles that appear in different characteristics like colour, shape, form.

Conclusions:
- Cross river sampling is difficult to achieve within this MSc. project.
- Multiple sieve mesh sizes, placed in descending order, extend sampling time as it avoids the large parts to clog smaller meshes.
- Smaller mesh sizes increase clogging risks.
- Wooden spacers are suggested so in case the filter clogs, water still escape without influencing the above placed sieves.
- After H_2O_2 and HNO_3 digestion, particles in the size range 0.125 mm up to 5 mm, of which most expected to be polymeric, can be manually isolated from the sample material by tweezers.
- Remnants of the digestion steps result in a brownish cloaking layer that hinders detection under light microscope. Particles can get overlooked.
- Density separation of particles is a useful and tested method for separating polymeric particles from inorganic sediment.

Appendix 4 Investigating probable negative aspects of hot acid digestion.

To examine the possible effects of acids during laboratory processing, an acid destruction test was performed with the following plastics (further: reference plastics):

1) 2 parts of a blue polystyrene mushroom cup (PS).
2) 2 pieces of polyethylene agriculture plastic (Green PE)
3) 2 parts of a polypropylene (PP) margarine tub.
4) 2 pieces of poly(vinylchloride) (PVC), grated off a grey coloured sewer pipe.
5) 2 preprocessed Chromospere™ polystyrene divinylbenzene red spherules (PSDVB).
6) 2 sheets of common sandwich bags (PE).

The plastics are shown in figure A4. They are arranged from left to right as in the list above. The type of polymer was verified based on the resin code on the product itself or on the product label. The nature of the agriculture plastic (2) and the common sandwich bags (6) were verified with Raman. They varied in size, but all measured above 2 mm. The red PSDVB spherules measured ø300 µm. The fragment sizes and the red beads were chosen in favour of increased distinctiveness.
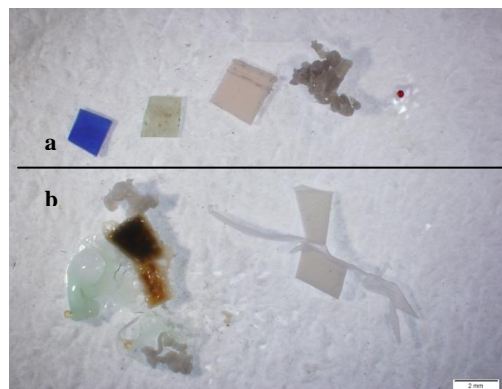
Figure A4. Effects of acid destruction on reference plastics (here: with HN0$_3$). Their nature and the observed effects after the test are presented in table A2. (a) Examples of reference plastics. From left to right: PS, Green PE, PP, PVC, PSDVB. The PE sheet is not shown. (b) The results of HNO3 destruction on similar reference plastics. Scale bar = 2mm

The acid destruction test was based on a standard Rijkswaterstaat procedure for metal extraction from organic material and sediment (procedure A4.408).This destruction test is performed once. The reference plastics were not weighed before or after treatment. In each of four clean and empty Teflon vessels, a set of reference plastics were placed. In the first vessel an aliquot of 10 ml HNO$_3$ (65%) was added, in the second 10 ml HCL (37%), in the third 10 ml aqua regia (HNO$_3$ and HCl in ratio 1:3). The fourth was used as blank just filled with 10 ml milliQ. Then each vessel was filled up with an aliquot of 10 ml milliQ. All three vessels were tightly closed and underwent a microwave destruction at 140º C for 40 minutes. After this, the vessels were filled up to 1 cm under the top, decanted and washed with milliQ above a Ø47 mm 0.7 µm glass fibre filter. The filters were directly studied under a stereomicroscope. Table A2 presents the observed effects to the reference plastics. The blank did not show to any observable effects suggesting that the temperature raise and the microwave radiation alone were no harm. For the samples containing acids. malformations, colour change and the fusion of plastics were observed. Fine debris on the micro pore filter suggests that plastics were also fragmentized.

Table A2. Summary of observed effects to a range of plastics after the acid destruction test. The test was performed with HCL, HNO3, aqua regia and a blank (MilliQ). The procedure is a standard to remove organic material from waste water and sediment with the aim of determining the presence of metals (A4.408). '---' stands for no observed effect.

	PS	Green PE	PP	PVC	PSDVB	PE sheet
Full name	Polystyrene	Polyethylene	Polypropylene	Poly (vinylchloride)	Polystyrene divinylbenzene	Polyethylene
Source	Mushroom cup (blue)	Agriculture plastic (green)	Margarine tub (white)	Sewer pipe (grey)	Chromospere™	Sandwich bag

	PS	Green PE	PP	PVC	PSDVB	PE sheet
Blank	---	---	---	---	---	---
HCl	Colour change to dark grey	Curled, more rigid structure.	---	Slightly lighter in colour	Slight colour change, still red.	Curled and shrunk.
HNO$_3$	Colour change to brown/grey. Malformed. Fused with Green PE.	Fused with PS and entangled with PVC and PSDVB.	Entangled with PE sheet.	Slightly lighter in colour, entangled with Green PE.	Colour change to brown, entangled with Green PE.	Curled and shrunk. Entangled with PP.
Aqua regia	Colour change to brown/grey.	Molten, 1 out of 2 entangled with all but PS.	1 out of 2 entangled with Green PE.	Slightly lighter in colour, 1 out of 2 entangled with Green PE.	Colour change to brown.	Curled and shrunk. Entangled with Green PE.

Appendix 5 Fourier-Transform and Raman spectra of the used references
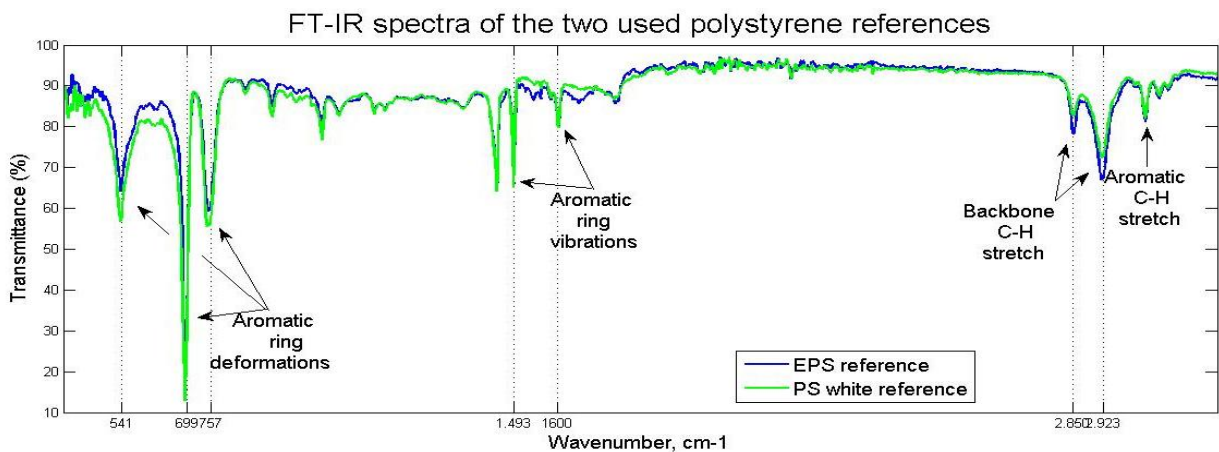
FT-IR

Figure A5. FT-IR spectra of the used polystyrene references. The transmittance is presented on the Y axis in %. The wavenumbers are presented on the X-axis, ranging from 400 cm^{-1} to 3200cm^{-1} (as no peaks were observed above 3200 cm^{-1}). The characteristic peaks are explained (Lobo and Bonilla 2003). Both references show clear similarity.
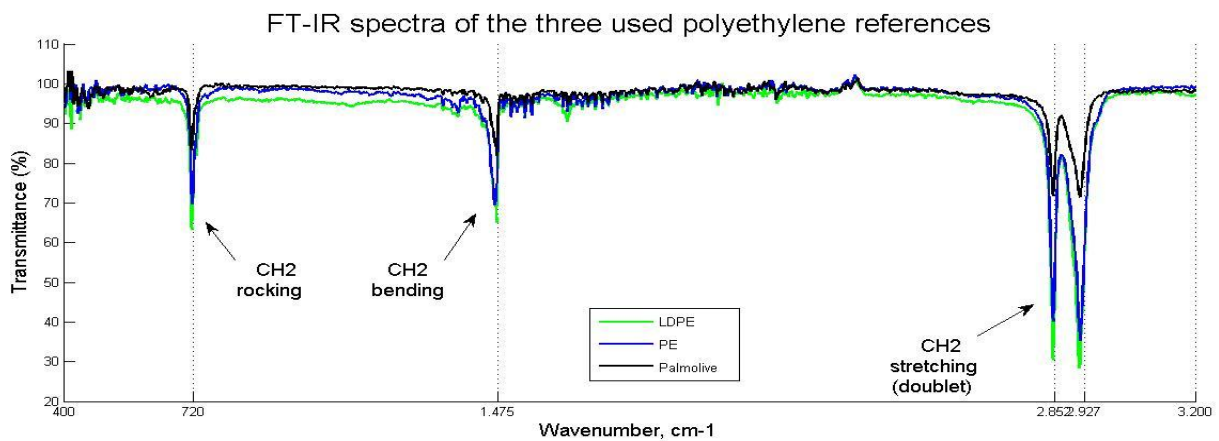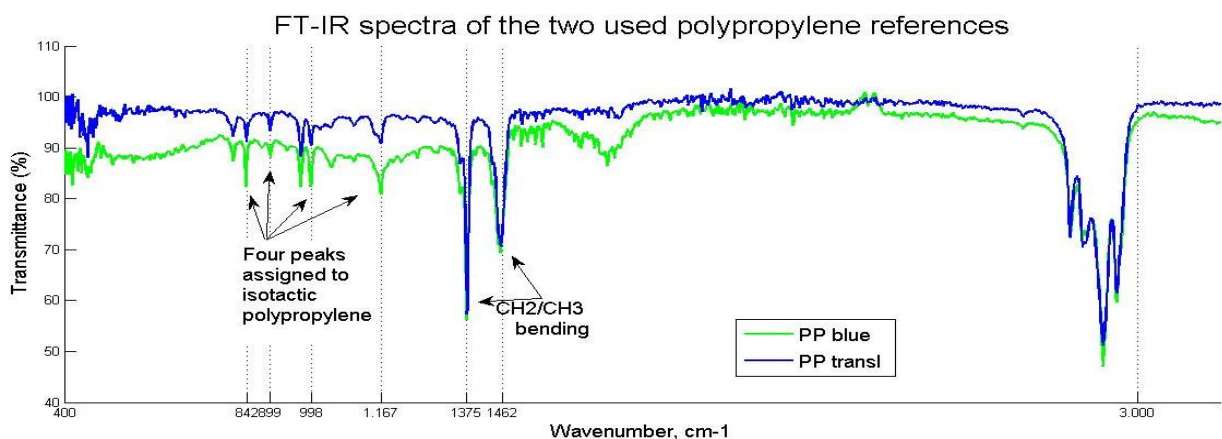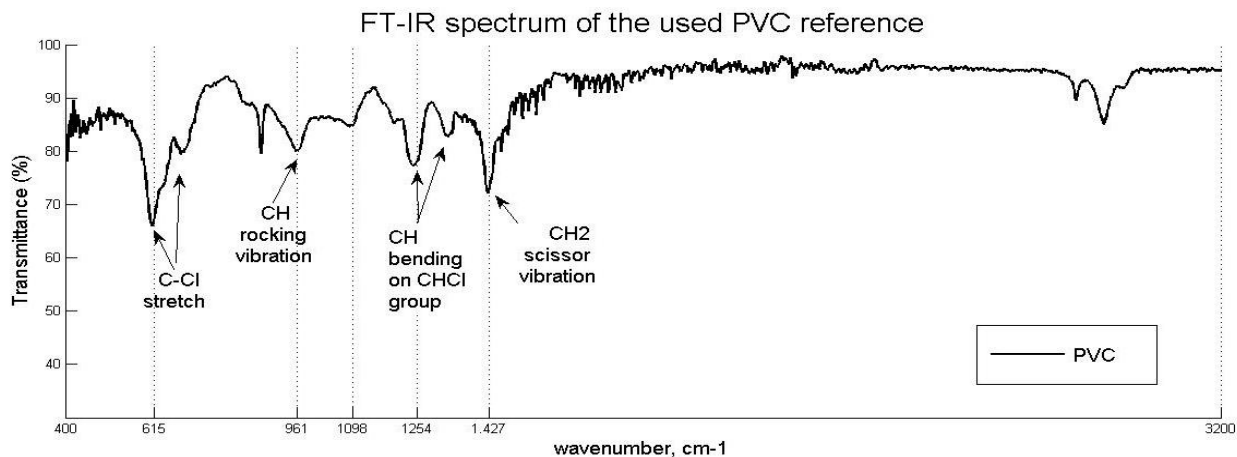

Figure A6. FT-IR spectra of the three used polyethylene references. The transmittance is presented on the Y axis in %. The wavenumbers are presented on the X-axis, ranging from 400 cm^{-1} to 3200cm^{-1} (as no peaks were observed above 3200 cm^{-1}). The characteristic peaks are explained (Lobo and Bonilla 2003). The three references show clear similarity.

Figure A7. FT-IR spectra of the two used polypropylene references. The transmittance is presented on the Y axis in %. The wavenumber is presented on the X-axis, ranging from 400 cm^{-1} to 3200cm^{-1} (as no peaks were observed above 3200 cm^{-1}). The characteristic peaks are explained, including their associated wavenumbers are given (Lobo and Bonilla 2003; Ozetti, De Oliveira Filho, Schuchardt & Mandelli, 2002). The two references show clear similarity.

FT-IR spectrum of the used PVC reference

Figure A8. FT-IR spectrum of the used polyvinyl reference. The transmittance is presented on the Y axis in %. The wavenumber is presented on the X-axis, ranging from 400 cm^{-1} to 3200cm^{-1} (as no peaks were observed above 3200 cm^{-1}). The characteristic peaks are pointed at, including the associated wavenumbers (Lobo and Bonilla 2003).

FT-IR spectra the used organic reference and the isolation foam reference
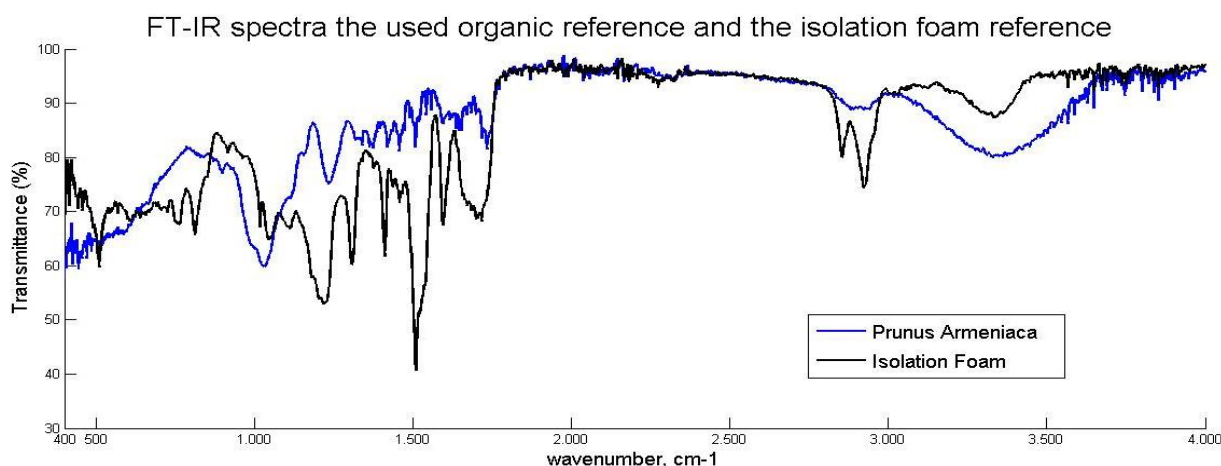
Figure A9. FT-IR spectra of the used organic reference (*Prunus armeniaca*) and the isolation foam reference. The transmittance is presented on the Y axis. The wavenumbers are presented on the X-axis, ranging from 400 cm^{-1} to 4000cm^{-1}. Verification of the vibrational groups of these two references with literature was not successful.

The loadings of PC1 plotted agains the mean centered data of EPS, PP and sample 80
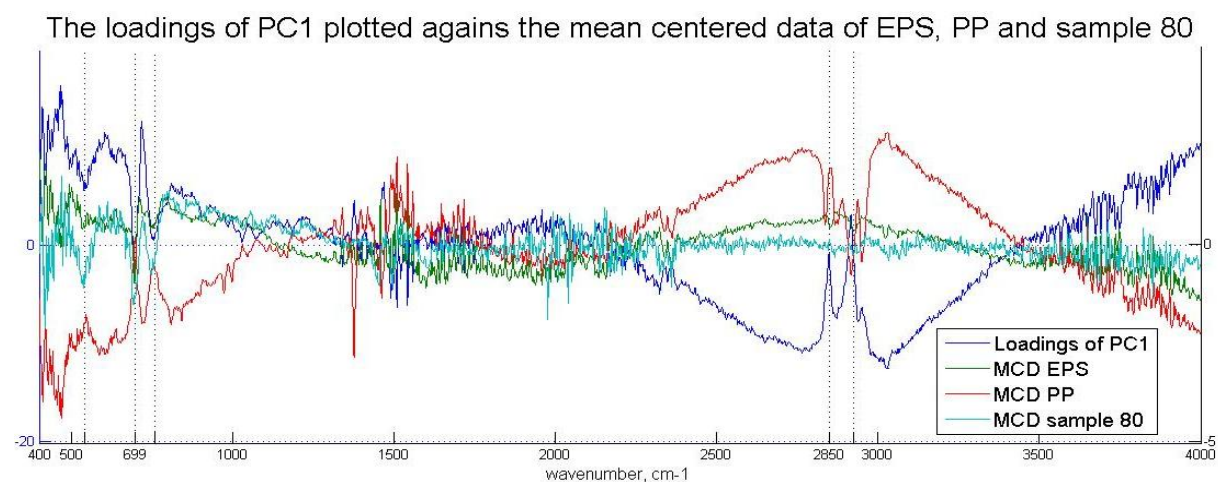
Figure A10. Line plots of the PC1 loadings (blue) versus the meancentered data of the PP reference (red), the meancentered data of the EPS reference (dark green) and the meancentered data of sample 80. The wavenumbers on which PS characteristics are expected, are indicated with the dotted lines. Notice the opposite direction of the PP peak with regard to the loading plot.

Raman
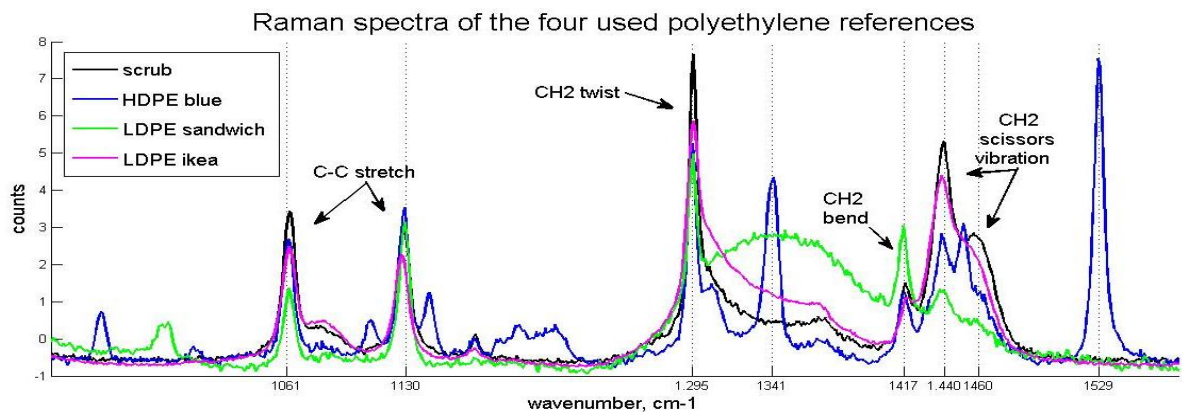
Figure A11. Raman spectra of the four used polyethylene references. Here the baseline corrected and scatter corrected spectra are plotted. On the X-axis, wavenumbers ranging from 925 cm^{-1} to 1575cm^{-1} (the finger print region). Laser wavelength: 785 um. The characteristic peaks for polyethylene are pointed at (Lobo and Bonilla, 2003, pages 223-235). The additional peaks for HDPE blue (the blue line) at 955 cm^{-1}, 1109 cm^{-1}, 1143 cm^{-1}, 1450 cm^{-1} and 1529 cm^{-1} are most probably assigned to the blue color pigment Copper Phthalocyanine (Bovill, McConnell, Nimmo & Smith, 1986) The wide peak for green line, between 1300 and 1400 cm^{-1}, is not explained, but is probably due to scattering which was regularly observed with semi-transparent polyethylene.
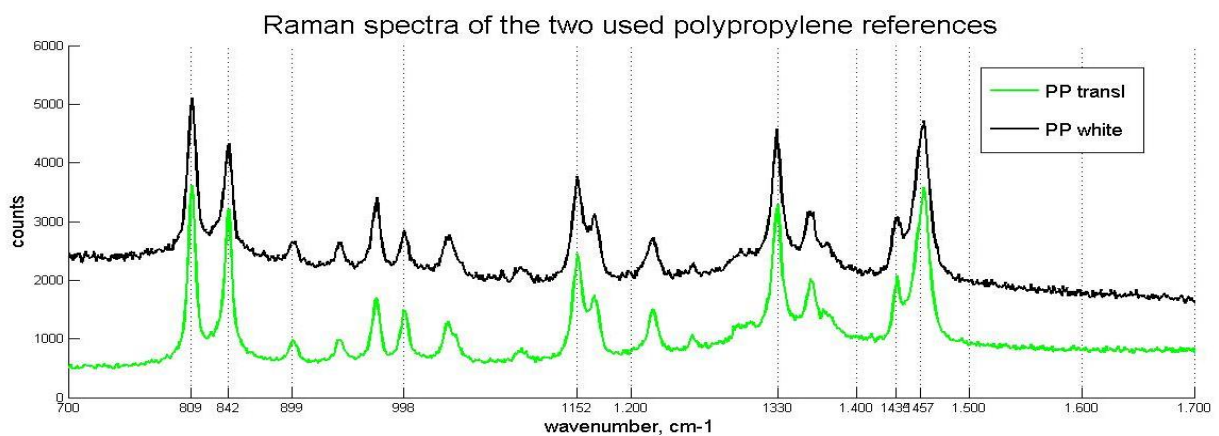
Figure A12. Raman spectra of the two used polypropylene references. The wavenumbers are presented on the X-axis, ranging from 700 cm^{-1} to 1700 cm^{-1} (the finger print region). Laser wavelength: 785 um. Similarity to isotactic polypropylene was verified with sample spectra from Lobo and Bonilla (2003, pages 236-241) and Shemouratov et al. (2008).
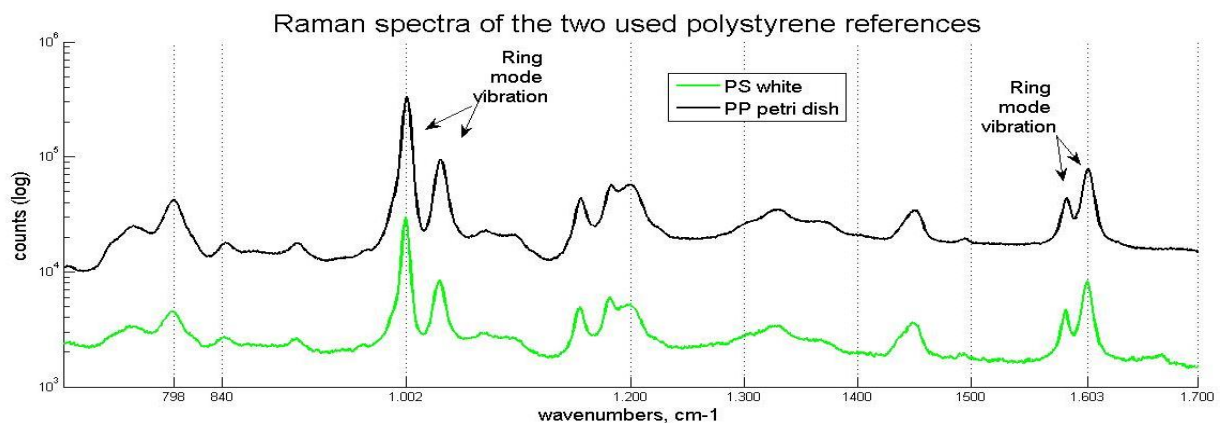
Figure A13. Raman spectra of the two used polystyrene references. The wavenumbers are presented on the X-axis, ranging from 700 cm^{-1} to 1700 cm^{-1} (the finger print region). The Y-scale is logarithmic. Laser wavelength: 785 um. No significant differences were observed between the solid white and the transparent references. Similarity to isotactic polypropylene was verified with Lobo and Bonilla (2003, pages 256-257).
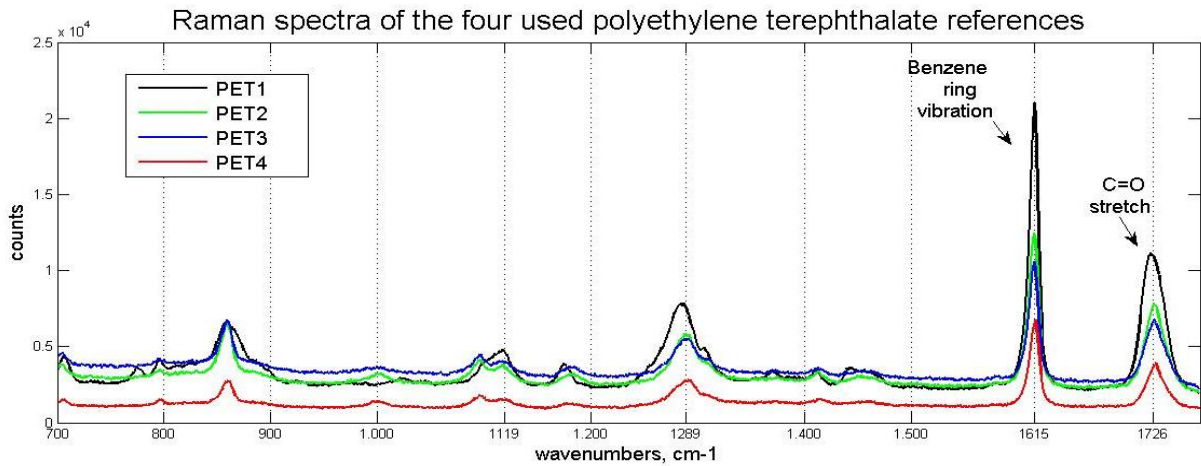
Figure A14. Raman spectra of the four used polyethylene terephthalate references. Laser wavelength: 785 um. The wavenumbers are presented on the X-axis, ranging from 700 cm^{-1} to 1760 cm^{-1} (the finger print region). Two characteristic peaks are explained in the figure. The carbonyl band at 1726 cm^{-1}, combined with the C-O-C ester bands at 1289 and 1119 cm^{-1} represent the features of the terephthalate ester (Lobo and Bonilla, 2003, pages 276-279).
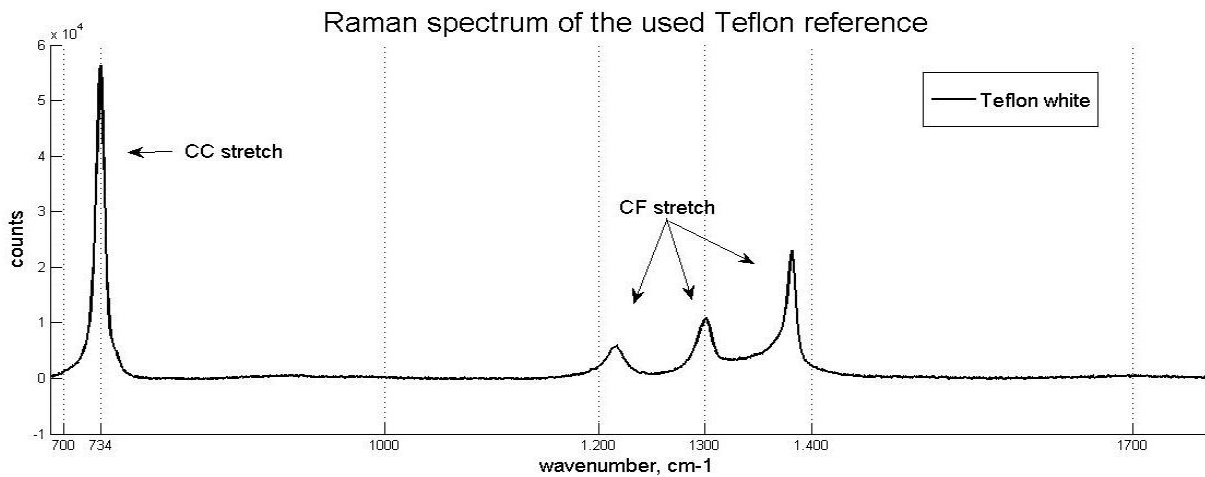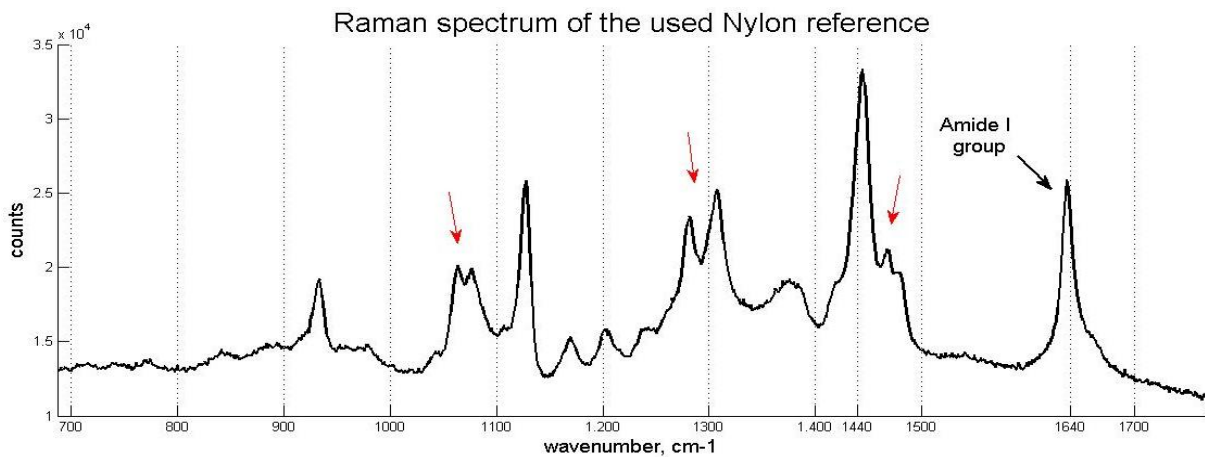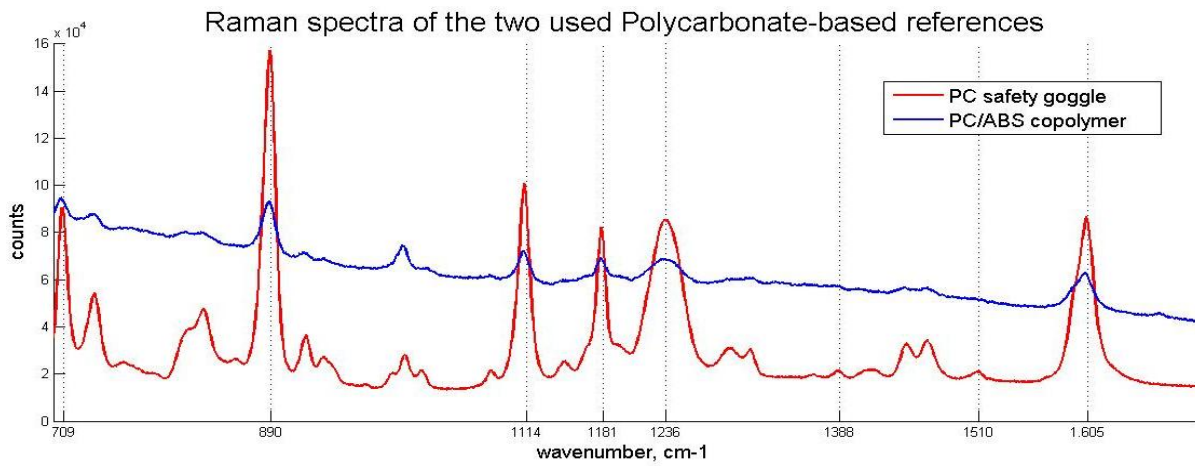

Figure A15. Raman spectrum of the used Teflon reference. Laser wavelength: 785 um. The wavenumbers are presented on the X-axis, ranging from 700 cm^{-1} to 1700cm^{-1} (the finger print region). Four characteristic peaks are described by Lobo and Bonilla (2003, page 253): three peaks contributed to C-F stretch vibration in between 1200 and 1400 cm^{-1} and one peak at 734 cm^{-1} due to skeletal C-C stretching vibrations.

Figure A16. Raman spectrum of the used nylon reference. The wavenumbers are presented on the X-axis, ranging from 700 cm^{-1} to 1700cm^{-1} (the finger print region). The polymer is identified as Nylon-6 (Lobo and Bonilla 2003, page 266, fig. 40). The red arrows point at characteristic comparable features. Laser wavelength: 785 um.

X

Figure A17. Raman spectra of the two used polycarbonate references. Laser wavelength: 785 um. The wavenumbers are presented on the X-axis, ranging from 700 cm^{-1} to 1700 cm^{-1} (the finger print region). The peak intensity differs, but individual line plots show clear similarity. Influences of ABS in the copolymer were not observed. Similarity to type A bis-phenol polycarbonate, commercially known as Lexan, was verified with Lobo and Bonilla (2003, page 330, fig. RS38).

Appendix 6. Regression analysis applied on turbidity and river discharge of the Meuse and Rhine

The river Rhine
This study investigated a probable relation between abundance at the one hand, and turbidity and river discharge at the other. Regression analysis is applied to observe a mutual possible relation between river discharge and turbidity. The daily averaged river discharges and the daily averaged NTU values of the Rhine are presented in figure A18. The starting dates of the samplings are presented on the X-axis. Similarity is suggested as both lines descend from January 10th and both rise and fall between approximately February 10th and February 19th. However, in between April 1st to May 27th, the NTU levels just seem to move in the opposite direction (at the right from the dashed line).
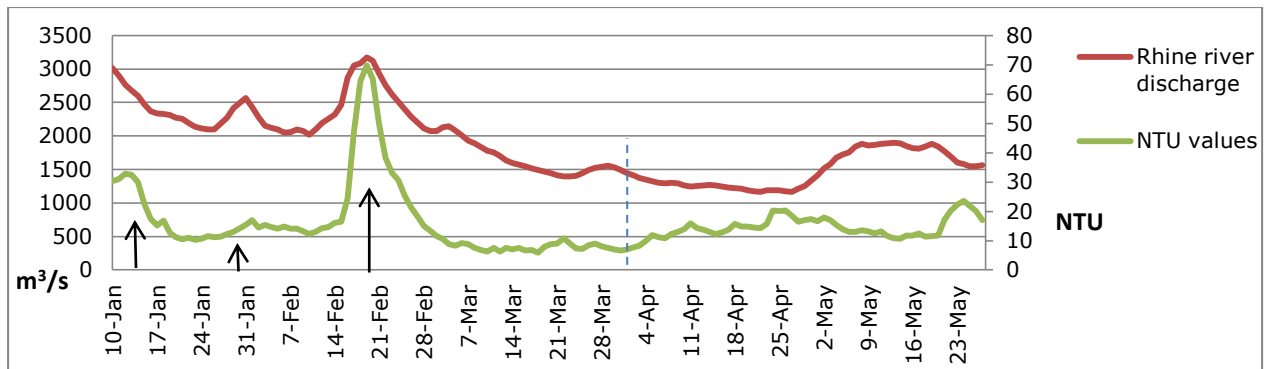
Figure A18. The daily averaged discharge and daily averaged NTU values of the river Rhine during the time path of this study. The black arrow points to a similar increase and/or decline. Right from the dashed line the movements seem opposite.

The mutual relationship between discharge rates and turbidity levels was further tested by applying regression analysis. NTU values and the discharge rates were loaded into Excel. Then each dataset was increasingly arranged on river discharge. Calculations were done in Excel with function regression.

For the river Rhine, two datasets were used:
1) The discharge rates and the NTU values during the actual samplings. Both were averaged over the sampling time. As there were 17 sampling series, 17 observations were included (figure A19). The p value reads 0.0178. Significance is determined at (1-p=) 98.2%, denoting high correlation.

2) The daily averaged discharge rates and the daily averaged NTU values of all days. Here, in total 137 observations were included (figure A20). The p value reads 0,004. Significance is determined at (1-p=) 99,6%, denoting very high correlation. Notice that above approximately 2900 m³/s the variance increases, but that discharge rates above 2900 m³/s are incidentally encountered in this study.

Historical recordings learn that in winter and spring both discharge and NTU values can easily exceed the levels recorded within this study's time path, so the here calculated correlation may not always apply.
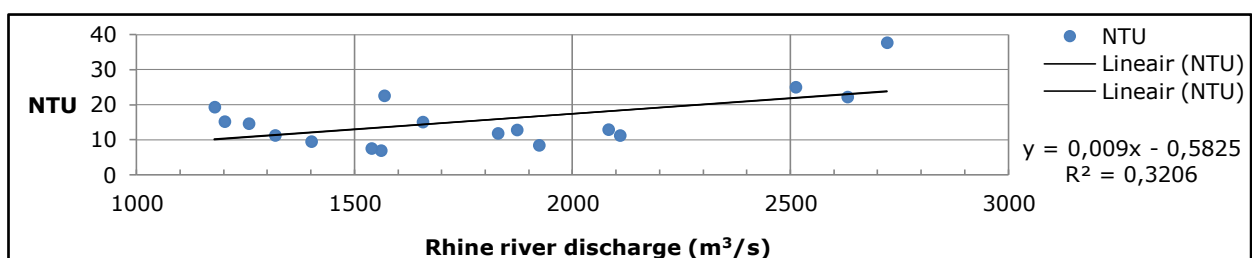

Figure A19. Regression analysis between turbidy (along the y-axis) and the Rhine river discharge (along the x-axis) based on 17 observations. Blue dots represent turbidity (NTU) values and the black line is the regression line.
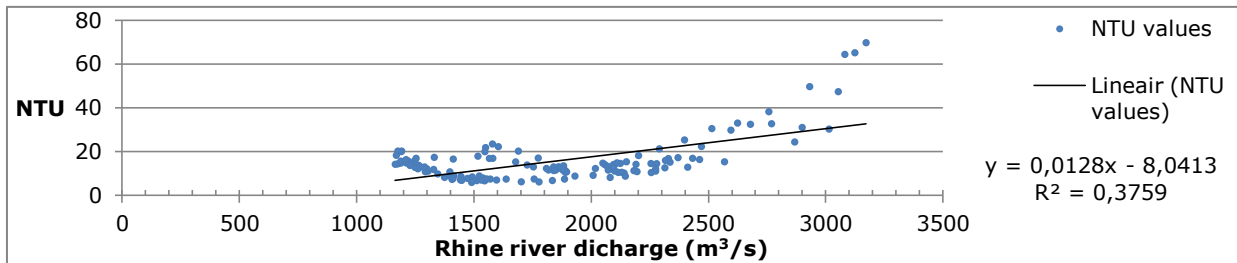
Figure A20. Regression analysis between turbidy (along the y-axis) and the Rhine river discharge (along the x-axis) based on 137 observations. Blue dots represent turbidity (NTU) values and the black line is the regression line.

The river Meuse

The daily averaged discharges and the daily averaged NTU values of the river Meuse are presented in figure A21. The starting dates of the samplings are presented on the X-axis. Dashed lines are drawn through the discharge up peaks to study the similarity of both line plots. In most cases the NTU line follows the discharge line, indicating a relationship. Before March 7th, the discharge rate was higher than the Lixhe power plant capacity of approximately 340 m^3/s and water was released over the full width of the dam. After this date, probably all river water was only led through the turbines. It is thinkable that the dam itself is a sediment trap causing relatively small levels of suspended matter to pass through. Differences between the contents of the suspension before and after March 7th cannot be excluded.
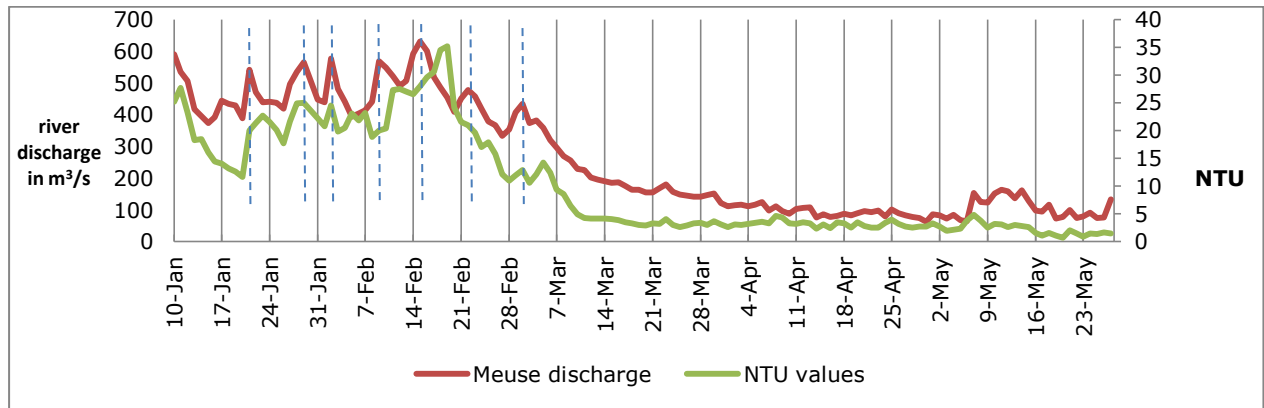

Figure A21. Daily averaged discharge (line plot along the primary Y-axis) and daily averaged NTU values (along the secondary Y-axis) of the river Meuse during the time path of this study.

For the river Meuse, regression analysis was only applied on the averaged values of the actual sampling periods (figure A22). Based on 15 observations, the correlation coefficient R read 0.986. As this is close to one, it indicates a very positive relationship between the observed data. The p value read 0,0001. Significance is determined at (1-p=) 99,99%, an extremely high correlation.
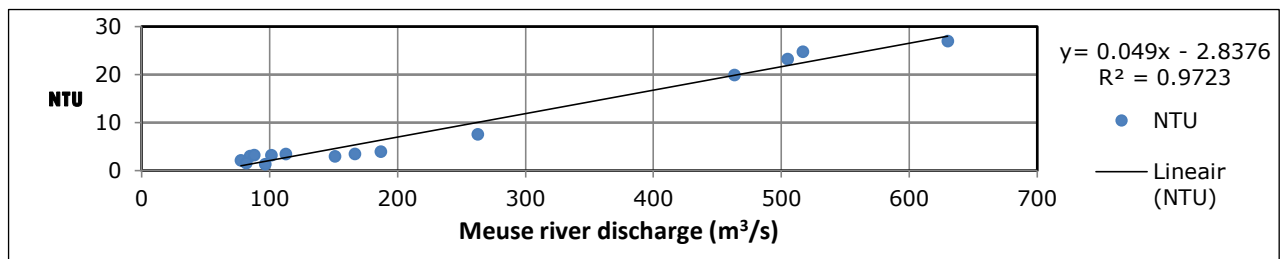

Figure A22. Regression analysis between turbidy (along the y-axis) and the Meuse river discharge (along the x-axis) based on 15 observations. Blue dots are daily averaged turbidity (NTU) values and the black line is the regression line. The correlation coefficient R approached 1.

XIII

Appendix 7. Contour map and cross section of the Rhine near the monitoring station at Lobith
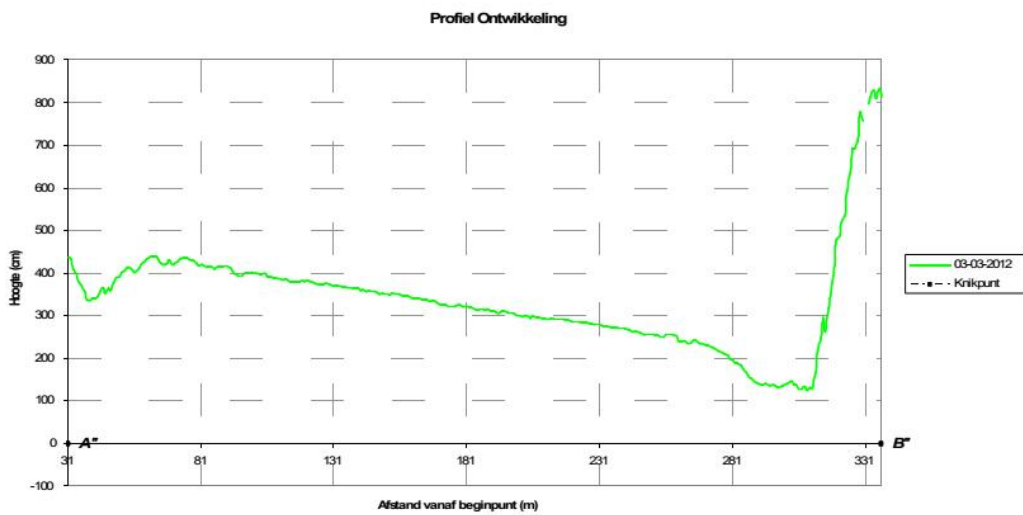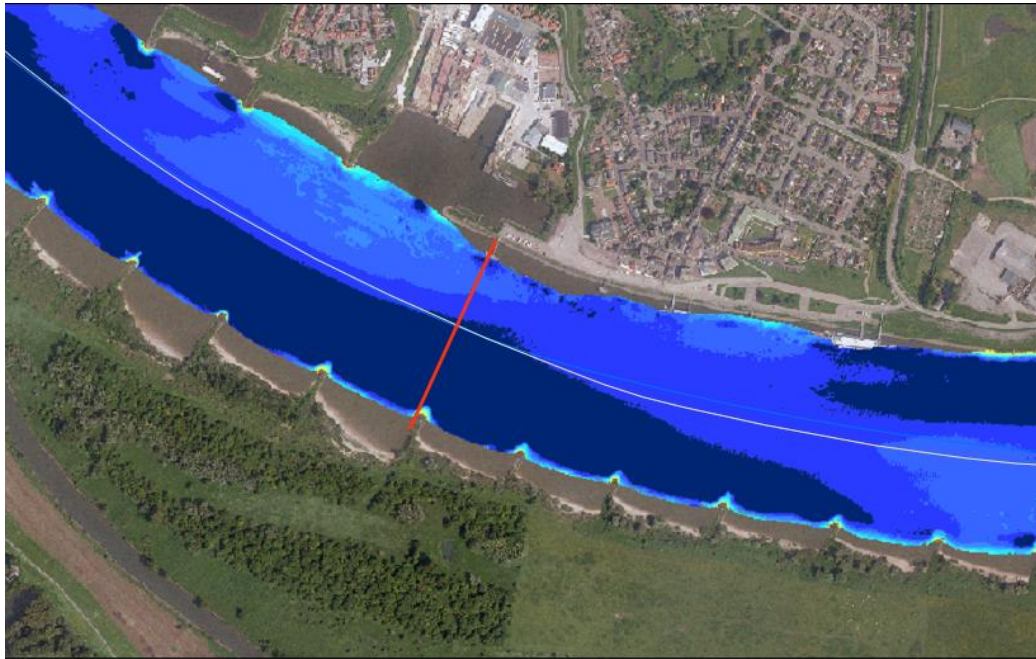
Figure A23. Contour map of the Rhine river at Lobith. The pontoon is located at the upper side of cross section line. Heights are distinguished in colours, from deep (dark blue) till less deep (light blue). For the green cross section inlay: A is at the right river bank (Lobith side) and B at the left river bank (Bimmen side).

Appendix 8. Contour map of the Meuse near the monitoring station at Eijsden
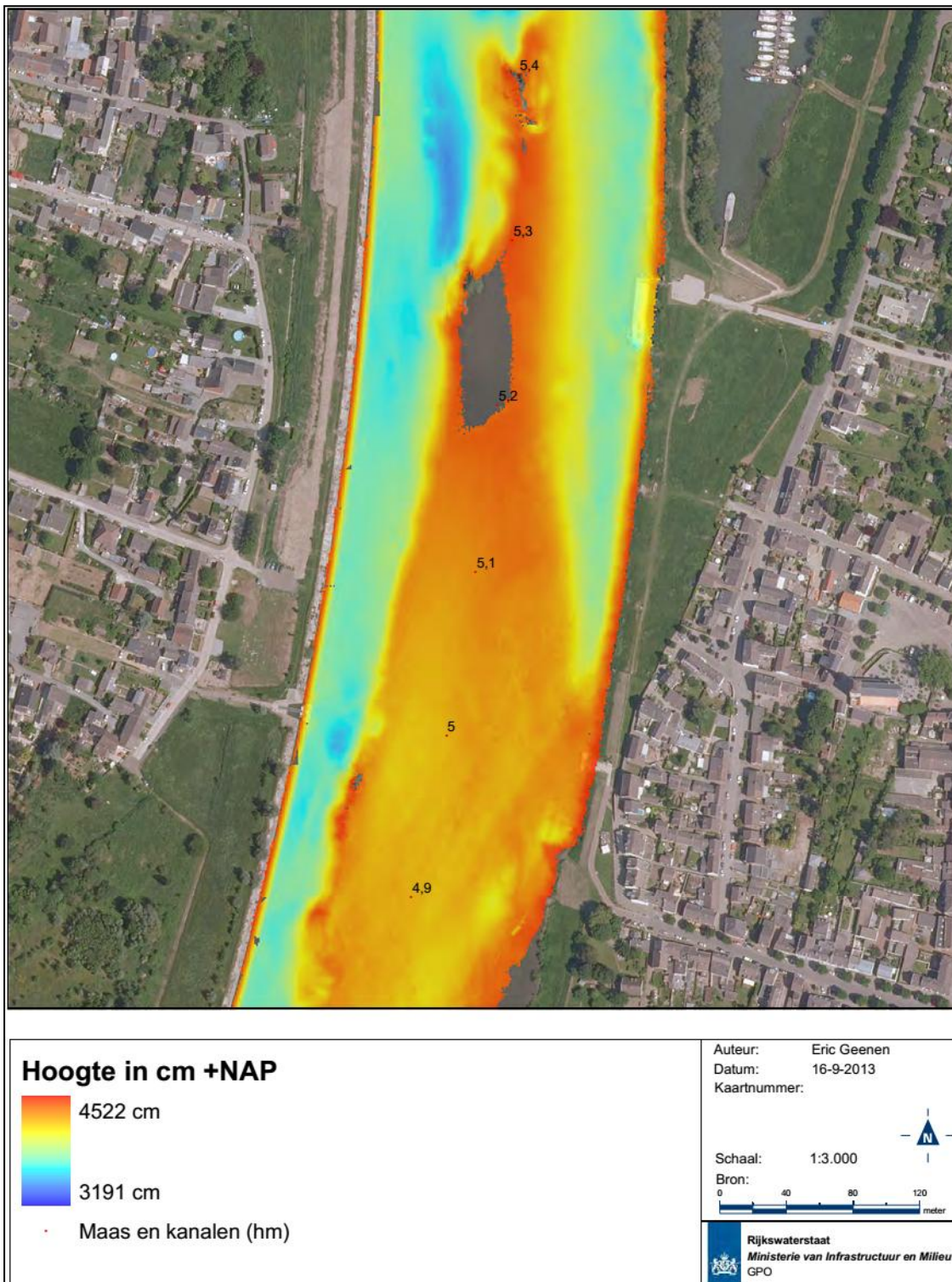

Figure A24. Contour map of the river Meuse at Eijsden. The pontoon is located at the right river bank in between 5.2 and 5.3 Meuse kilometers. Heights are distinguished by colours, from deep (blue) till less deep (red). The grey oval is an island that rises above the water surface.